Palestine Polytechnic University

College of Engineering & Technology

Mechanical Engineering Department

Mechatronics Engineering Program

Bachelor Thesis

Graduation Project

Solar-Fuel-Cell Hybrid System Control Strategy Oriented for Off-Grid Systems

Project Team

Shadi I. Ajweh **Mohammad I. Ajarmeh**

Project Supervisor

Dr. Momen sughayyer

Hebron – Palestine

May, 2013

Palestine Polytechnic University

College of Engineering & Technology

Mechanical Engineering Department

Hebron-Palestine

Solar-Fuel-Cell Hybrid System Control Strategy Oriented for Off-Grid Systems

Project Team

Shadi I. Ajweh ***Mohammad I. Ajarmeh***

According to the orientations of the supervisor on the project and the examined committee is by the agreement of a staffers all, sending in this project to the Mechanical Engineering Department are in the college of the engineering and the technology by the requirements of the department for the step of the bachelor's degree.

Project supervisor signature

……..……

Committee signature

....

Department head signature ……

Dedication

We dedicate this simple work:

To our parents

To our brothers

To our friends

To our nation

To any person working hard …

Acknowledgments

First and for most we should offer our thanks, obedience and gratitude to Allah.

Our appreciation to:

Palestine Polytechnic University

College of Engineering & Technology

Mechanical Engineering Department

Our supervisor: Dr. Momen sughayyer

Eng. Huseen Amro

Eng. Khalid Tamizi

Eng. Ahmad Balasi

Eng. Sami Salameen

Eng. Makaway Hraiz

Anyone who helped us

Abstract

Socio-economic development requires delivering electrical energy efficiently either form traditional or renewable sources. The final cost of delivering this energy depends on the many factors, which include economic and environment impacts. This has led to attract more attention to renewable energy sources and to develop its applications. However, each source is efficient only for specific situations and applications. Thus, integrating different renewable sources could provide more effective solutions. This trend requires the development of energy management and control strategies, especially when off-grid applications are the target.

The geographical location of Palestine lies within a considerably high solar belt, which is up to 5-6 kWh solar energy falling per square meter per day, and sunshine is about 3000 hour per year. Fuel-cell and hydrogen fuel technologies have attracted special attention due to their potential for replacing traditional internal combustion engines that runs on fossil fuels. Fortunately, hydrogen could be generated from bio-waste material available locally using economic technologies.

This contribution will introduce a control strategy for effective integration of fuel-cell and solar energy oriented for off-grid systems. The effectiveness of the proposed strategy will be proved using MatLab/Simulink software for applying solar-fuel-cell hybrid system on a study case. A typical energy consumption pattern for a Palestinian home will be used. In addition, the project will provide a sizing and optimization of system using PSO algorithm, also a modeling of the proposed system. Experimental results obtained for a reduced scale model parts built in the lab to give insight into the system technical details.

ملخص

فكرة المشروع تقوم على تطوير استراتيجية تحكم في طاقة النظام الهجين الذي يستخدم كلا من الخلايا الشمسية وخلايا الهيدروجين بالاضافة الى البطاريات لانتاج الطاقة، سيتم اثبات فعالية هذه الاستراتيجية باستخدام برناج الماتلاب لتطبيقها على حالة حقيقة لبيت في جنوب فلسطين ودراسة نتائجها.

ايضا في هذا المشروع تم استخدام نظرية سرب الطيور لتحديد الحجم الأمثل لكل جزء في النظام بهدف تقليل التكلفة وزيادة الاعتمادية على النظام، بالاضافة الى عمل models باستخدام الماتلاب لكل جزء في النظام. بعد ذلك تم عمل نموذج في المختبر بهدف محاكاة النظام الحقيقي وتم فيه تثبيت الجهد ب 1.2 فولت ليحاكي الجهد في المنزل 220 فولت.

List of Contents:

CHAPTER 5 : Optimization and Sizing

CHAPTER 6 : Experiments and results

CHAPTER 7 : Conclusion and Recommendations

List of Figures:

Chapter 1

Introduction

1.1 Introduction

1.2 Project Idea

1.3 Project Objectives

1.4 Recognition of the need

1.5 Literature review

1.6 Project Schedule

1.7 Budget

1.8 Thesis content

1.1 Introduction:

1.1.1 Renewable Energy

As awareness of global warming increases and conventional fuel sources begin to decrease, alternative energy sources attract the attention of the community more and more every day. Since the political issues decrease the desirability of nuclear power, a large amount of research and investments focus on renewable energy. Renewable energy is generated from natural resources like sunlight, wind, hydro, geothermal energies or from biodiesel fuels. Energy produced from renewable resources have no major waste products and the resources are naturally replenished. Although the resources are cost-free and environmentally friendly, current high initial costs of equipment, low energy conversion efficiencies and intermittent nature of energy sources decrease economic viability of the renewable energy against the fossil fuels. However, as the renewable technologies step forward, the practical use of renewables is growing. During the last decade, many governments have advanced their support for renewables.

1.1.2 Solar energy

Solar energy is one of the major sources of renewable energy with the amount of solar radiation reaching the Earth from the Sun. It is a well known fact that the world's one year energy demand can be supplied by the Sun in one hour if it was possible to collect all the solar energy falling on the earth. There are two commonly used ways of benefiting from sunlight; solar energy can be used to produce hot water or air via thermal solar panels or it is possible to convert solar energy into electricity by photovoltaic (PV) cells. Photovoltaic electricity generation has various advantages and disadvantages. Main disadvantages are; high initial cost of the equipment, low efficiency in converting solar energy into electricity and intermittent energy production due to natural reasons such as no sunlight being available during the night and low solar radiation throughout the winter seasons. But, once the PV panels are built, the operation cost of the system is very low and the panels can

work up to 20 years without any special maintenance need. Energy produced by the PV panels is cost-free and there is not any waste product. With conventional PV technologies 12 to 18% of solar energy can be converted into electricity.

1.1.3 Fuel Cells

Fuel cells are electrochemical devices that convert chemical energy in fuels into electrical energy directly, promising power generation with high efficiency and low environmental impact. Because the intermediate steps of producing heat and mechanical work typical of most conventional power generation methods are avoided, fuel cells are not limited by thermodynamic limitations of heat engines such as the Carnot efficiency. In addition, because combustion is avoided, fuel cells produce power with minimal pollutant. However, unlike batteries the reductant and oxidant in fuel cells must be continuously replenished to allow continuous operation. Fuel cells bear significant resemblance to electrolyzers. In fact, some fuel cells operate in reverse as electrolyzers, yielding a reversible fuel cell that can be used for energy storage.

1.1.4 Stand Alone Power System

A Stand Alone Power System (SAPS) is an off-grid electricity system that can operate without any external power input. Energy input to the system is usually from renewable sources which used to produce Hydrogen to used by fuel cell. Stand alone power systems are mostly used in remote locations where transporting electricity is either very difficult or expensive. Main elements of such systems are the solar energy source, photovoltaic panels, electrolyzer, fuel-cell and the hydrogen tank. Also some auxiliary equipment is needed for the system to work properly. Hydrogen which can be produced sustainably with no emission of carbon dioxide from renewable energy source like solar panel, a wind turbine or a micro-hydro generator to convert the radiant energy of sunlight into electrical power, which drives an electrolyzer. The electrolyzer breaks apart water producing hydrogen and oxygen gases. The hydrogen is stored for use by the fuel cell and the oxygen is released into

the atmosphere. Thus when the sun shines, the wind blows or the water flows, the electrolyzer can produce hydrogen.

A power system incorporating hydrogen from renewable sources and a fuel cell is a closed system, as none of the products or reactants, water, hydrogen and oxygen are lost to the outside environment. The water consumed by the electrolyzer is converted to gases. The gases are converted back to water. The electrical energy produced by the solar panel is transferred to chemical energy in the form of gases. The gases can be stored and transported, to be reconverted back to electricity (Fig. 1.1).

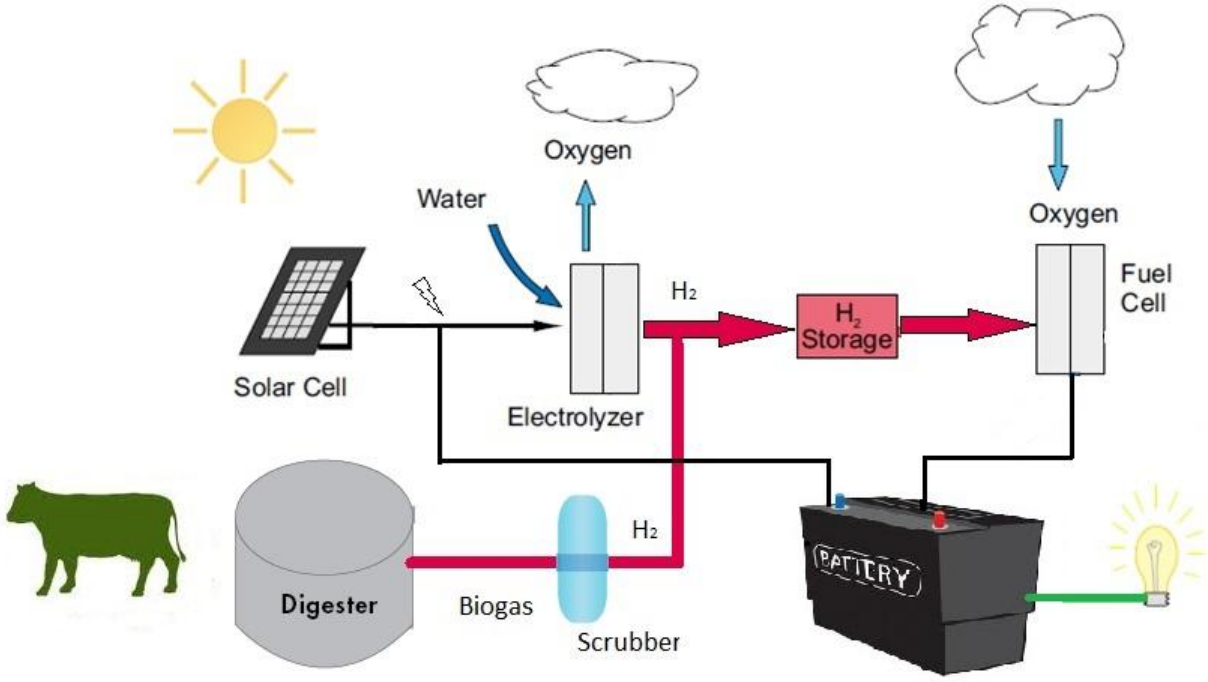

Figure 1.1: Electrical power from renewable energy sources.

1.2 Project Idea :

The main idea of this project is to study the stand alone power system based on solar-hydrogen energy for remote area power supply in Palestine and improve a power management strategy to control the hybrid system components, increase the efficiency and reduce the cost of the system. Then using practical swarm optimization (PSO) algorithm to Optimize and size the system components to reduce the costs and increase reliability.

By using a reduced scale model parts built in the lab to give insight into the system technical details and to keep the voltage of the system within 1.2V to simulate the voltage of loads in houses.

The presented work seeks to improve both theoretical and empirical understanding of solar-hydrogen power systems, and hence make significant additional contribution of the current body of knowledge on solar-hydrogen power systems.

1.3 Project objectives :

The overall objectives of this project are thus to:

- Review pervious work on the development and performance evaluation of Stand alone power systems.
- Develop and improve theoretical analysis of single-cell solar-hydrogen power systems.
- Develop a computer based simulation model based on theoretical analysis to predict the performance of and assist in designing solar-hydrogen power systems.
- Design, construct and measure the performance of experimental on solar-hydrogen power system employing PEM electrolyzer components.
- Design a control system to manage the power in solar-hydrogen power system.
- Identify opportunities for developing solar-hydrogen power systems with improved performance and cost effectiveness.

- Develop control scheme oriented to increase efficiency of the system.
- Using Practical swarm optimization algorithm for sizing and optimization the system cost and reliability.

1.4 Recognition of the need

Remote areas in Palestine are suffering from lack of electricity supply, which are indispensable for development and that because of the Israeli occupation and its policy that deprive Palestinians in these areas of electricity in addition to the large cost of the electricity network if it was reached to these areas.

Supply these areas with electricity using traditional methods like the use of diesel generators increase environmental problems such as pollution and global warming, since the world these days is moving towards the use of renewable sources of energy production, the ideal solution for these regions is using solar-hydrogen stand alone power systems which uses both solar energy and hydrogen energy and where it is possible to extract hydrogen from methane CH4, the use of this system contributes to the exploitation of agricultural waste by fermented and extract methane gas which is used to produce hydrogen and use the remainder of this waste as an organic fertilizer for crops in these lands.

The power management and sizing of the stand alone power system is the main challenge to engineers and designers; so in this project we will build a solar-hydrogen stand alone power system and also build controller to manage the power in this system with maximizing the efficiency of the system as possible, also to use a Practical Swarm Optimization algorithm (PSO) in sizing the system to get minimum cost and increase readability.

1.5 Literature review

Stand-Alone Power Systems based on different renewable energies is a developing topic in the literature. Most of the studies serve as "proof of concept" to using hydrogen as seasonal energy storage for intermittent renewable energy sources. The main focus of studies is proving technical viability of this kind of systems. According to economic point of view, the systems are usually evaluated as not being feasible with the current prices and efficiencies of the equipments used. Investment return is usually found to be over 20 years. Detailed knowledge about renewable energy and system equipment is required to design Stand-Alone Power Systems. Experimental testing or computational techniques can provide the necessary information. There are several works in the literature on the design, operation and simulation processes of renewable energy systems.

Experimental testing on small scaled energy systems is usually expensive and time consuming compared to computational methods. Therefore, the number of computational researches on this topic is greatly higher than experimental studies. Only some of them will be looked over in this section. A typical renewable energy system with hydrogen as energy storage contains electrolyzers, fuel cells, batteries, hydrogen storage tanks, DC/DC convertors, DC/AC inverters and PV panels. Each component should be modeled separately before forming the whole system.

Miland and Ulleberg [4] used a test facility to report the system performance and operational experience of individual components, subsystems and complete renewable power systems. To be able to investigate seasonal performance of the system, PV arrays have been emulated using a programmable power supply unit. Since a real time testing during a whole year is very time consuming, 7 days with different solar energy profiles have been selected to investigate seasonal behavior of the system in a weekly testing. The programmable power supply feeds the emulated PV power to the system consisting of PEM electrolyzer and fuel cell, metal hydride tank, hydrogen purifier, control panels and load. The efficiencies of singular component, subsystems and complete system have been found

and ways to improve them have been proposed. The real time operating efficiency of system, excluding PV array efficiency, has been found over 50%.

Agbossou et al. [5] investigated the performance of a hydrogen stand alone power system. A wind turbine and PV panels are used together as the energy generators. Alkaline electrolyzers, PEM fuel cells, hydrogen storage, batteries, controllers, DC/DC convertors and DC/AC inverters are the other components of the system. The controller defines the flow path of energy in the system. Batteries are used to cover energy demand during peak load powers and load power transients. After 30 days of operation, stand alone power system based on hydrogen as energy storage is found to be safe and reliable.

Kelly et al. [6] designed and constructed a system to produce hydrogen for fuelcell electric vehicles by solar energy. The system consisted of high efficiency PV panels and high pressure electrolyzers. The average efficiency of the system was increased to 8.5% by matching PV panel voltage at maximum power point output and electrolyzer voltage at nominal operating power. The authors claimed that solar-to-hydrogen efficiency of the system is one of the highest values reported in the literature.

Dufo-Lopez et al. [7] developed a method for controlling stand-alone hybrid renewable electrical systems with hydrogen storage. The method optimized the control of the hybrid system by minimizing the total cost throughout its lifetime. The optimized hybrid system can be composed of renewable sources, batteries, fuel cell, AC generator and electrolyzer. Also, the control strategy optimizes how the spare energy is used. The important point of this study is; the control strategy determines the most economical way to meet the energy deficit, when the amount of energy demanded by the loads is higher than the one produced by the renewable sources.

Pedrazzi et al [8] developed a complete mathematical model for a solar hydrogen energy system. Each component and subsystem has been modeled separately by using the information available in the literature. Then the individual models were combined together to form the virtual system. The simulations were conducted on commercial software

MATLAB Simulink. The annual simulations suggested that the system was able to perform as a stand alone power system without any energy need from grid. Thermodynamic, energy and economic analysis's was planned to be done by using the reference system modeled.

1.6 Project Schedule

The time plan views the stages of establishing the project with its components, divided into two semesters as shown in the following tables.

Table 1.1: Timing schedule of the First Semester

Process	Week														
	1	2	3	4	5	6	7	8	9	10	11	12	13	14	15
Collecting data and literature															
Analyzing the data of pervious works															
Make some on components experiments															
Build a simulation model of each component															
Writing the documentation															
Advanced features															

Table 1.2: Timing schedule of the Second Semester

Process	Week														
	1	2	3	4	5	6	7	8	9	10	11	12	13	14	15
Full Designing															
Build a Power Management Strategy															
Optimization and sizing using PSO															
Build The Prototype															
Documentation															

1.7 Project budget

This project required equipments and part to be completed, Majority of these equipments founded in the university and the project team will use it, some few of other equipments needed (capacitors, resistor, battery,…) but its cost is low and not excess 50$.

1.8 Thesis Content

This chapter gives an introduction about the system and the idea of the and the recognition of the need and the budget of this project.

Chapter two contains an introduction about hybrid system and give some information about its components (Photovoltaic Panels, Fuel cells, and Battery).

In chapter three the solar hydrogen stand alone power system parts modeling and simulation using Matlab/SIMULINK has been presented.

In chapter four the Power Management Strategy presented and the SIMULINK/State Flow model also shown.

Chapter five display optimization and sizing of hybrid system use PSO algorithm.

In chapter six some of experiment and its results done in last semester were presented, also the building of hybrid system prototype and the problems we faced is presented.

Chapter seven contains the problems faced due the work, conclusion of the project and recommendations.

Chapter 2

Introduction

2.1 Introduction

2.2 Photovoltaic Panels

2.3 Fuel Cells

2.4 Batteries

2.1 Introduction

A Stand Alone Power System is an off-grid electricity system that can operate without any external power input. Energy input to the system is usually from a renewable source. Stand alone power systems are mostly used in remote locations where transporting electricity is either very difficult or expensive.

Main elements of such systems are the solar energy source, photovoltaic panels, electrolyzer, fuel-cell and the hydrogen tank. Also some auxiliary equipment is needed for the system to work properly.

In the following sections the main components of the system will be introduced.

2.2 Photovoltaic Panels

Photovoltaic conversion is the direct conversion of sunlight into electricity with no intervening heat engine. Photovoltaic devices are solid state; therefore, they are rugged and simple in design and require very little maintenance. Perhaps the biggest advantage of solar photovoltaic devices is that they can be constructed as standalone systems to give outputs from microwatts to megawatts. That is why they have been used as the power sources for calculators, watches, water pumps, remote buildings, communications, satellites and space vehicles, and even megawatt-scale power plants. Photovoltaic panels can be made to form components of building skin, such as roof shingles and wall panels. With such a vast array of applications, the demand for photovoltaics is increasing every year. In 2003, 750 MWp (peak MW or MW under peak solar radiation of 1 kW/m^2) of photovoltaic panels were sold for the terrestrial markets and the market is growing at a phenomenal rate of 30% per year worldwide [29].

The sun fills the requirements of a clean energy-source, but why are people not making use of all the energy that surrounds us in form of sunlight? The answer to this is to be found in the solar cell, the component used to transform the sunlight into electricity.

Solar cells are used in different areas. Solar cell as the gadget that will help to solve the energy problem, though the thought of using the sun as an energy-source is very tempting. The obstacle in the way of the ultimate solution is the solar cell itself.

2.2.1 Materials Used for the Construction of Photovoltaic Cells

Special materials are used for the construction of photovoltaic cells. These materials are called semiconductors. The most commonly used semiconductor material for the construction of photovoltaic cells is silicon. Several forms of silicon are used for the construction; they are single-crystalline, multi-crystalline and amorphous. Other materials used for the construction of photovoltaic cells are polycrystalline thin films such as copper indium dieseline, cadmium telluride and gallium arsenide

- **Silicon - The Most Popular Material for Solar Cells**

A number of the earliest photovoltaic (PV) devices have been manufactured using silicon as the solar cell material and it is still the most popular material for solar cells today. The molecular structure of single-crystal silicon is uniform. This uniformity is ideal for the transfer of electrons efficiently through the material. However, in order to make an effective photovoltaic cell, silicon needs to be "doped" with other elements. Multi-crystalline silicon is normally considered less efficient than single-crystal silicon.
On the other hand, multi-crystalline silicon devices are less expensive to produce. Casting process is the most common means of producing multi-crystalline silicon on a commercial scale.

Amorphous silicon can absorb 40 times more solar radiation than single-crystal silicon. This is one of the main reasons why amorphous silicon can reduce the cost of photovoltaic's. Amorphous silicon can be coated on low-cost substrates such as plastics and glass. This makes amorphous silicon ideal for building-integrated photovoltaic products.

- **Copper Indium Dieseline**

Copper indium dieseline or CIS for short, has an extremely high absorptive. This means that 99% of the light illuminated on CIS will be consumed in the first micrometer of the material. The addition of a small amount of gallium will improve the efficiency of the photovoltaic device. This is commonly referred to as copper indium gallium dieseline or CIGS photovoltaic cell.

- **Cadmium Telluride**

Cadmium telluride or CdTe is another well-known polycrystalline thin-film material. Similar to copper indium dieseline, CdTe also has a very high absorptive and can be produced using low-cost techniques. The properties of CdTe can be altered by the addition of alloying elements such as mercury and zinc.

2.2.2 Physical characteristics of the solar cell

The p–n Junction Diode

Anyone familiar with semiconductors will immediately recognize that what has been described thus far is just a common, conventional p–n junction diode, the characteristics of which are presented in Fig. 2.1. If we were to apply a voltage Vd across the diode terminals, forward current would flow easily through the diode from the p-side to the n-side; but if we try to send current in the reverse direction, only a very small (≈10−12 A/cm^2) reverse saturation current I_0 will flow. This reverse saturation current is the result of thermally generated carriers with the holes being swept into the p-side and the electrons into the n-side. In the forward direction, the voltage drop across the diode is only a few tenths of a volt [14].

The symbol for a real diode is shown here as a blackened triangle with a bar; the triangle suggests an arrow, which is a convenient reminder of the direction in which current flows easily. The triangle is blackened to distinguish it from an “ideal” diode. Ideal diodes have no voltage drop across them in the forward direction, and no current at all flows in the reverse

direction. The voltage–current characteristic curve for the p–n junction diode is described by the following Shockley diode equation [14]:

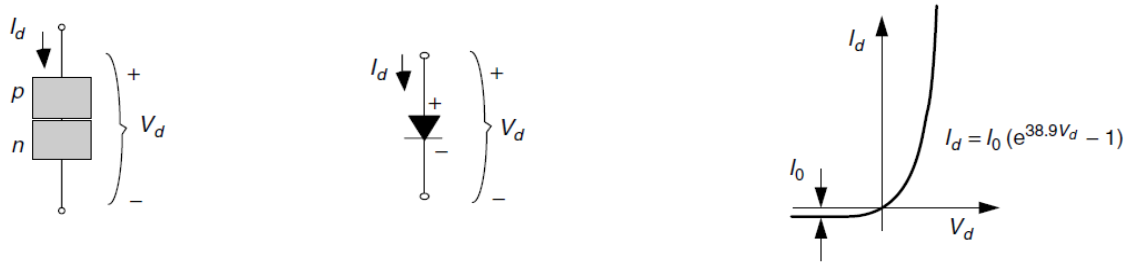

Figure 2.1: A *p*–*n* junction diode allows current to flow easily from the *p*-side to the *n*-side, but not in reverse. (a) *p*–*n* junction; (b) its symbol; (c) its characteristic curve.)

$$I_d = I_0\left(e^{\frac{qV_d}{KT}} - 1\right) \tag{2.1}$$

where:

I_d: is the diode current in the direction of the arrow.

V_d :is the voltage across the diode terminals from the p-side to the n-side (V).

I_0: is the reverse saturation current (A).

q: is the electron charge (1.602×10^{-19}C).

k :is Boltzmann's constant (1.381×10^{-23} J/K).

T: is the junction temperature (K).

$$\frac{qV_d}{kT} = \frac{1.602 \times 10^{-19}\text{C}}{1.381 \times 10^{-23}\text{ J/K}} \cdot \frac{V_d}{T(K)}$$

at T= 25°c

$$I_d = I_0(e^{38.9\,V_d} - 1) \tag{2.2}$$

A simple equivalent circuit model for a photovoltaic cell consists of a real diode in parallel with an ideal current source as shown in Fig 2.2. The ideal current source delivers current in proportion to the solar flux to which it is exposed.

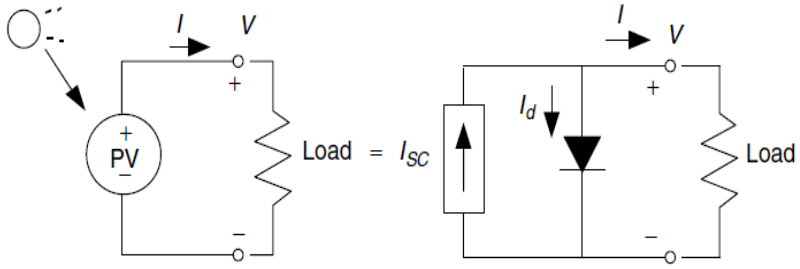

Figure 2.2: A simple equivalent circuit for a photovoltaic cell consists of a current source driven by sunlight in parallel with a real diode [29].

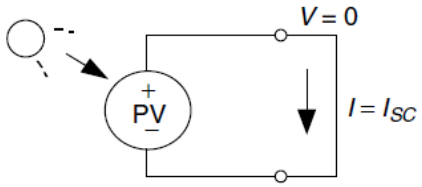

a (Short-circuit current)

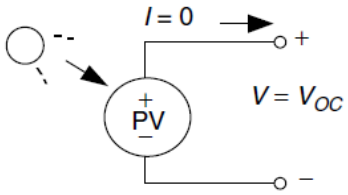

b(Open-circuit voltage)

Figure 2.3:Two important parameters for photovoltaic's are the short-circuit current I_{SC} and the open-circuit voltage V_{OC}.

There are two conditions of particular interest for the actual PV and for its equivalent circuit. As shown in 2.3, they are:

(1) The current that flows when the terminals are shorted together (the short-circuit current, I_{SC})

(2) The voltage across the terminals when the leads are left open (the open-circuit voltage, V_{OC}).

When the leads of the equivalent circuit for the PV cell are shorted together, no current flows in the (real) diode since $V_d = 0$, so all of the current from the ideal source flows through the shorted leads. Since that short-circuit current must equal ISC, the magnitude of

the ideal current source itself must be equal to I_{SC}. Now we can write a voltage and current equation for the equivalent circuit of the PV cell shown in Fig. 2.3.b. Start with [30]

$$I = I_{sc} - I_d \tag{2.3}$$

And then substitute Eq. (2.2) into Eq. (2.3) to get

$$I = I_{sc} - I_0(e^{38.9\,V_d} - 1) \tag{2.4}$$

When the leads from the PV cell are left open, I = 0 and we can solve Eq. (2.4) for the open-circuit voltage V_{OC}:

$$V_{oc} = \frac{KT}{q}\ln\left(\frac{I_{sc}}{I_0} + 1\right)$$

$$V_{oc} = 0.0257\ln\left(\frac{I_{sc}}{I_0} + 1\right) \tag{2.5}$$

In both of these equations, short-circuit current, I_{SC}, is directly proportional to solar insulation, which means that we can now quite easily plot sets of PV current–voltage curves for varying sunlight. Also, quite often laboratory specifications for the performance of photovoltaic's are given per cm^2 of junction

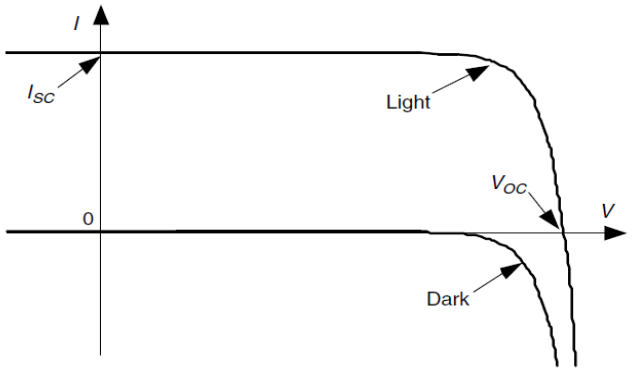

Figure 2.4: Photovoltaic current–voltage relationship for "dark" (no sunlight) and "light" (an illuminated cell).

2.2.3 A More Accurate Equivalent Circuit for a PV Cell

There are times when a more complex PV equivalent circuit than the one shown in Fig.2.5 is needed In our simplified equivalent circuit for the shaded cell, the current through that cell's current source is zero and its diode is back biased so it doesn't pass any current either (other than a tiny amount of reverse saturation current). This means that the simple equivalent circuit suggests that no power will be delivered to a load if any of its cells are shaded. While it is true that PV modules are very sensitive to shading, the situation is not quite as bad as that. So, we need a more complex model if we are going to be able to deal with realities such as the shading problem. Fig. 2.5 shows a PV equivalent circuit that includes some parallel leakage resistance R_p. The ideal current source I_{SC} in this case delivers current to the diode, the parallel resistance, and the load [4]:

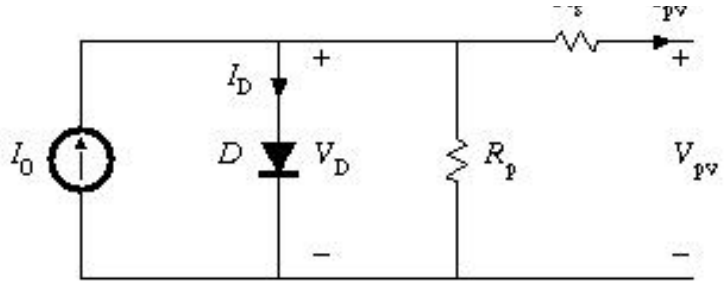

Figure 2.5: Equivalent Circuit for a PV Cell

$$\mathrm{I}_{sc} = I_d + I_p + \mathrm{I} \tag{2.6}$$

$$I = I_{SC} - I_d = I_{SC} - I_O\left(e^{qv/Kt} - 1\right) \tag{2.7}$$

$$V_d = V + R_s I \tag{2.8}$$

$$I = I_{SC} - I_0\left\{exp\left[\frac{q(V + I.R_s)}{KT}\right] - 1\right\} \tag{2.9}$$

$$I = I_{SC} - I_0\left[e^{38.9\,(V+I.R_S)} - 1\right] - \frac{1}{R_P}(V + I.R_S) \tag{2.10}$$

And the Values Of : $R_p > \dfrac{100V_{oc}}{I_{sc}}$, $R_S < \dfrac{0.01V_{oc}}{I_{sc}}$

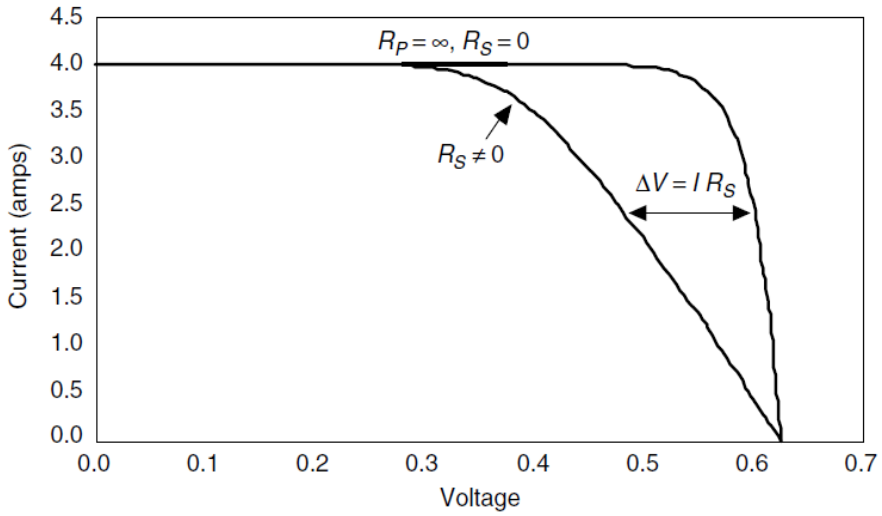

Figure 2.6: Adding series resistance to the PV equivalent circuit causes the voltage at any given current to shift to the left by $V = IR_S$.

2.2.4 From Cells To Modules To Arrays

Since an individual cell produces only about 0.6 V, it is a rare application for which just a single cell is of any use. Instead, the basic building block for PV applications is a module consisting of a number of pre-wired cells in series, all encased in tough, weather-resistant packages. A typical module has 36 cells in series and is often designated as a "12-V module" even though it is capable of delivering much higher voltages than that. Some 12-V modules have only 33 cells, which, as will be seen later may, be desirable in certain very simple battery charging systems. Large 72-cell modules are now quite common, some of which have all of the cells wired in series, in which case they are referred to as 24-V modules. Some 72-cell modules can be field-wired to act either as 24-V modules with all 72 cells in series or as 12-V modules with two parallel strings having 36 series cells in each. Multiple modules, in turn, can be wired in series to increase voltage and in parallel to increase current, the product of which is power. An important element in PV system design is deciding how many modules should be connected in series and how many in parallel to

deliver whatever energy is needed. Such combinations of modules are referred to as an array [29].

From Cells to a Module

When photovoltaics are wired in series, they all carry the same current, and at any given current their voltages add as shown in Fig. 2.7. That means we can continue the spreadsheet.

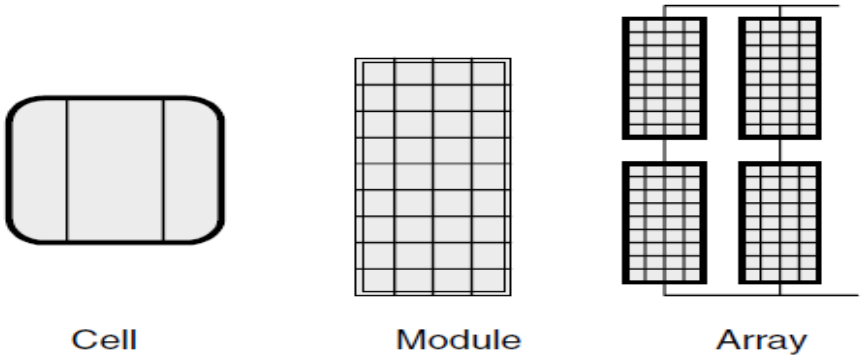

Figure 2.7:Photovoltaic cells, modules, and arrays.

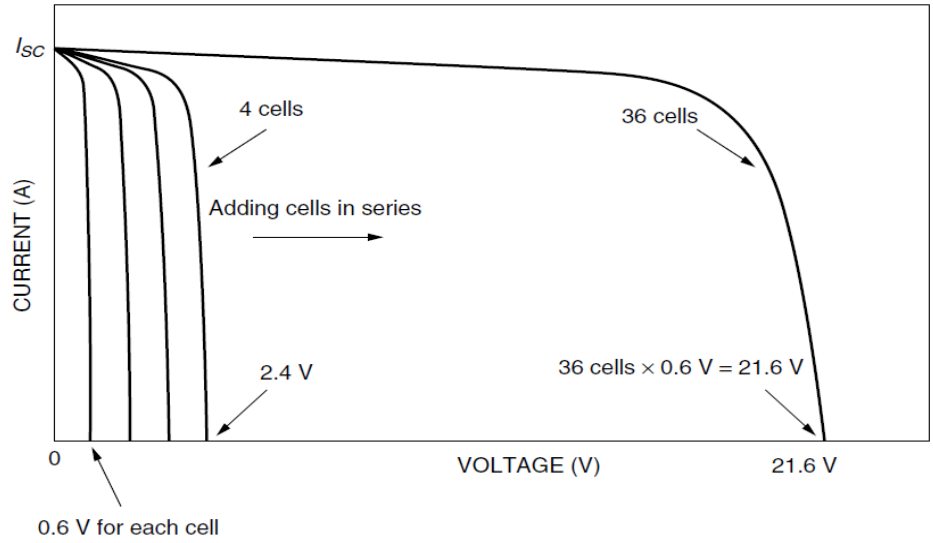

Figure 2.8: For cells wired in series [30].

To find value of the module voltage (V):

$$V_{module} = n(V_d - IR_s) \tag{2.11}$$

To find power of module (KW):

$$P = V_{module} * I \tag{2.12}$$

From Modules to Arrays

Modules can be wired in series to increase voltage, and in parallel to increase current. Arrays are made up of some combination of series and parallel modules to increase power. For modules in series, the I –V curves are simply added along the voltage axis. That is, at any given current (which flows through each of the modules), the total voltage is just the sum of the individual module voltages as is suggested in Fig2.9. For modules in parallel, the same voltage is across each module and the total current is the sum of the currents. That is, at any given voltage, the I –V curve of the parallel combination is just the sum of the individual module currents at that voltage. Fig.2.10 shows the I–V curve for three modules in parallel. When high power is needed, the array will usually consist of a combination of series and parallel modules for which the total I –V curve is the sum of the individual module I –V curves. There are two ways to imagine wiring a series/parallel combination of modules: The series modules may be wired as strings, and the strings wired in parallel as in Fig.2.11a, or the parallel modules may be wired together first and those units combined in series as in Fig2.11b. The total I –V curve is just the sum of the individual module curves, which is the same in either case when everything is working right. There is a reason, however, to prefer the wiring of strings in parallel Fig.2.11a. If an entire string is removed from service for some reason, the array can still deliver whatever voltage is needed by the load, though the current is diminished, which is not the case when a parallel group of modules is removed.

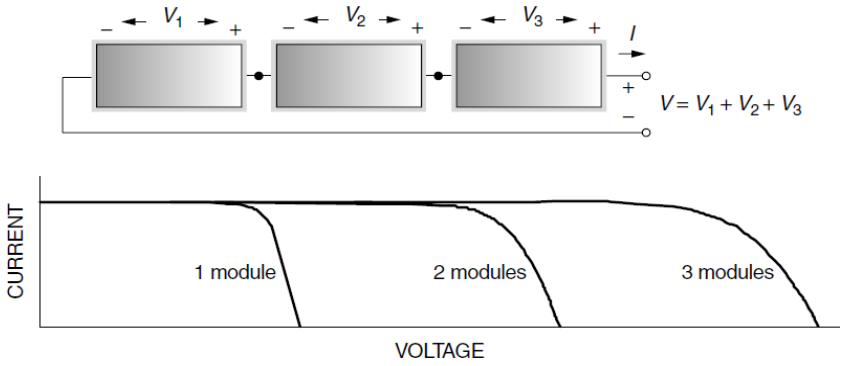

Figure 2.9: For modules in series, at any given current the voltages add.

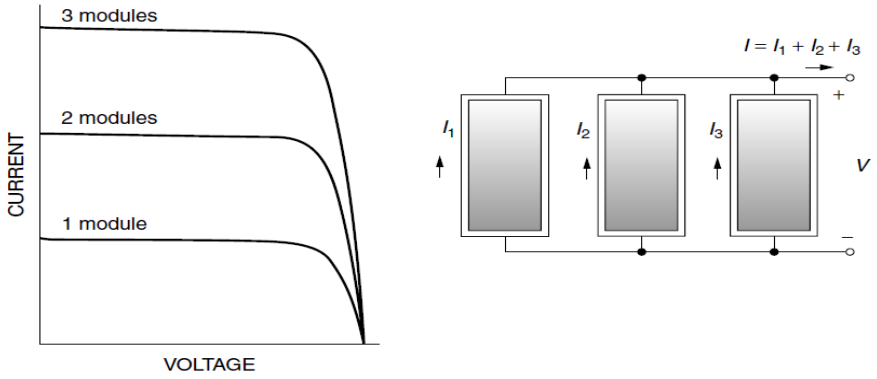

Figure 2.10: For modules in parallel, at any given voltage the currents add.

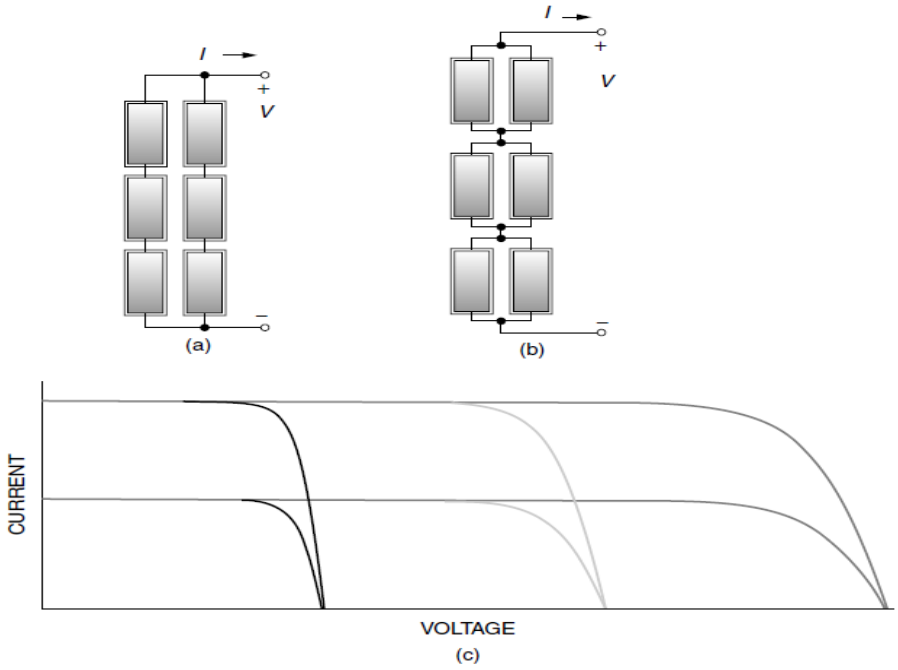

Figure 2.11 :Two ways to wire an array with three modules in series and two modules in parallel.. The total I –V curve of the array is shown in (c) [30].

2.2.5 Impacts of Temperature and Insulation on I–V curves

As seen in these I-V curves Fig2.12, as the irradiance level incident on the PV device changes, the short circuit current (I_{sc}) changes proportional to the irradiance. However, the open circuit voltage (V_{oc}) remains almost the same.

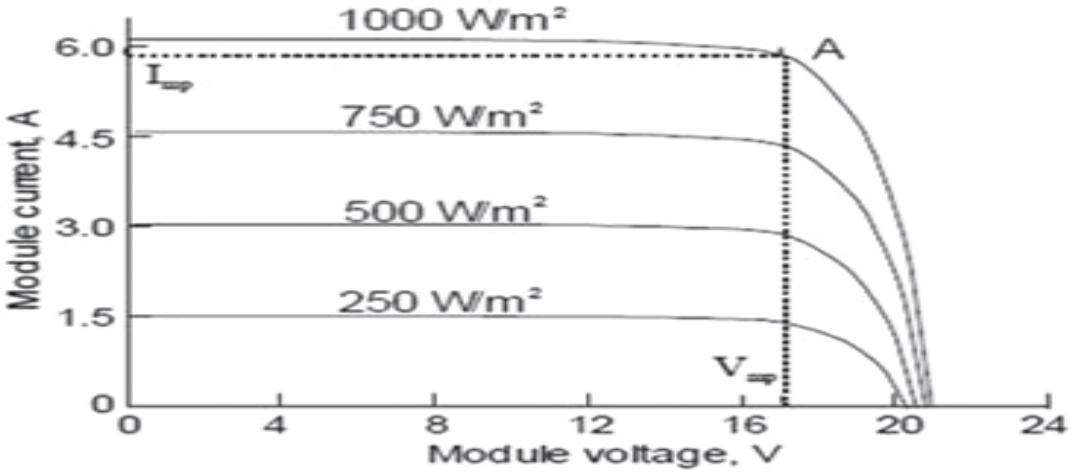

Figure 2.12: Dependence of current and voltage on incident sunlight levels [15].

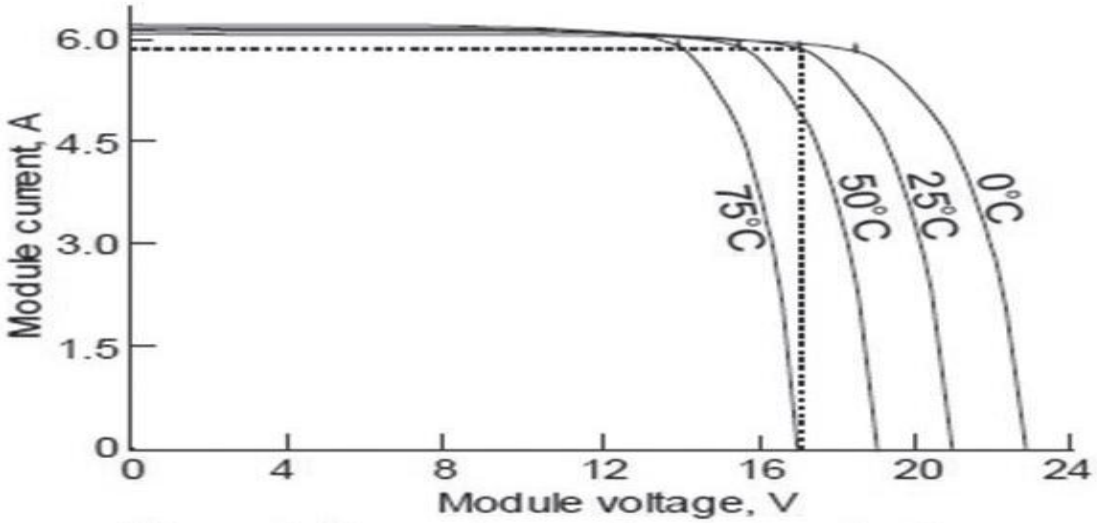

Figure 2.13: Dependence of current and voltage on temperature for sunlight of 1000W/m^2.

As seen in these I-V curves Fig2.13, as the temperature of the PV device changes, the open circuit voltage V_{oc} changes inversely proportional to the temperature. However, the short circuit current I_{sc} remains almost the same.

Because of the effects of both irradiance and temperature on the I-V curve characteristics and the resulting Maximum Power Point (MPP), a set of test conditions had to be established that establishes the values of both irradiance and temperature at which PV manufacturers rate the output of their devices. This set of test conditions is known as the "STC" or Standard Test Conditions for the PV industry. By having the nameplate data of solar panels based upon these conditions, the PV designer who is evaluating various PV panel products knows the irradiance and temperature conditions under which the nameplate data was measured.

In the PV industry, STC specifies a temperature of 25°C and an irradiance of 1000 W/m2 with an air mass 1.5 (AM 1.5) spectrums. These correspond to the irradiance and spectrum of sunlight incident on a clear day upon a sun-facing 37°-tilted surface with the sun at an angle of 41.81° above the horizon. This condition approximately represents solar noon near the spring and autumn equinoxes in the continental United States with surface of the cell aimed directly at the sun.

Similarly, when testing PV modules in the field prior to installation, the measurements for I_{sc}, V_{oc}, or better yet the I-V curve itself must be recalculated to the Standard Test Conditions of 1000 Watts per Square Meter of irradiance and 25 degrees Celsius in order to compare the measurements against the nameplate data.

2.3 Fuel Cell

Fuel cells are electrochemical devices that convert chemical energy in fuels into electrical energy directly, promising power generation with high efficiency and low environmental impact. Because the intermediate steps of producing heat and mechanical work typical of most conventional power generation methods are avoided, fuel cells are not limited by thermodynamic limitations of heat engines such as the Carnot efficiency. In addition, because combustion is avoided, fuel cells produce power with minimal pollutant. However, unlike batteries the reductant and oxidant in fuel cells must be continuously replenished to allow continuous operation. Fuel cells bear significant resemblance to electrolyzers. In fact,

some fuel cells operate in reverse as electrolyzers, yielding a reversible fuel cell that can be used for energy storage.

Though fuel cells could, in principle, process a wide variety of fuels and oxidants, of most interest today are those fuel cells that use common fuels (or their derivatives) or hydrogen as a reductant, and ambient air as the oxidant.

At present, fuel cells are routinely used in space applications, and have been under intensive development for terrestrial use, such as for utilities and zero-emission vehicles. There exist a variety of fuel cells, which are classified based on their operating temperature and the type of ion migrating through the electrolyte. However, the choice of electrolyte defines the properties of a fuel cell. Therefore, fuel cells are often named by the nature of their electrolyte. There are presently six major fuel cell technologies at varying stages of development and commercialization: alkaline, phosphoric acid, polymer electrolyte membrane, molten carbonate, solid oxide, and direct methanol fuel cell (DMFC).

Most fuel cell power systems comprise a number of components:

- Unit cells, in which the electrochemical reactions take place
- Stacks, in which individual cells are modularly combined by electrically connecting the cells to form units with the desired output capacity
- Balance of plant which comprises components that provide feed stream conditioning (including a fuel processor if needed), thermal management, and electric power conditioning among other ancillary and interface functions

2.3.1 Fuel Cell Types

A variety of fuel cells are in different stages of development. The most common classification of fuel cells is by the type of electrolyte used in the cells and includes 1) polymer electrolyte fuel cell (PEFC), 2) alkaline fuel cell (AFC), 3) phosphoric acid fuel cell (PAFC), 4) molten carbonate fuel cell (MCFC), and 5) solid oxide fuel cell (SOFC).

Broadly, the choice of electrolyte dictates the operating temperature range of the fuel cell. The operating temperature and useful life of a fuel cell dictate the physicochemical and thermomechanical properties of materials used in the cell components (i.e., electrodes, electrolyte, interconnect, current collector, etc.). Aqueous electrolytes are limited to temperatures of about 200 °C or lower because of their high vapor pressure and rapid degradation at higher temperatures. The operating temperature also plays an important role in dictating the degree of fuel processing required. In low-temperature fuel cells, all the fuel must be converted to hydrogen prior to entering the fuel cell. In addition, the anode catalyst in low temperature fuel cells (mainly platinum) is strongly poisoned by CO. In high-temperature fuel cells, CO and even CH4 can be internally converted to hydrogen or even directly oxidized electrochemically. Table 2.1 provides an overview of the key characteristics of the main fuel cell types [10].

In parallel with the classification by electrolyte, some fuel cells are classified by the type of fuel used:

- Direct Alcohol Fuel Cells (DAFC). DAFC (or, more commonly, direct methanol fuel cells or DMFC) use alcohol without reforming. Mostly, this refers to a PEFC-type fuel cell in which methanol or another alcohol is used directly, mainly for portable applications.
- Direct Carbon Fuel Cells (DCFC). In direct carbon fuel cells, solid carbon (presumably a fuel derived from coal, pet-coke or biomass) is used directly in the anode, without an intermediate gasification step. Concepts with solid oxide, molten carbonate, and alkaline electrolytes are all under development. The thermodynamics of the reactions in a DCFC allow very high efficiency conversion. Therefore, if the technology can be developed into practical systems, it could ultimately have a significant impact on coal-based power generation.

Table 2.1 : Summary of Major Differences of the Fuel Cell Types

	PEFC	**AFC**	**PAFC**	**MCFC**	**SOFC**
Electrolyte	Hydrated Polymeric Ion Exchange Membranes	Mobilized or Immobilized Potassium Hydroxide in asbestos matrix	Immobilized Liquid Phosphoric Acid in SiC	Immobilized Liquid Molten Carbonate in LiAlO2	Perovskites (Ceramics)
Electrodes	Carbon	Transition metals	Carbon	Nickel and Nickel Oxide	Perovskite and perovskite /metal cermet
Catalyst	Platinum	Platinum	Platinum	Electrode material	Electrode material
Interconnect	Carbon or metal	Metal	Graphite	Stainless steel or Nickel	Nickel, ceramic, or steel
Operating Temperature	40 – 80 °C	65°C – 220 °C	205 °C	650 °C	600-1000 °C
Charge Carrier	H^+	OH^-	H^+	$CO3^=$	$O^=$
External Reformer for hydrocarbon fuels	Yes	Yes	Yes	No, for some fuels	No, for some fuels and cell designs
External shift conversion of CO to hydrogen	Yes, plus purification to remove trace CO	Yes, plus purification to remove CO and CO2	Yes	No	No
Prime Cell Components	Carbon-based	Carbon-based	Carbon-based	Stainless-based	Ceramic
Product Water Management	Evaporative	Evaporative	Evaporative	Gaseous Product	Gaseous Product
Product Heat Management	Process Gas + Liquid Cooling Medium	Process Gas + Electrolyte Circulation	Process Gas + Liquid cooling medium or steam generation	Internal Reforming + Process Gas	Internal Reforming + Process Gas

2.3.2 Polymer Electrolyte Fuel Cell (PEMFC)

Polymer Electrolyte Fuel Cell is a type of fuel cell being developed for transport applications as well as for stationary fuel cell applications and portable fuel cell applications. The PEMFCs usually operate at about $80^{O}C$ and 1–8 atm pressure. The pressures, in general, are maintained equal on either side of the membrane. Operation at high pressure is necessary to attain high power densities, particularly when air is chosen as the cathodic reactant. They are a leading candidate to replace the aging alkaline fuel cell technology, which was used in the Space Shuttle.

Cell Components

Typical cell components within a PEFC stack include:

• The ion exchange membrane.

• An electrically conductive porous backing layer.

• An electro-catalyst (the electrodes) at the interface between the backing layer and the membrane.

• Cell interconnects and flow plates that deliver the fuel and oxidant to reactive sites via flow channels and electrically connect the cells Fig. 2.14.

PEFC stacks are almost universally of the planar bipolar type. Typically, the electrodes are cast as thin films that are either transferred to the membrane or applied directly to the membrane. Alternatively, the catalyst-electrode layer may be deposited onto the backing layer, then bonded to the membrane.

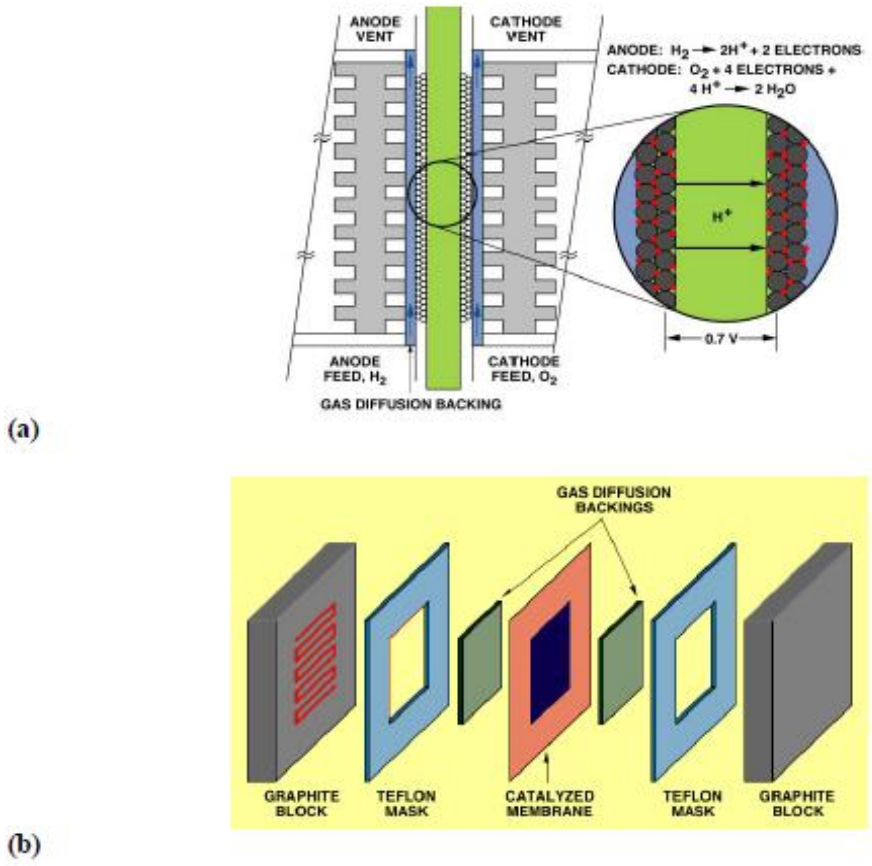

Figure 2.14: (a) Schematic of Representative PEFC (b) Single Cell Structure of Representative PEFC [10].

2.3.3 Basic Operating Principle

In a PEM fuel cell, two half-cell reactions take place simultaneously, an oxidation reaction (loss of electrons) at the anode and a reduction reaction (gain of electrons) at the cathode. These two reactions make up the total oxidation-reduction (redox) reaction of the fuel cell, the formation of water from hydrogen and oxygen gases.

As in an electrolyzer, the anode and cathode are separated by an electrolyte, which allows ions to be transferred from one side to the other Fig. 2.15. The electrolyte in a PEM fuel cell is a solid acid supported within the membrane. The solid acid electrolyte is saturated with water so that the transport of ions can proceed.

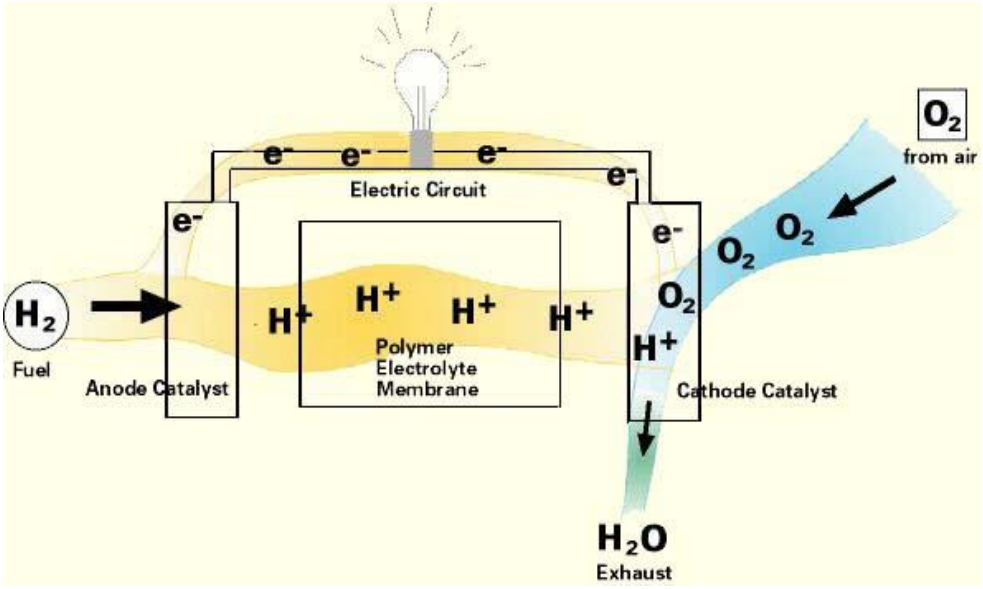

Figure 2.15: Diagram of a single PEM fuel cell [11].

PEM Fuel Cell:

Anode reaction: $\mathbf{H_2 \rightarrow 2H^+ + 2e^-}$ (2.13)

Cathode reaction: $\mathbf{\frac{1}{2} O_2 + 2H^+ + 2e^- \rightarrow H_2O}$ (2.14)

Overall cell reaction: $\mathbf{H_2 + \frac{1}{2} O_2 \rightarrow H_2O}$ **+Heat Generated +Electric Energy.** (2.15)

At the anode, the hydrogen molecules first come into contact with a platinum catalyst on the electrode surface. The hydrogen molecules break apart, bonding to the platinum surface forming weak H-Pt bonds. As the hydrogen molecule is now broken the oxidation reaction can proceed. Each hydrogen atom releases its electron, which travels around the external circuit to the cathode (it is this flow of electrons that is referred to as electrical current). The remaining hydrogen proton bonds with a water molecule on the membrane surface, forming a hydronium ion (H_3O^+). The hydronium ion travels through the membrane material to the cathode, leaving the platinum catalyst site free for the next hydrogen molecule.

At the cathode, oxygen molecules come into contact with a platinum catalyst on the electrode surface. The oxygen molecules break apart bonding to the platinum surface forming weak O-Pt bonds, enabling the reduction reaction to proceed. Each oxygen atom then leaves the platinum catalyst site, combining with two electrons (which have travelled through the external circuit) and two protons (which have travelled through the membrane) to form one molecule of water. The redox reaction has now been completed. The platinum catalyst on the cathode electrode is again free for the next oxygen molecule to arrive.

To prevent the membrane dry out leading to local hot-spot (and crack) formation, performance degradation, and lifetime reduction, both fuel and oxidant streams are fully humidified, and the operating temperature is limited by the saturation temperature of water corresponding to the operating pressure. The liquid water formed at the cathode does not dissolve in the electrolyte membrane, and is usually removed from the cell by the excessive oxidant gas stream. The accumulation of liquid water in the cathode backing layer blocks the oxygen transfer to the catalytic sites, thus resulting in the phenomenon called water-flooding that causes performance reduction. Local hot and cold spots will cause the evaporation and condensation of water. Thus, an integrated approach to thermal and water management is critical to PEMFCs' operation and performance, and a proper design must be implemented.

2.3.4 Major Technological Problems

For practical applications, PEMFC performance in terms of energy efficiency, power density (both size and weight) and capital cost must be further improved. This can be accomplished by systematic research in:

i. New oxygen-reduction electrocatalysts: this includes the reduction of precious-metal platinum and its alloys loading from 4 mg/cm2 to 0.4 mg/cm2 or lower without affecting the long-term performance and the lifetime, and the development of CO-tolerant catalysts.

ii. New types of polymer electrolyte with higher oxygen solubility, thermal stability, long life and low cost. A self-humidified membrane or a polymer without the need of humidification will be ideal for PEMFC operation and performance enhancement with significant simplification of system complexities and reduction of the cost.
iii. Profound changes in oxygen (air) diffusion electrode structure to minimize all transport-related losses. The minimization of all transport losses is the most promising direction for PEMFC performance improvement.
iv. Optimal thermal and water management throughout the individual cells and the whole stack to avoid local hot and dry spot formation and to avoid water-flooding of the electrode.

In addition to the above issues, the development of low-cost, light-weight materials for construction of reactant gas flow fields and bipolar plates is one of the major barriers to PEMFCs' large-scale commercialization. The successful solution of this problem will further increase the output power density. Additional issues include optimal design of flow fields with the operating conditions, and an appropriate selection of materials and fabrication techniques. It has been reported that over 20% improvement in the performance of PEMFC stacks can be obtained just by appropriate design of flow channels alone. The current leading technologies for bipolar plate design include: injection-molded carbon-polymer composites, injection molded and carbonized amorphous carbon, assembled three piece metallics, and stamped unitized metallics.

2.3.5 Open Circuit Voltage

The fuel cell directly converts chemical energy into electrical energy. The chemical energy released from the fuel cell can be calculated from the change in Gibbs free energy (Δgf) which is the difference between Gibbs free energy of the product and the Gibbs free energy of the reactants. For chemical energy the *point of zero energy can be define as almost*

anywhere. "Gibbs free energy of formation", G_f is used when this convention is used. Therefore, the Gibbs free energy of formation is zero for the input state, thus simplifying calculations and creating a standard. The Gibbs function of formation is defined below:

$$\bar{g} = \bar{h} - T\bar{s} \tag{2.16}$$

where $\bar{h}$ is enthalpy per mole, T is temperature, and $\bar{s}$ is entropy per mole.

The Gibbs function at a state other than the standard state is found by adding the Gibbs free energy of the standard state with that of the specific Gibbs function of the state of interest as expressed below [17]:

$$\bar{g}(T,p) = \bar{g}_f^0 + \left[\bar{g}(T,p) - \bar{g}\left(T_{ref}, p_{ref}\right)\right]$$

$$= \bar{g}_f^0 + \Delta\bar{g} \tag{2.17}$$

where $\bar{g}_f^0$ is the absolute Gibbs energy at 25^oC and 1 atm. Applying Eq. (2.16) to Eq. (2.17) we obtain the equation below:

$$\Delta\bar{g} = \left[\bar{h}(T,p) - \bar{h}\left(T_{ref}, p_{ref}\right)\right] - \left[T\bar{s}(T,p) - T\bar{s}\left(T_{ref}, p_{ref}\right)\right] \tag{2.18}$$

Enthalpy in Eq. (2.16) is defined as:

$$\bar{h} = \bar{u} + p\bar{v} \tag{2.19}$$

where $\bar{u}$ is the specific internal energy per mole, p is pressure, and $\bar{v}$ is the specific volume. Entropy is defined as:

$$S_2 - S_1 = \left(\int_1^2 \frac{\delta Q}{T}\right)_{Int\ Rev} \tag{2.20}$$

where δQ is the heat transfer at a part of the system boundary during a portion of the cycle, and T is the temperature. Assuming ideal gas behavior entropy at any temperature and pressure is determined by:

$$\bar{s} = \bar{s}\left(T, p_{ref}\right) + \left[\bar{s}(T,p) - \bar{s}\left(T, p_{ref}\right)\right] \tag{2.21}$$

which can be expanded to:

$$\bar{s}(T,p) = \bar{s}^0(T) - \bar{\bar{R}}\ln\left(\frac{p}{p_{ref}}\right) \tag{2.22}$$

where $\bar{s}^0$ is the absolute entropy at temperature T and pressure p. The absolute entropy is defined as:

$$\bar{s}^0(T) = \int_0^T \frac{c_p(T)}{T} dT \tag{2.23}$$

The Gibbs free energy is used to present the available energy to do external work. For the hydrogen/oxygen fuel cell, the basic chemical reaction is

$$H_2 + \frac{1}{2} O_2 \rightarrow H_2O \tag{2.24}$$

And the change in the Gibbs free energy Δgf is

$$\Delta gf = gf\ of\ product - gf\ of\ reactants = (gf)_{H2O} + (gf)_{H2} + (gf)_{O2} \tag{2.25}$$

The change in Gibbs free energy varies with both temperature and pressure. It can be shown that

$$\Delta fg = \Delta g_f^\circ - \bar{R} T_{fc} \ln \left[\frac{p_{H2} p_{O2}^{\frac{1}{2}}}{p_{H2O}} \right] \tag{2.26}$$

Where Δg_f° is the change in Gibbs free energy at standard pressure (1 Bar) which varies with the temperature,T_{fc} of the fuel cell, in Kelvin. The partial pressure, p_{H2}, p_{O2}, and p_{H2O} of the hydrogen, oxygen, and vapor, respectively are expressed in Bar. $\bar{R}$ is the universal gas constant 8.31451 J/(kg.K). The change in Gibbs free energy of the reaction in Eq. (2.24) at standard pressure Δg_f° is given in Table 2.2 for various reaction temperatures. The value of Δg_f° is negative which means that the energy is released from the reaction.

If the fuel cell process were "reversible", all of the Gibbs free energy would be converted to electrical energy, which is the electrical work used to move electrical charge around a circuit. For each mole of hydrogen, two moles of electrons pass around the external circuit and electrical work done (charge × voltage) is

$$\text{Electrical work done} = -2FE \quad \text{Joules} \tag{2.27}$$

where F is the Faraday Constant (=96485 Coulombs) which represent the electric charge of one mole of electrons and E is the voltage of the fuel cell. This electrical work done would be equal to the change in Gibbs free energy if the system were considered reversible

$$\Delta fg = -2FE \qquad (2.28)$$

Table 2.2 : Gibbs free energy for water for various temperatures and states [17].

Form of water product	Temp ^oC	$\Delta\bar{g}_f$ kJ/mole	Max EMF	Efficiency limit
Liquid	25	-237.2	1.23V	83%
Liquid	80	-228.2	1.18V	80%
Gas	100	-225.3	1.17V	79%
Gas	200	-220.4	1.14V	77%
Gas	400	-210.3	1.09V	74%
Gas	600	-199.6	1.04V	70%
Gas	800	-188.6	0.98V	66%
Gas	1000	-177.4	0.92V	62%

Thus, using equation (2.15), the reversible voltage of the fuel cell can be written as

$$\boldsymbol{E} = \frac{-\Delta_{fg}}{2F} = \frac{-\Delta g_f^{\circ}}{2F} + \frac{\bar{R}T_{fc}}{2F}\ln\left[\frac{p_{H2}p_{O2}^{\frac{1}{2}}}{p_{H2O}}\right] \qquad (2.29)$$

In practice, the fuel cell process is not reversible, some of the chemical energy is converted to heat, and the fuel cell voltage,V_{fc}, is less than that in Eq. (2.27). Voltage E in Equation (2.28) is called varies from standard state (25^{o}C and 1 atm) reference potential (1.229 V) in accordance with the temperature in the form

$$-\frac{\Delta g_f^{\circ}}{2F} = 1.229 + \left(T_{fc} - T_0\right)\left(\frac{\Delta S^0}{2F}\right) \qquad (2.30)$$

Where T_0 the standard is state temperature (298.15 K) and ΔS^0 is the entropy change. Since the variation in specific heat with expected change in temperature is minimal, the entropy change of a given reaction is approximately constant and can be set to the standard value, thus

$$-\frac{\Delta g_f^{\circ}}{2F} = 1.229 - \frac{298.15\ .\Delta s_0^0}{2F} + \left(\frac{\Delta S^0}{2F}\right) T_{fc} \qquad (2.31)$$

Using thermodynamic values of standard state entropy change, Equation (2.16) if further expanded and yields

$$\boldsymbol{E} = 1.229\ \ - 0.85 \times 10^{-3}\left(T_{fc} - 298.15\right) +\ \ 4.3085$$

$$\times\ 10^{-5} T_{fc}\ \ \left[ln(p_{H2}) + \frac{1}{2} ln(p_{O2})\right] \qquad \text{Volts} \qquad (2.32)$$

In Eq. (2.32), T_{fc} is expressed in Kelvin, and p_{H2}, and p_{O2} are expressed in atm. When the fuel cell operates, the actual voltage of the cell is less than the value calculated by Eq. (2.32), as shown in a typical fuel cell performance plot in Fig. (2.16). The differences are a result of losses or irreversibilities. In figure 3.3, cell voltage is the actual voltage of the fuel cell, v_{cell} , and the current density, i , is define as cell current. which equals stack current I_{st} (A), per cell active area, A_{fc} (cm^2).

$$\boldsymbol{i} = \frac{\boldsymbol{I_{st}}}{\boldsymbol{A_{fc}}} \qquad (2.33)$$

The cell current is equal to the stack current, I_{st}, because the stack is formed by connecting the fuel cells in series. The losses are attributed to three categories the activation loss, the ohmic loss, and the concentration loss. Plots of voltage drops caused by each of the losses are shown in Fig. 2.17. Each of these losses is considered and modeled separately in the following sections.

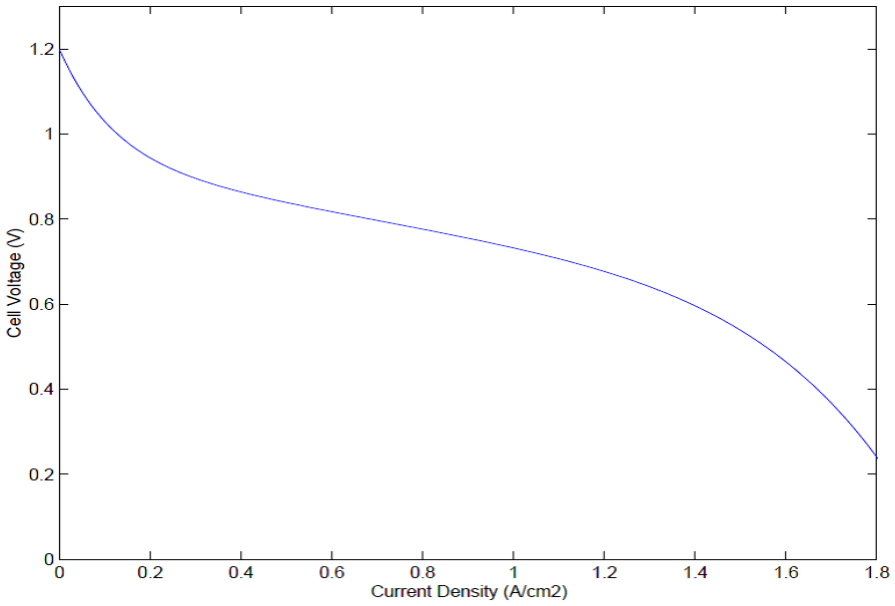

Figure 2.16: Typical Fuel Cell Polarization Curve

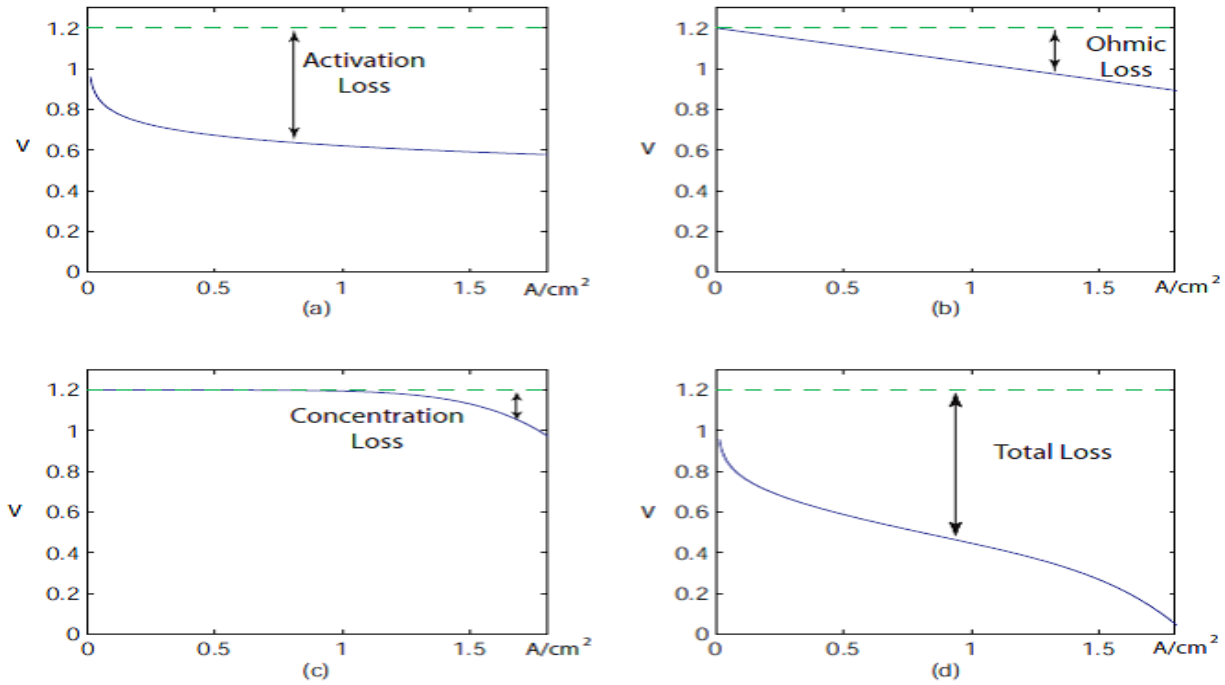

Figure 2.17: Voltage drops caused by different types of losses in fuel cell: (a) Activation losses only (b) Ohmic losses only (c) Concentration losses only (d) Total losses.

2.3.6 Fuel Cell Performance

Understanding the impacts of variables such as temperature, pressure, and gas constituents on performance allows fuel cell developers to optimize their design of the modular units and it allows process engineers to maximize the performance of systems applications.

A logical first step in understanding the operation of a fuel cell is to define its ideal performance. Once the ideal performance is determined, losses arising from non-ideal behavior can be calculated and then deducted from the ideal performance to describe the actual operation.

2.3.7 Fuel Cell Efficiency

The efficiency of a fuel cell is determined by the Gibbs free energy, $\Delta\bar{g}_{f,}$ and the "enthalpy of formation" ,$\Delta\bar{h}_f$, The "enthalpy of formation" is the value given to the heat that would be produced by burning the fuel. The "enthalpy of formation" is more commonly referred to as the "calorific value." The efficiency of a fuel cell is given by:

$$\frac{electrical\ energy\ produced\ per\ mole\ of\ fuel}{-\Delta\bar{h}_f} = \frac{\Delta\bar{g}_f}{\Delta\bar{h}_f} \tag{2.34}$$

The efficiency equation, Eq. (2.29), can be ambiguous in that the enthalpy of formation, $\Delta\bar{h}_f$, depends on the state of the H_2O product in the governing combustion equation. The product H_2O can be in the form of either steam or liquid. For the product H_2O in the form of steam being produced, $\Delta\bar{h}_f$ = −241.83*kJ=mole*, whereas, for H_2O in the form of liquid being produced, $\Delta\bar{h}_f$= −285.84*kJ=mole*. The difference in the two enthalpy of formation values is due to the molar enthalpy of vaporization of water. The enthalpy of formation $\Delta\bar{h}_f$=−285.84 *kJ=mole*, corresponding to the H_2O in the liquid state is known as the higher heating value (HHV). The enthalpy of formation, $\Delta\bar{h}_f$ = −241.83*kJ=mole*, corresponding to the H_2O is known as the lower heating value (LHV). The heating value is a common term applied to a fuel, and it is a positive number equal to the enthalpy of combustion. The

higher heating value is the value given when the product of the combustion is a liquid and the lower heating value is the value corresponding to when the product is in the gas form. The enthalpy of formation is easily calculated from the equation below:

$$\bar{h}_{RP} = \sum_{P} n_e \left(\bar{h}_f^o + \delta\bar{h}\right)_e - \sum_{R} n_i \left(\bar{h}_f^o + \delta\bar{h}\right)_i \tag{2.35}$$

where P and R correspond to the products and reactants, respectively, in any general combustion equation, n corresponds to the respective coefficients of the reaction equation giving the moles of reactants and products per mole of fuel, and $\bar{h}$ is the enthalpy. Therefore, the maximum efficiency for a fuel cell is determined by Eq. (2.36):

$$Maximum\ efficiency\ possible = \frac{\Delta\bar{g}_f}{\Delta\bar{h}_f} \times 100\% \tag{2.36}$$

where the maximum efficiency of any system is the actual energy produced by the reaction, $\bar{g}_f$ divided by the ideal energy produced by the reaction $\bar{h}_f$. The Gibbs free energy $\bar{g}_f$, is the actual energy produced by the combustion reaction, and the enthalpy of formation, $\bar{h}_f$, is the ideal energy that can be produced by the combustion reaction if the maximum energy was produced by the combustion reaction. Table 2.2 gives the value of maximum efficiency for a range of operating temperatures. Some interesting points about the efficiency of a fuel cell are:

- Even though a fuel cell is more efficient at lower temperatures as shown in Table 2.2, the voltage losses are much less in higher temperature fuel cells. Therefore, it is more advantageous to run a fuel cell at a higher temperature yet lower efficiency to produce higher operating voltages.
- Fuel cells operating at higher temperatures will produce more heat which can be harnessed and used in a much more efficient manner than the low heat produced by low temperature fuel cells.
- Fuel cells do not necessarily have a higher efficiency than heat engines. A heat engine is actually more efficient at higher temperatures depending on the specific fuel cell being analyzed.

2.4 Batteries

In stand-alone photovoltaic systems, the electrical energy produced by the PV array can not always be used when it is produced. Because the demand for energy does not always coincide with its production, electrical storage batteries are commonly used in PV systems. The primary functions of a storage battery in a PV system are to:

1. *Energy Storage Capacity and Autonomy:* to store electrical energy when it is produced by the *PV array* and to supply energy to *electrical loads* as needed or on demand.

2. ***Voltage and Current Stabilization****:* to supply power to *electrical loads* at stable voltages and currents, by suppressing or 'smoothing out' *transients* that may occur in PV systems.

3. ***Supply Surge Currents****:* to supply surge or high peak operating currents to *electrical loads* or appliances.

2.4.1 Battery Types and Classifications

Many types and classifications of batteries are manufactured today, each with specific design and performance characteristics suited for particular applications. Each battery type or design has its individual strengths and weaknesses. In PV systems, *lead-acid* batteries are most common due to their wide availability in many sizes, low cost and well understood performance characteristics. In a few critical, low temperature applications *nickel-cadmium* cells are used, but their high initial cost limits their use in most PV systems. There is no “perfect battery” and it is the task of the PV system designer to decide which battery type is most appropriate for each application.

In general, electrical storage batteries can be divided into to major categories, *primary* and *secondary* batteries.

Primary Batteries

Primary batteries can store and deliver electrical energy, but *can not be recharged*. Typical carbon-zinc and lithium batteries commonly used in consumer electronic devices are primary batteries. Primary batteries are not used in PV systems because they can not be recharged.

Secondary Batteries

A secondary battery can store and deliver electrical energy, and *can also be recharged* by passing a current through it in an opposite direction to the discharge current. Common *lead-acid* batteries used in automobiles and PV systems are secondary batteries.

2.4.2 Battery Performance Characteristics

Terminology and Definitions

Ampere-Hour (Ah): The common unit of measure for a battery's electrical storage capacity, obtained by integrating the discharge current in amperes over a specific time period. An ampere-hour is equal to the transfer of one-ampere over one-hour, equal to 3600 coulombs of charge. For example, a battery which delivers 5-amps for 20-hours is said to have delivered 100 ampere-hours.

Capacity: A measure of a battery's ability to store or deliver electrical energy, commonly expressed in units of *ampere-hours*. Capacity is generally specified at a specific discharge rate, or over a certain time period. The capacity of a battery depends on several design factors including: the quantity of active material, the number, design and physical dimensions of the plates, and the electrolyte specific gravity. Operational factors affecting capacity include: the discharge rate, depth of discharge, cut off voltage, temperature, age and cycle history of the battery. Sometimes a battery's energy storage capacity is expressed in kilowatt-hours (kWh), which can be approximated by multiplying the rated capacity in amperehours by the nominal battery voltage and dividing the product by 1000.

Cut Off Voltage: The lowest voltage which a battery system is allowed to reach in operation, defining the battery capacity at a specific discharge rate. Manufacturers often rate capacity to a specific cut off, or end of discharge voltage at a defined discharge rate. If

the same cut off voltage is specified for different rates, the capacity will generally be higher at the lower discharge rate.

Cycle: Refers to a discharge to a given depth of discharge followed by a complete recharge. A 100 percent depth of discharge cycle provides a measure of the total battery capacity.

Discharge: The process when a battery delivers current, quantified by the discharge current or rate. Discharge of a lead-acid battery involves the conversion of lead, lead dioxide and sulfuric acid to lead sulfate and water.

Charge: The process when a battery receives or accepts current, quantified by the charge current or rate. Charging of a lead-acid battery involves the conversion of lead sulfate and water to lead, lead dioxide and sulfuric acid.

Rate of Charge/Discharge: The rate of charge or discharge of a battery is expressed as a ratio of the nominal battery capacity to the charge or discharge time period in hours. For example, a 4-amp discharge for a nominal 100 ampere-hour battery would be considered a C/20 discharge rate.

Negative (-): Referring to the lower potential point in a dc electrical circuit, the negative battery terminal is the point from which electrons or the current flows during discharge.

Positive (+): Referring to the higher potential point in a dc electrical circuit, the positive battery terminal is the point from which electrons or the current flows during charging.

Open Circuit Voltage: The voltage when a battery is at rest or steady-state, not during charge or discharge. Depending on the battery design, specific gravity and temperature, the open circuit voltage of a fully charged lead-acid battery is typically about 2.1-volts.

2.4.3 Battery System Design and Selection Criteria

Battery system design and selection criteria involve many decisions and trade offs. Choosing the right battery for a PV application depends on many factors. While no specific battery is appropriate for all PV applications, common sense and a careful review of the battery literature with respect to the particular application needs will help the designer narrow the choice. Some decisions on battery selection may be easy to arrive at, such as physical properties, while other decisions will be much more difficult and may involve making tradeoffs between desirable and undesirable battery features. With the proper application of this knowledge, designers should be able to differentiate among battery

types and gain some application experience with batteries they are familiar with. Table 2.3 summarizes some of the considerations in battery selection and design.

Table 2.3 : Battery Selection Criteria [31]

·Type of system and mode of operation	· Temperature and environmental conditions
· Charging characteristics; internal resistance	· Cyclic life and/or calendar life in years
· Required days of storage (autonomy)	· Maintenance requirements
· Amount and variability of discharge current	· Sealed or unsealed
· Maximum allowable depth of discharge	· Self-discharge rate
· Daily depth of discharge requirements	· Maximum cell capacity
· Accessibility of location	· Energy storage density
· Size and weight	· Susceptibility to freezing
· Gassing characteristics	· Susceptibility to sulfation
· Electrolyte concentration	· Terminal configuration

Chapter 3

Modeling and Simulation

3.1 Introduction

In this part of the project we will built a model of stand-alone power system based on photovoltaic panels and hydrogen fuel cells, produce electrical energy and store it in a battery stack.

In this part of project the model of PV panels, electrolyzer, fuel cell, and batteries will be building using Matlab/Simulink software to be used in the control design of the system that will be present in the next chapter.

The system consists of PV arrays, fuel cell stack, hydrogen storage tank, electrolyzer, batteries, power converter and controllers. Dynamic component models, used in this project, are summarized in the following sections

3.2 PV panels

Poly-Si PV modules are used in the system [12]. PV specifications are given in Table 2.

Modeling of PV panels

The basic mathematical model is used to calculate the maximum power output from the PV panels. The power output of the PV panel is rated according to maximum points for current and voltage as follows [12].

Fig. 3.1 shows the equivalent circuit of the one-diode model of PV cell [13].

Using Kirchhoff's current law, the terminal current through the PV cell can be expressed from the following equations. The photocurrent (I_{ph}) mainly depends on solar irradiation and cell's operating temperature, which is given by [14,15],

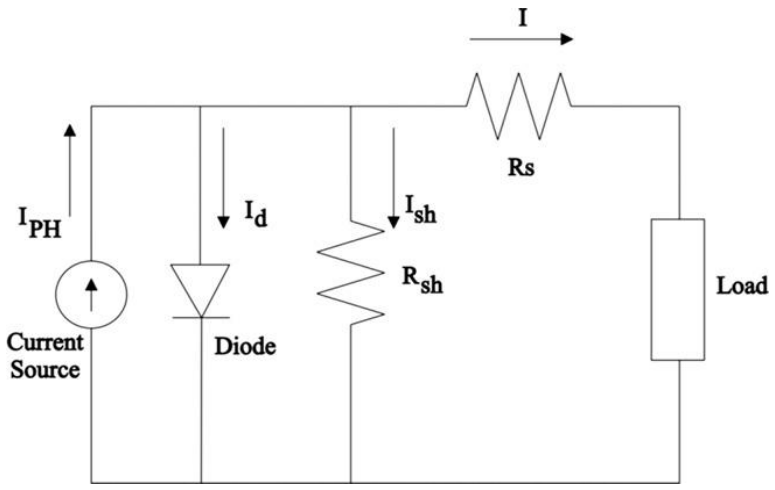

Figure 3.1: Equivalent circuit of PV cell.

$$I_{ph} = \left[I_{SC} + K_I\left(T_C - T_C^{ref}\right)\right]G \tag{3.1}$$

$$I_s = I_{RS}\left(\frac{T_c}{T_c^{ref}}\right)\exp\left[\frac{qE_G}{kA}\left(\frac{1}{T_c^{ref}} - \frac{1}{T_c}\right)\right] \tag{3.2}$$

$$I = I_{ph} - I_s\left\{exp\left[\frac{q(V + IR_s)}{kT_cA}\right] - 1\right\} - \frac{V + IR_S}{R_{sh}} \tag{3.3}$$

where, I_{SC} is the cell's short-circuit current. K_I, is the cell's temperature coefficient during short-circuit. T_c^{ref} , is the cell's reference temperature. G, is the solar irradiance in kW/m^2. I_{ph} is the light-generated current or photocurrent. I_S, is dark current for the cell saturation. q is the charge of an electron (1.6×10^{-19} C). k is the Boltzmann's constant (1.38×10^{23} J/K).

T_C, is the cell's working temperature. A , is the ideal factor of the PV cell. R_{sh}, is the shunt resistance, and R_S is the serial resistance, I_{RS}, is the cell's reverse saturation current at reference temperature and solar irradiation, E_G, is the band gap energy of the semi-

conductor used in the cell [16]. Ideal factor and band gap values of PV cells are presented in Table 3.1.

Table 3.1: Ideal factor (A) and band gap (E_G) values of different PV cell types.

Cell type	A	E_G
Mono-Si	1.026	1.12
Poly-Si	1.025	1.14
a-Si:H	1.8	1.65
a-Si:H tandem	3.3	2.9
a-Si:H triple	3.09	1.6
CdTe	1.5	1.48
CIS	1.5	1
AsGa	1.3	1.43

The MATLAB/Simscape® model and submodel of the Poly Si PV panels are presented in Fig.3.2.

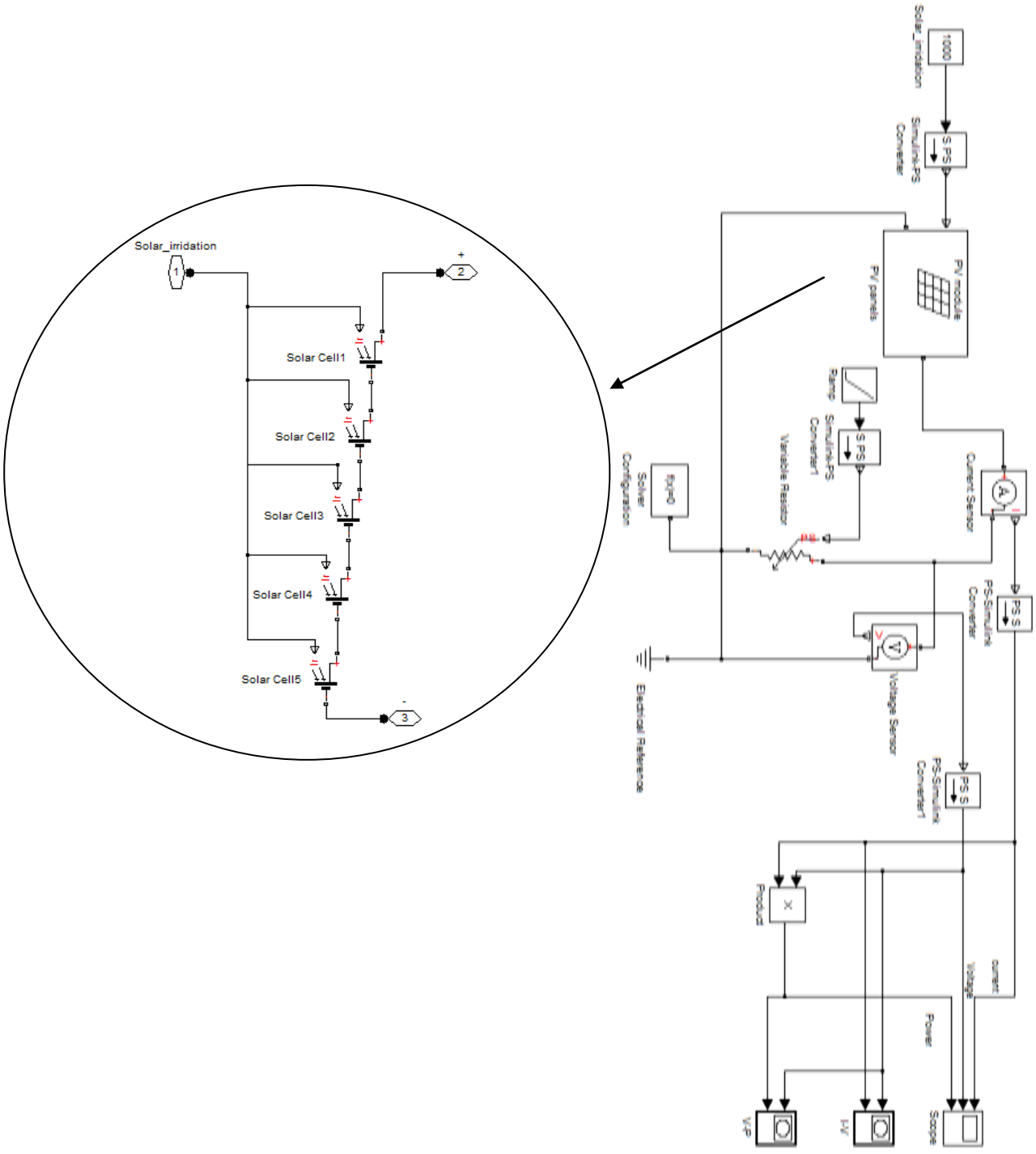

Figure 3.2: The MATLAB/Simscape® model and submodel of PV panels.

3.3 PEM electrolyzer

Electrolyzers are electrochemical devices to produce pure hydrogen and oxygen. For the hydrogen electrolyzer, two electrons pass through the external circuit for each water molecule consumed, and each molecule of hydrogen produced [17].

Modeling of the electrolyzer

A basic PEM electrolyzer unit consists of an anode, a cathode, power supply, a membrane, and electrodes. A direct current (DC) is applied to maintain the electrons flow from the negative terminal of the DC source to the cathode at which the electrons are consumed by hydrogen ions (protons) to form hydrogen gas.

A PEM electrolyzer consists of several electrolyzer cells connected in series. The proposed model aims to express the relationship between cell voltage and cell current. The real cell voltage in an electrolytic cell is higher than the ideal open circuit voltage and can be expressed as [11],

$$V = V_{OC} + V_{act} + V_{ohm} + V_{con} \tag{3.4}$$

Where, Voc is open circuit voltage. V_{act} is the activation over potential. V_{ohm} is the ohmic over potential. V_{con} is the concentration over potential. The reversible potential or open circuit voltage at the cell (V_{oc}) can be derived from the Nernst equation for water electrolysis [18].

$$V_{OC} = E_0 + \frac{RT}{2F}\left[\ln\left(\frac{pH_2 pO_2^{\frac{1}{2}}}{pH_2O}\right)\right] \tag{3.5}$$

$$E_0 = 1.229 - 0.9 \times 10^{-3}(T - 298) \tag{3.6}$$

According to the Nernst equation for hydrogen reaction, the ideal cell potential at a given temperature can be increased by operating at higher reactant pressures, and

improvements in fuel cell performance have, in fact, been observed at higher pressures [19].

According to Dalton's law of partial pressures,

$$pH_2O = \frac{610}{10^5}\exp\left[\frac{T}{T+238.3}\times 17.2694\right] \tag{3.7}$$

$$pO_2 = p_{anode} - pH_2O \tag{3.8}$$

$$pH_2 = p_{cathode} - pH_2O \tag{3.9}$$

where, E_0, Nernst potential; p_{anode}, anode pressure; $p_{cathode}$, cathode pressure; pH_2O, partial pressure of water; pO_2, partial pressure of oxygen; pH_2, partial pressure of hydrogen; T, the temperature in Kelvin (273+°C); R, the gas constant = 8.314472 J/K.mol = 0.08314 (bar.L/K.mol); F, the Faraday constant = 96,485 C.mol^{-1}.

The activation over potential (V_{act}) is highly affected from these values, which depend on the used electro catalyst and the temperature [20]. Initially, assuming to only charge transfer limitations (accurate approximation only for low current densities) the Butlere-Volmer Eq. (3.10) relates the current density to the activation over potential for each electrode, which takes into account the kinetics of the charge transfer reaction [21];

$$i = i_0\left[exp\left(\frac{\alpha_1 F}{RT}V_{act}\right) - exp\left(-\frac{\alpha_2 F}{RT}V_{act}\right)\right] \tag{3.10}$$

$$V_{act} = V_{act,a} + V_{act,c} \tag{3.11}$$

$$V_{act,a} = \frac{RT}{F}\sinh^{-1}\left[\frac{1}{2}\left(\frac{i}{i_{0,a}}\right)\right] \tag{3.12}$$

$$V_{act,c} = -\frac{RT}{F}\sinh^{-1}\left[\frac{1}{2}\left(\frac{i}{i_{0,c}}\right)\right] \tag{3.13}$$

where, $V_{act,a}$, activation over potential at anode; $V_{act,c}$, activation over potential at cathode; α_1, the cathodic charge transfer coefficient; α_2, the anodic charge transfer coefficient; i, the electrode current density; $\alpha_1 = \alpha_2$, assuming Eqs. (3.12) and (3.13) can be inverted [22]; $i_{0,a}$ and $i_{0,c}$, are the exchange current densities for each electrode.

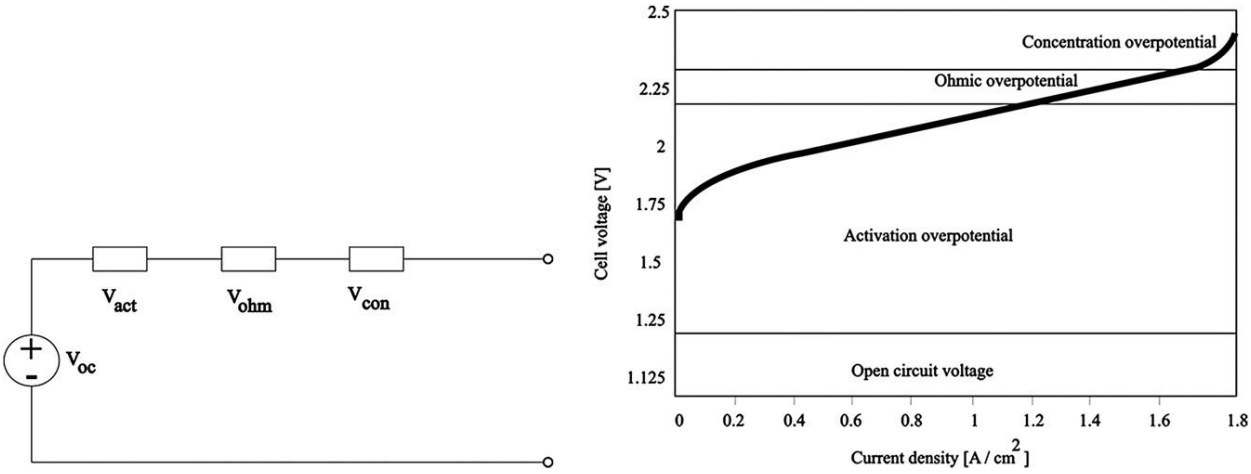

Figure 3.3: Polarization curve and simple equivalent circuit of the PEM electrolyzer.

For Pt based catalysts, $i_{0,a}$, also much dispersed in a range between 10^{-13} and 10^{-6} A/cm^2, $i_{0,c}$, 10^{-3} A/cm^2 [23].

An ohmic over potential appears due to the ohmic resistance of the current collectors, bipolar plates and electrode surfaces [24]. Following Ohm's law, these losses can be grouped and equations as;

$$V_{ohm} = iR_{ohm} \tag{3.14}$$

$$R_{ohm} = t_m/\sigma_m \tag{3.15}$$

where, σ_m is the conductivity of the membrane which is calculated from water content of the membrane λ_m. t_m is membrane thickness (mm). The electrolyzer operation temperature is T [25,26].

$$\sigma_m = (0.00514\lambda_m - 0.00326)\exp\left[1268\left(\frac{1}{303} - \frac{1}{T}\right)\right] \tag{3.16}$$

Concentration losses are caused by the mass transportation, which affects the concentration of the hydrogen and oxygen at high current densities [26]. Additionally, operating electrolyzers at high current densities result in a high rate of hydrogen production but at a low efficiency.

$$V_{con} = V_{con,a} + V_{con,c} \tag{3.17}$$

$$V_{con,a} = \frac{RT}{2F} ln\left[\left(\frac{p^I O_2}{pO_2}\right)^{1/2}\right] \tag{3.18}$$

$$V_{con,c} = \frac{RT}{2F}\ln\left(\frac{p^I H_2\, pH_2O}{pH_2\, p^I H_2O}\right) \tag{3.19}$$

where, p^I represents the partial pressures at the electrode-electrolyte interface [27].

The MATLAB/Simulink® model of the electrolyzer is presented in Fig.3.4.

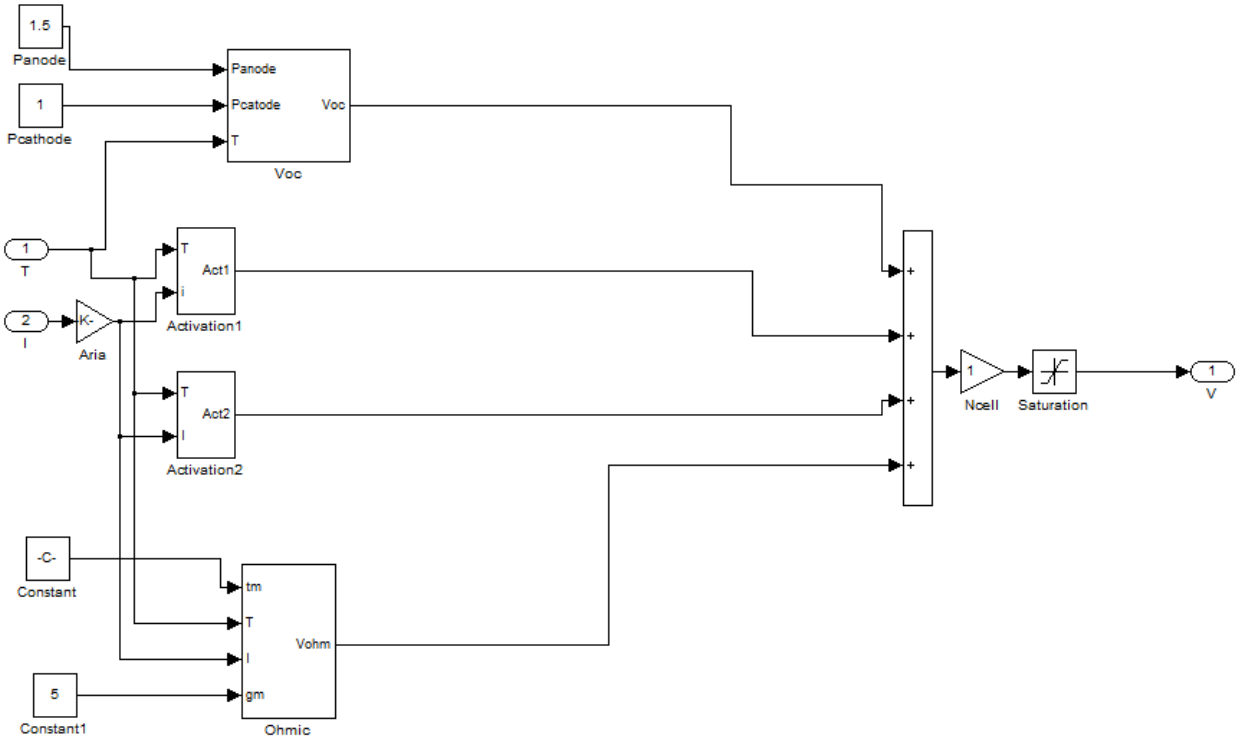

Figure 3.4: MATLAB/Simulink® model of the electrolyzer.

The hydrogen production [28];

$$H_2 production = \eta_f \frac{n_c(RITt)}{Fpz} \tag{3.20}$$

where, n_C, the number of PEM electrolyzer cell stacks; I, the current supplied to electrolyzer (ampere); t, the period of time current supplied to electrolyzer (second); p, the ambient pressure = 101325 Pa; z, the excess number of electrons which is 2 for hydrogen and 4 for oxygen.

The ratio between the actual and the theoretical maximum amount of hydrogen produced in the electrolyzer is known as Faraday efficiency. Assuming that the working temperature of the electrolyzer is 40°C, Faraday efficiency is calculated by the following equation,

$$\eta_F = 96.5e^{(0.09/i - 75.5/i^2)} \tag{3.21}$$

i is the electric current in the equivalent electrolyzer circuit.

3.4 Fuel Cell

There is a need for a reliable mathematical model. Such model can allow the evaluation of the PEMFC dynamic performance for small size electrical energy generation systems, reducing cost and time along the design stage and tests. Such need motivated us to conduct electrochemical modeling to determine the open circuit voltage and the voltage drops of the cells for each operating point. In power generation systems, the dynamic response is extremely important for the planner of control and management systems; especially when there is injection of energy into the grid.

Modeling of PEM Fuel cell

The basic mathematical model is used to calculate the maximum power output from the fuel cell stakes. The power output of the fuel cell is rated according to maximum points for current and voltage as follows.

Using fuel cell module discussed in chapter two the terminal current and voltage through the fuel cell can be expressed from the following equations:

$$E_{OC} = K_c E_n \tag{3.22}$$

$$i_o = \frac{zFk(PH_2 + PO_2)}{Rh} e^{-\frac{\Delta G}{RT}} \tag{3.23}$$

$$A = \frac{RT}{z\alpha F} \tag{3.24}$$

where R = 8.3145 J/(mol K), F = 96485 A s/mol, z : Number of moving electrons, E_n : Nernst voltage, which is the thermodynamics voltage of the cells and depends on the temperatures and partial pressures of reactants and products inside the stack (V), α: Charge transfer

coefficient, which depends on the type of electrodes and catalysts used, PH_2: Partial pressure of hydrogen inside the stack (atm), PO_2: Partial pressure of oxygen inside the stack (atm), k: Boltzmann's constant = 1.38 × 10–23 J/K, h: Planck's constant = 6.626×10^{-34} (J.s) , ΔG : Size of the activation barrier which depends on the type of electrode and catalyst used, T : Temperature of operation (K), K_c: Voltage constant at nominal condition of operation.

$$E_n = \frac{-\Delta \bar{g}_f^o}{2F} + \frac{RT}{2F} \ln\left(\frac{P_{H_2} P_{O_2}^{\frac{1}{2}}}{P_{H_2O}}\right) \tag{3.25}$$

The MATLAB/Simscape® model of the PEM fuel cell stake are presented in Fig 3.5.

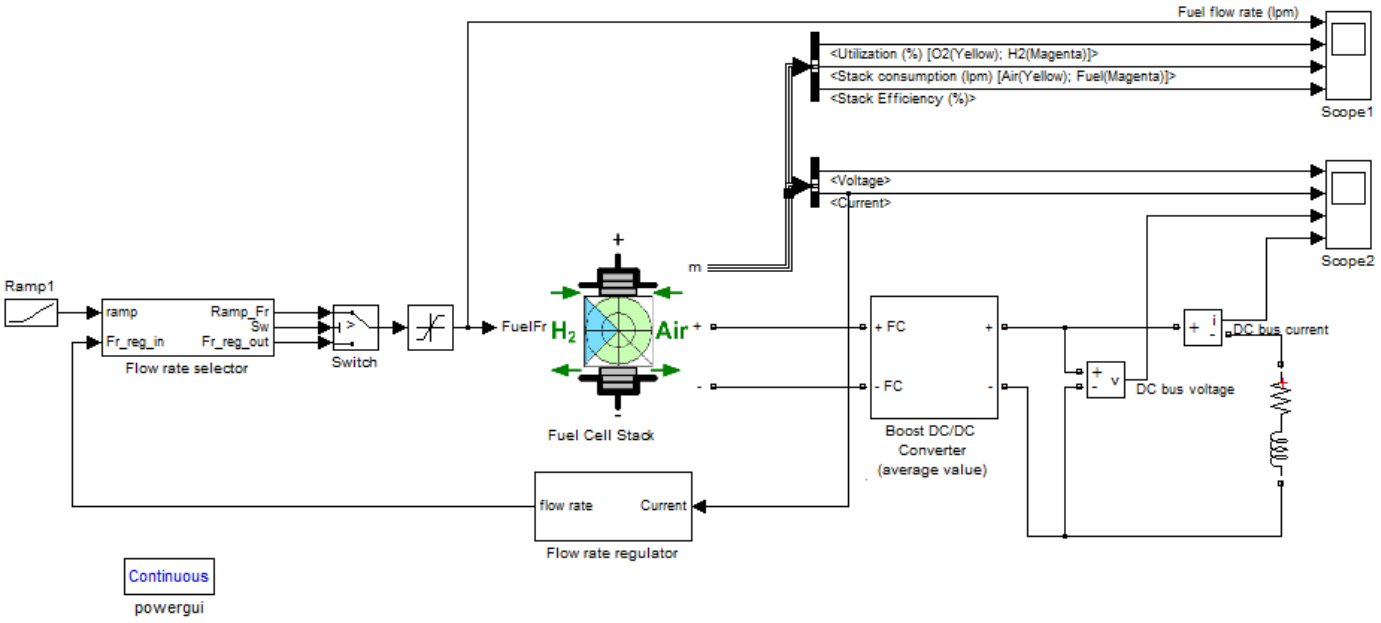

Figure 3.5: The MATLAB/Simscape® model of the PEM fuel cell stake.

Chapter 4

Power Management Strategy

4.1 Introduction

Power systems based on Renewable Energy Sources (RES) offer off-grid energy supply for various applications. These systems contains PV pan The design, analysis and optimization of such systems require the development of mathematical models for all individual components. The proper sizing of the various subsystems is a major challenge that depends on weather conditions at the place of installation, the selected operating policy and of course economic data (e.g., cost of purchase, maintenance, operation and so forth).

Nevertheless, little is reported about the influence that key variables like the operation limits of SOC of the accumulator and the output power of the fuel cell have on the operation time and operation variables (e.g. hydrogen inventory) of the stand-alone power system, but caution was mainly given to the operation of the accumulator as a sensitive subsystem. For example, low SOC_{min} limits (increased depth of discharge, DOD) might lead to increased hydrogen inventory, but at the expense of more intense usage of the accumulator. The identification of such key variables could be used in optimization studies that would take into account the operation costs along with the key variables and guide the designer to suitable decisions on enhancing the performance of the system for an economical and reliable operation.

In the present work, proposed PMS that ultimately aim to ensure the reliable satisfaction of the system load requirement and safeguard the units from undesirable operating conditions. The performance of the entire power system under PMS is then estimated.. The key decision parameters in the PMS are the level of the power provided by the RES and the SOC levels of the accumulator. Also the proposed logical block diagrams are given.

4.2 Power Management Strategy

The main aim for the applied Power Management Strategy (PMS) in the adopted hybrid system is to satisfy the load requirements off grid for home use. The operation of the fuel cell should satisfy the load pattern requirements in terms of duration and power level for the various operation times.

Unfortunately, frequent start-up and shut-down actions for the fuel cell will eventually degrade its performance and possibly reduce its lifespan according to various studies. Therefore, the lead-acid battery becomes an essential component of the system that aims at absorbing the short-term variability of the renewable energy system power generation. On the other hand, the operation cycles that storage capacity undergoes affect its lifespan and subsequently influence the operating and maintenance costs of the entire system, but at lower costs.

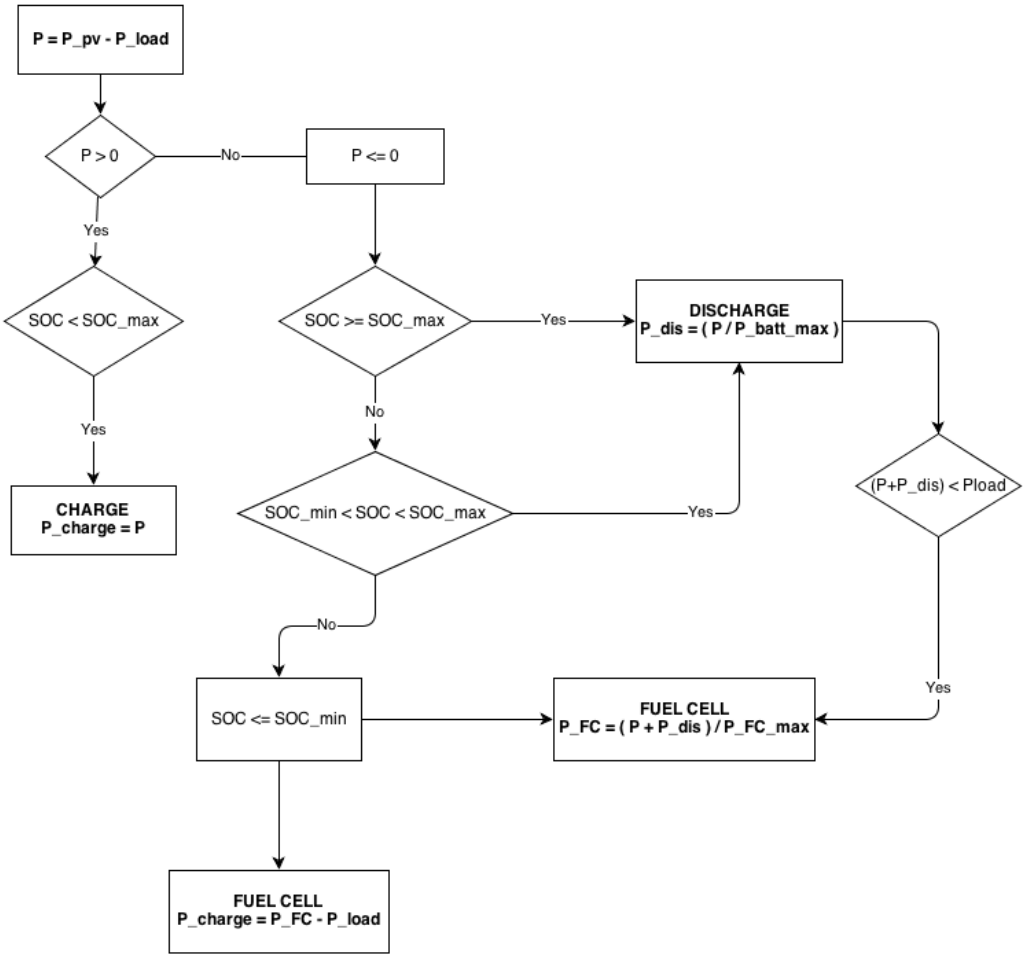

Figure 4.1: Logical block diagram for PMS.

The logical block diagram for PMS is shown in Figure 4.1. It is built on the bases of power sources states and load demand pattern with the priority given to solar energy supply, thus if power difference between solar and load $P \leq 0$, based on instantaneous power supply, then the necessary power to satisfy the load is provided by the lead-acid batteries or the fuel cell. The source of additional power is determined based on the *SOC* of the batteries. If $SOC > SOC_{min}$ then the batteries provides the necessary power to the system. If $SOC \leq SOC_{min}$, then the fuel cell provides the necessary power to meet the total load demand, and the excess power from the fuel cell will charge the batteries. If the batteries work with its maximum power and cannot cover the load demand, also the fuel cell will work together with batteries to cover the load demand. In the case that the output power of the fuel cell is higher than the power deficit, the excess power is sent to the batteries. If $P > 0$ then the excess power is sent to the batteries if $SOC \leq SOC_{max}$.

The adopted PMS is built to provide operating modes under variable weather conditions that would ensure the satisfaction of the power requirements and maintain the operating costs at a reasonable level for the target communities.

4.3 Hybrid System Model

A hybrid solar–Hydrogen energy system consists of Photovoltaic Panels, Fuel cell, battery bank, converter, electrolyser and other accessory devices and cables. In order to predict the hybrid system performance, individual components need to be modeled first as in Chapter 3 and then their mix can be evaluated to meet the load demand.

4.4 System Sizing

Sizing of system is very important to improve the control strategy efficiency and cost, so by using A typical load pattern for home electric power requirements and also a typical solar radiation pattern the control strategy simulated.

4.4.1 Load Demand

A typical load pattern for home electric power requirements is obtained and given in Figure 5.2 in chapter 5. The shown data is the consumed energy during 24/4/2012, the maximum consumed power 4.5kW and average 1.32kW.

4.4.2 Solar Radiation

A typical solar radiation pattern is for one average day at southern Palestinian villages shown in Figure 5.3 in chapter 5. The solar radiation is obtained for 24 hour on 24/4/2012, and the solar radiation average in this daylight (6:30 AM to 19:30 PM) is 0.538 kW/m^2.

4.4.3 PV Sizing

By using Mono-crystalline (efficiency=0.1495) which available in Palestine and it has an acceptance cost.

In the first the area of PV panels is required so:

$$\text{Area of PV} = \frac{E_d}{\eta_{CH} \times \eta_I \times ASR \times \eta_{PV}} \quad (4.1)$$

where :Ed: daily energy consumption

η_{CH}: efficiency of charge control

η_I: efficiency of inverter

ASR: average solar radiation

η_{PV}: efficiency of PV panels

Using Area module mono-crystalline =1.67m^2, the number of modules needed is :

Table 4.2: PV module specifications.

AYAVA SALAR AY Series Monocrystalline

Maximum Power (Wp)	250
Maximum Power Voltage (V)	48.5
Maximum Power Current (A)	5.15
Open Circuit Voltage (V)	58.1
Short Circuit Current (A)	5.58
Size of Module (mm)	1580 × 1058 × 46

4.4.4 Battery sizing

The chosen battery in standalone power system is regular lead acid battery; the efficiency of this technology is about 90%, and their life time is 5 years. In standalone power system batteries are used for daily storage to assist the fuel cell in the peak hours. The battery input power can be positive or negative depending on the charge or discharge mode. The state of charge (SOC) is obtained from the battery power and efficiency

$$SOC_{bat} = \int \left(P_{Bat,charge} \times \eta_{Bat} - P_{Bat,discharge} \right) dt \qquad (4.2)$$

The battery stack has a maximum and a minimum allowable fractional state of charges (SOC_{max} and SOC_{min}) set to 0.8 and 0.4 because of the safety and efficiency reasons .
The battery power is obtained from the equations :

$$P_{Bat} = P_{PV} + P_{FC} - P_{Load} \qquad (SOC \leq SOC_{min}) \qquad (4.3)$$

$$P_{Bat} = P_{PV} - P_{Load} \qquad (SOC > SOC_{min}) \qquad (4.4)$$

Energy daily consumption before losses in charger controller and inverter =1845Wh

$$\text{Battery Power Capacity} = \frac{E_d}{\eta_{CH} \times \eta_I} \quad (4.5)$$

where :Ed: daily energy consumption

η_{CH}: efficiency of charge control

η_I: efficiency of inverter

$$\text{Battery Power Capacity} = \frac{1323}{0.9 \times 0.85} = 1730 \text{ Wh}$$

4.4.5 Fuel Cell sizing

The fuel cells supply the required load when there is not enough solar radiation. Fuel cells use hydrogen as fuel under normal temperature conditions (from 30 to 200 and can work with a pressure of 1 atm). The fuel cell power can be calculated according to the maximum load required. Stack electrical efficiency for commercial fuel cell is about 46%, nominal power is 1.26 KW and operating temperature of fuel cell is 55°C. Life time of fuel cell is about 5000 hours of fuel cell performances.

Table 3.4: Fuel Cell Specification

Fuel cell nominal parameters	
Nominal stack power	1.26 KW
Nominal stack voltage	24.23 V
Nominal stack current	52 As
Nominal stack efficiency	46 %
Operating temperature	55 °C
Number of cells	42

4.5 Simulation of proposed power management

By using the models of each component of system (PV, FC, Battery) which build using SIMULINK/MATLAB software and the control strategy which build using State Flow/MATLAB shown in figure 4.2.

To prove its effectiveness of the proposed power management strategy .The module inputs are the Load Pattern, Solar Radiation Pattern, and the limits of batteries SOC minimum and maximum states. These inputs are evaluated by PMS Control to gives the values of the output powers from each component of the hybrid system (PV, Batteries, and Fuel Cell).

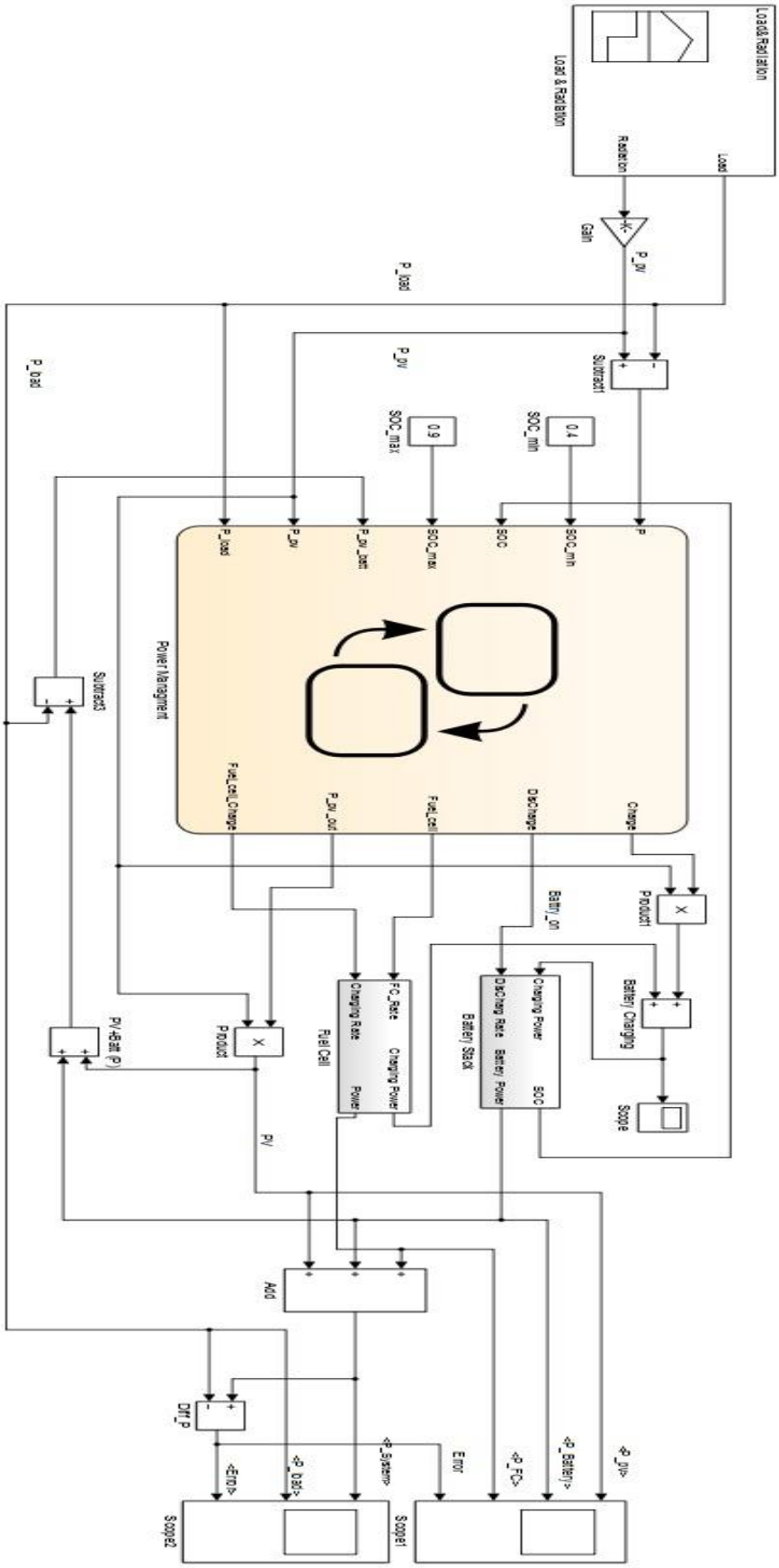

Figure 4.2: Simulink and State Flow model of oriented PMS.

Case 1: Morning (5:00 AM – 11:00 AM)

In this period of day the sun rise and the solar radiation will increase slowly so the batteries will provide the needed low power demand, but when the PV and batteries cannot satisfy the load requirements during the morning hours, the fuel cell will be turn on to compensate the lack of energy supply as shown in Figure 4.3.

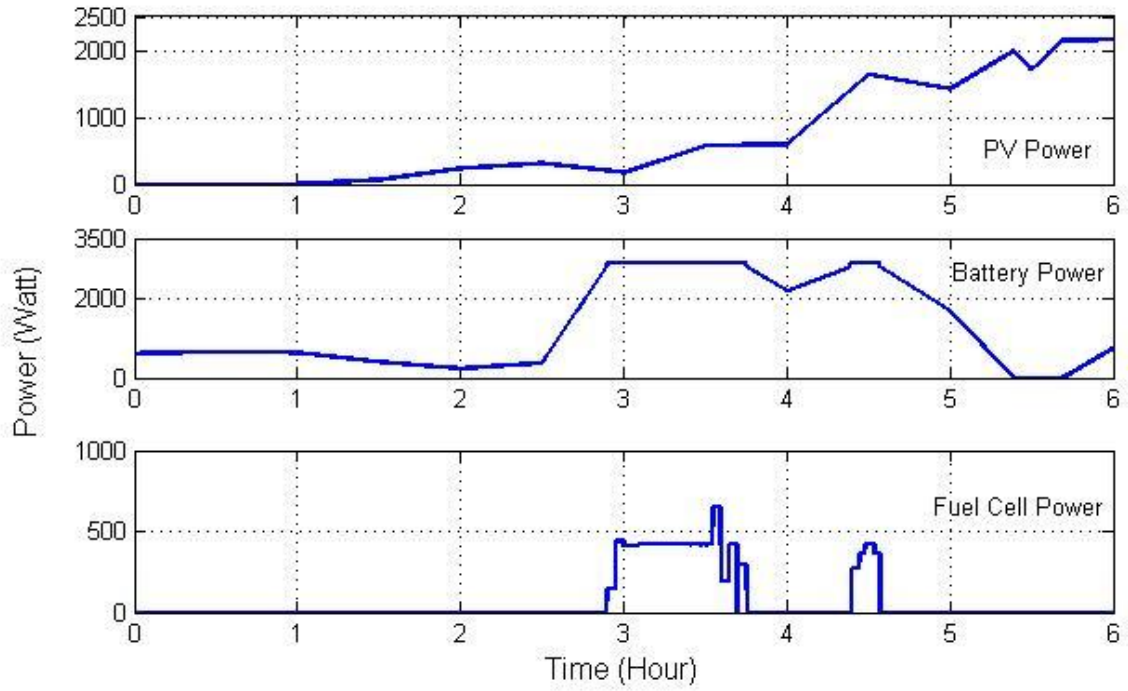

Figure 4.3: PV, Battery, Fuel Cell power Load Power and Error during the morning.

Figure 4.4 also shows the power output from the hybrid system and its values almost matching to the load pattern, the maximum value is about 4.5kW and minimum is about 0.5kW, in addition, the error is very small; approximately 6% at maximum in this period.

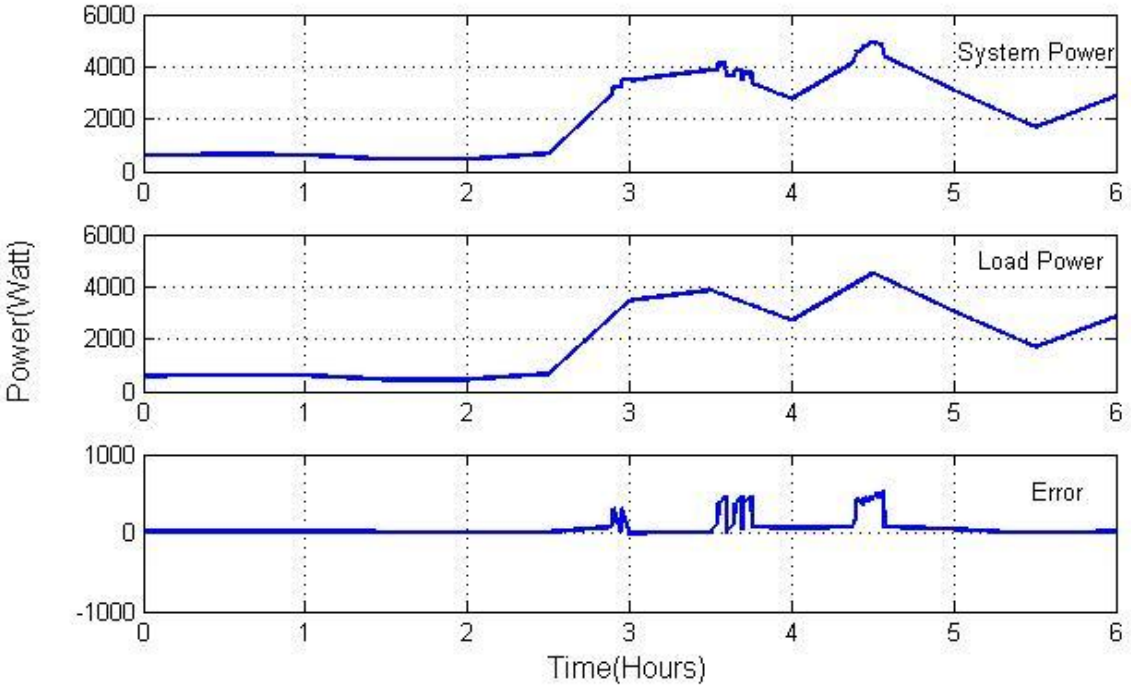

Figure 4.4: System Power, Load Power and Error during the morning

Case 2: Afternoon (10:00 AM – 8:00 PM)

During this period the solar radiation will increase to reach its maximum values. Thus the power output from the PV panels can meet the load demand until the solar radiation decreases at the sunset. The batteries will supply power to give the needed power difference to meet the load as shown in Figure 4.5. During this period the Fuel cell still shutdown, and also the batteries will be charged with exceeds power from PV panels.

As shown in Figure 4.6 the system power is close to the load pattern and so the error is close to zero. But when the Batteries shutdown and the fuel cell operated the error increase for very small of time because of fuel cell response. In this period the output power of system is exactly the same as the load pattern, error is almost zero; this value because the load pattern varying slowly over time.

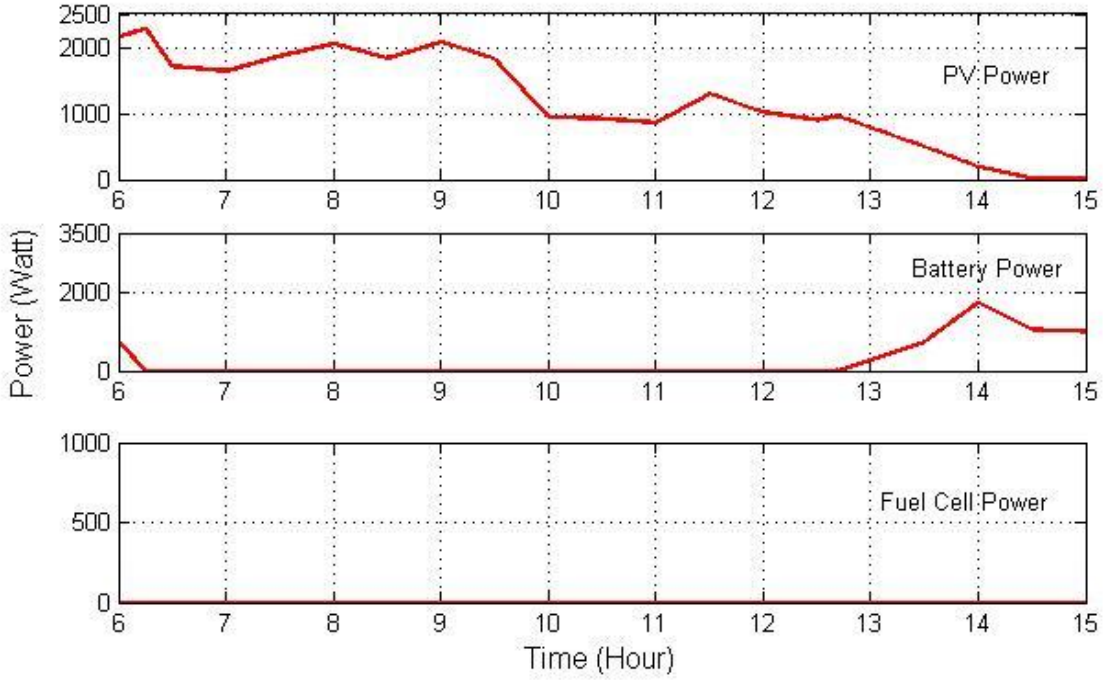

Figure 4.5: PV, Battery, Fuel Cell power Load Power and Error during the afternoon.

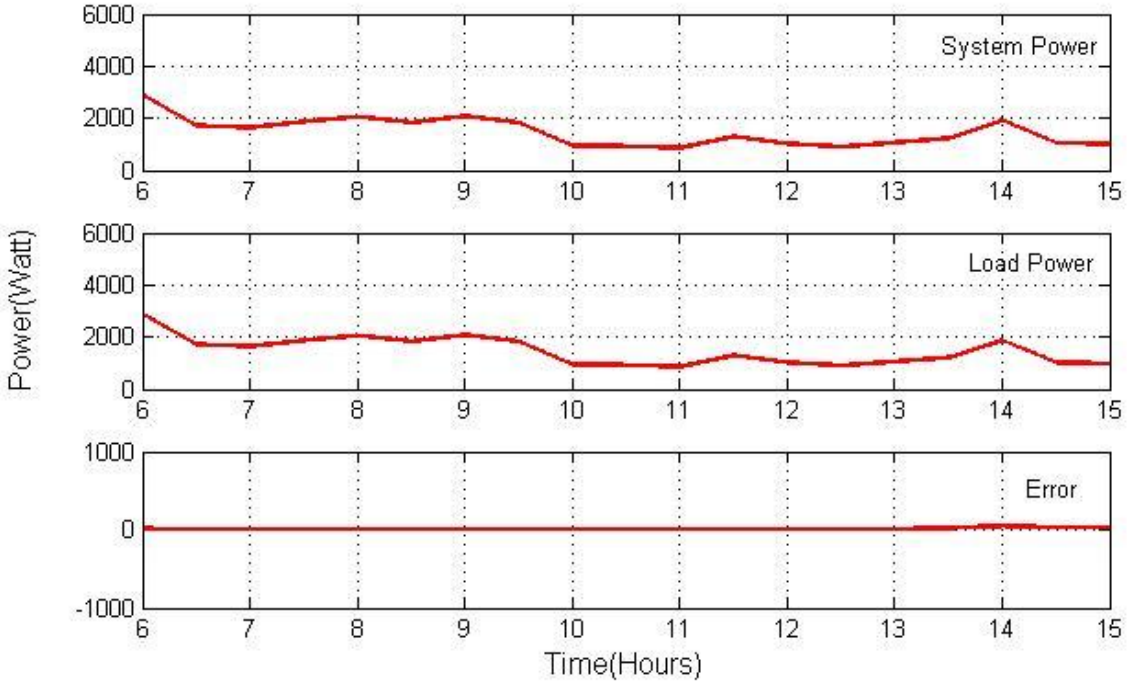

Figure 4.6: System Power, Load Power and Error during the afternoon.

Case 3: Evening (8:00 PM – 5:00 AM)

During this time no sunlight exists, so the PV power output equals zero. The batteries and fuel cell must give the required power to meet the load demand.

In the begging of the evening period the batteries *SOC* > *SOCmin*, thus the batteries gives the needed power until its *SOC* reach *SOCmin*, then the fuel cell is operated to meet the load demand and the excess power will charge the batteries as shown in Figure 4.7.

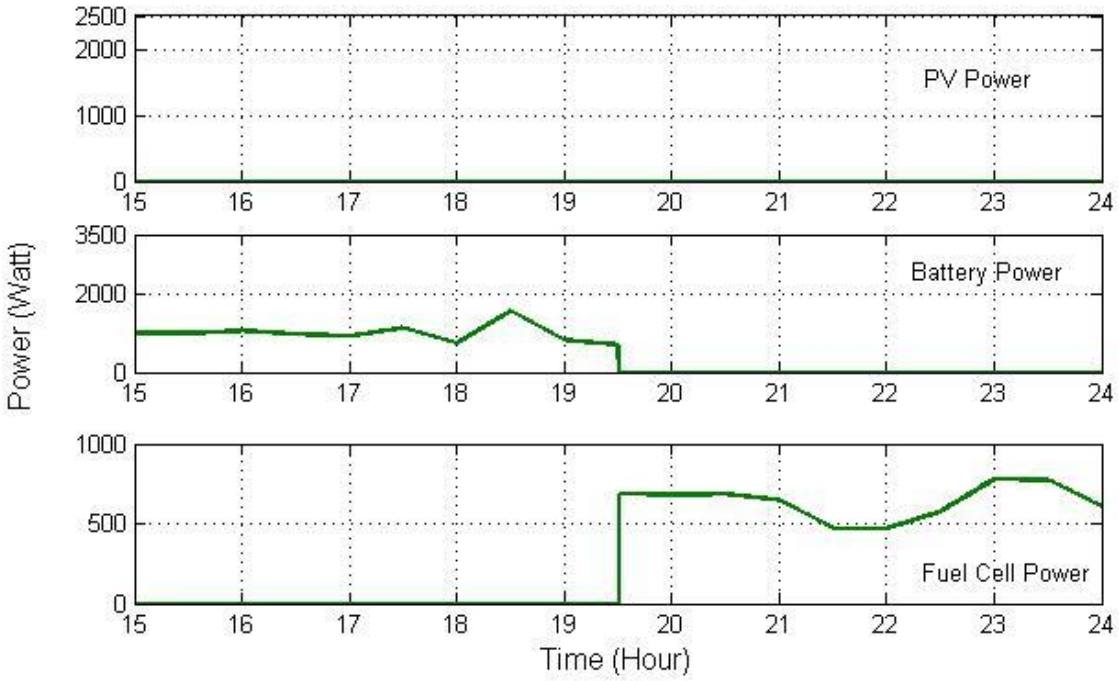

Figure 4.7: PV, Battery, Fuel Cell power Load Power and Error during the evening.

In figure 4.8 The system power is close to the load pattern and so the error is close to zero. But when the batteries are shutdown and the fuel cell work up the error increase for very small of time because of fuel cell response.

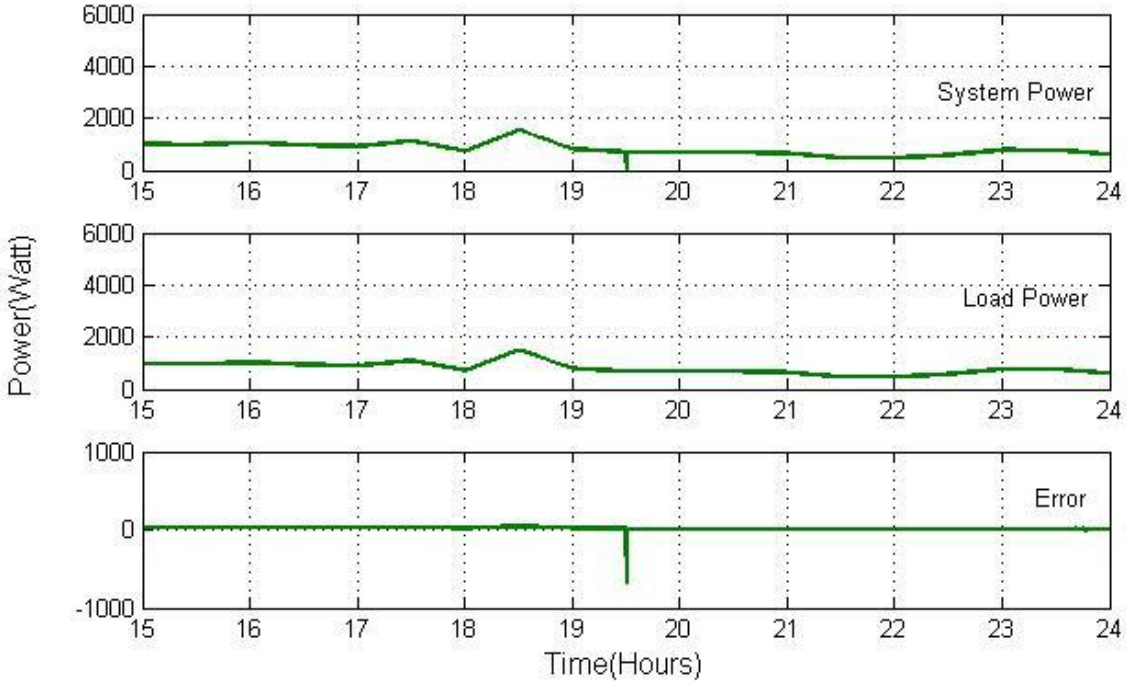

Figure 4.8: System Power, Load Power and Error during the evening.

Chapter 5

Optimization and Sizing

5.1 Introduction

In order to produce electricity for a domestic stand-alone system, the classical solution associating photovoltaic (PV) cells and batteries presents limits when required to feed a system throughout one year cycle. Indeed, the battery and the solar generator have to be over-sized to respond to the critical periods when the solar insulation delivers a very small amount of energy. Currently, most of the systems avoid over-sizing by adding a diesel generator which supplies the load during critical periods. A possible solution consists in adding a proton exchange membrane fuel cell (PEM FC). This kind of fuel cell (FC) has the advantage to produce electricity without greenhouse emissions when the fuel is hydrogen. However, when the fuel is methane, for example, CO_2 emissions are produced. Figure 5.1 show the tow configurations considered in this project.

The configuration in Figure 5.1(a) consists of a PV generator, a battery and a FC fed by hydrogen (H_2) from an external source to supply the system during critical periods (i.e. winter). A second configuration is shown in Figure 5.1(b) that does not use batteries to store energy .

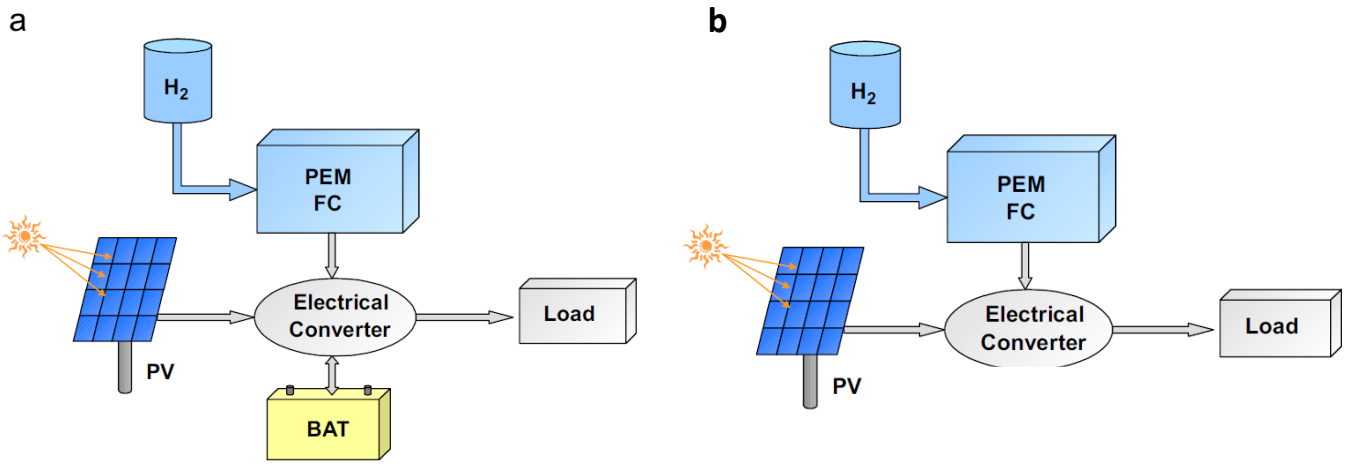

Figure 5.1: Configurations layouts. (a) Configuration 1: PV, battery, FC is fed by an external hydrogen tank; (b) PV, FC is fed by an external hydrogen tank

5.2 System Sizing and Configuration

In order to efficiently and economically utilize the solar-hydrogen hybrid Energy System, an optimum design sizing method is necessary. Various optimization techniques such as the genetic algorithm, ant colony optimization, and simulated annealing method have been recommended by researchers. In this chapter, one optimal sizing model based on Practical Swarm Optimization Algorithm (PSO) for a stand-alone hybrid solar-hydrogen system is developed. The optimization procedure aims to find the configuration that yields the best compromise between the two considered objectives: efficiency and total cost. These configurations can be obtained by an optimization technique such as PSO, which it is generally robust in finding global optimal solutions, especially in multi-objective optimization problems, where the location of the global optimum is a difficult task.

In the next section a traditional method for sizing the system is used and then the sizing is done by PSO algorithm to show the deference between configurations and method of sizing.

5.2.1 Consumption estimation

The first step to size the sources and the other devices is to evaluate the load profile. The chosen profile is presented in Fig. 5.2; the load average power is 1.32 KW which represents an annual energy consumption of 11.6 MWh. This consumption evolution is based on a domestic consumption in a hose at village in south of Palestine.

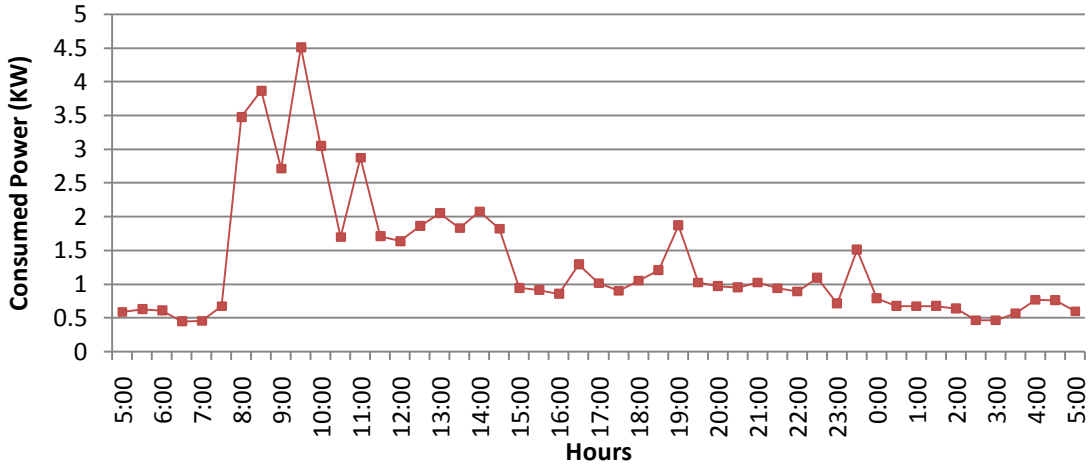

Figure 5.2: Daily load pattern obtained in 24/4/2012.

5.2.2 Solar Radiation Data

A typical solar radiation pattern is for one average day at southern Palestinian villages shown in Figure 5.3. The solar radiation is obtained for 24 hour on 24/4/2012, and the solar radiation average in this daylight (6:30 AM to 19:30 PM) is 0.538 kW/m^2 , On this site, the total annual solar energy received on 1m^2 is about 4.72 MWh. Assuming that a PV generator with polycrystalline technology presents an efficiency of 10%, 472 kWh are annually obtained using 1m^2 PV array.

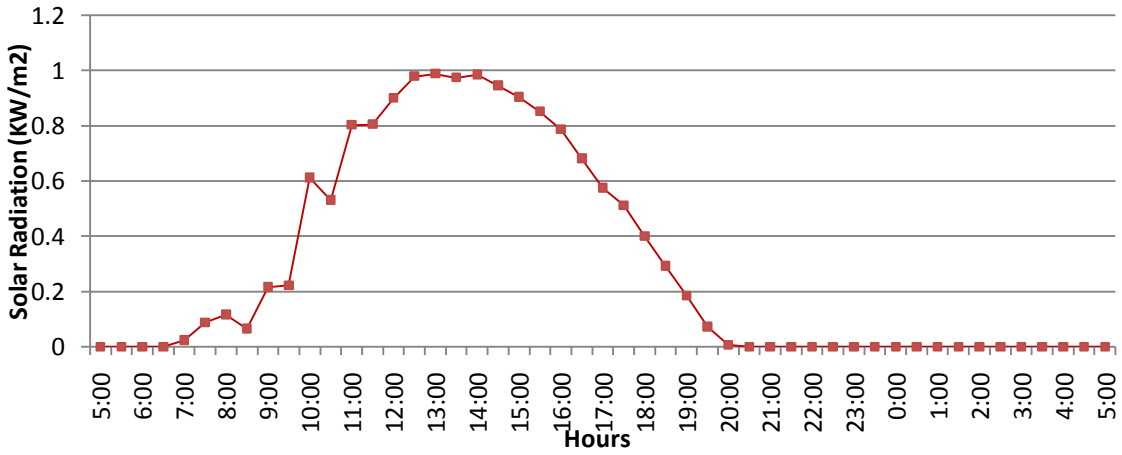

Figure 5.3: Solar radiation pattern obtained on 24/4/2012.

5.2.3 Technology choice

In order to obtain a precise energy cost, the technologies of each device have to be understood. For the FC, a PEM (proton exchange membrane) cell is considered. This kind of FC operates with hydrogen as fuel under normal temperature conditions (from 30 to 200 1C and can work with a pressure of 1 atm. Moreover, this technology becomes commercialized with stack electrical efficiency about 40%.

The chosen battery is a regular lead-acid battery. This technology has a good efficiency, low cost and low self-discharges (less than 5% per month). The main drawback for this battery is its weight, but in a stationary system, that is not important.

The polycrystalline PV cells are currently the best choice in terms of quality and price. They present an efficiency lower than the monocrystalline technology (respectively, about 10–13% compared to 15–22%) but they are cheaper. That is why this technology is commonly used in most of PV systems.

5.2.4 Element sizing

The last step of the sizing is to find the power or capacity of each device. It depends on the considered configuration. Several solutions are available and an optimization is needed. The following section details a first approach, without using optimization but only the analytical relations.

5.3 Sizing using traditional method

5.3.1 First configuration

First, for the configuration number 1 as in Fig. 1(a), the FC power is fixed. FC net power can be equal to the load average power (1.32 KW). The load surplus is generated by another device (PV if available or battery). Considering that the FC auxiliary systems need about 20% of the net power (for cooling and air pressurization), it is necessary to use a 1.6 KW FC gross power.

The PV surface can be easily calculated assuming that solar generator delivers the whole energy consumed.

$$SPV = \frac{E_{consumed \ \ on\ 1\ year}}{E_{produced \ \ on\ 1\ year\ \ with\ \ 1m^2}} \tag{5.1}$$

$$=11600/472 = \mathbf{24.5\ m^2}$$

This surface represents a 2450 W peak PV panel.

For battery sizing we use Energy daily consumption before losses in charger controller and inverter which equal 1323 Wh

$$\text{Battery Power Capacity} = \frac{E_d}{\eta_{CH} \times \eta_I} \tag{5.2}$$

where :Ed: daily energy consumption

η_{CH}: efficiency of charge control

η_I: efficiency of inverter

Battery Power Capacity =1323/0.9*0.85=1730Wh

The cost of 20 year life time of the system is calculated using equations (5.5 and 5.6) and variable of table 5.1 and equal **473649 $**.

5.3.2 Second configuration

As in the first configuration, FC power has to be determined first. In this configuration shown in Figure 5.1(b), the FC must be able to supply the load all by itself. So, the FC net power is 4.5 KW (load maximum power) and considering auxiliary systems consuming 20% of this power, the gross power is 5.4 KW.

The PV surface can be easily calculated assuming that solar generator delivers the whole energy consumed Equation (5.2).

=11600/472

= 24.5 m^2

This surface represents a 2450 W peak PV panel.

The cost of 20 year life time of the system is calculated using equations (5.5 and 5.6) and variable of table 5.1 and equal **1103153 $**.

5.4 Optimization Using Particle Swarm Algorithm

5.4.1 PSO Algorithm

Particle Swarm Optimization (PSO) is an approach to problems whose solutions can be represented as a point in an n-dimensional solution space. In this approach a number of *particles* are randomly set into motion through this space. At each iteration, each particle keeps track of previous best position and the best particle in the swarm. The previous best value is the best solution it has achieved so far. This value is called *pbest*. Another "best" value that is tracked by the PSO is the global best value, obtained so far by any particle in the population. This best value is called *gbest* .The new velocity and positions of each particle are dynamically updated by the following equations :

$$v_{id}(t+1) = \omega v_{id}(t) + c_1 r_1\big(pbest - x_{id}(t)\big) + c_2 r_{12}\big(gbest - x_{id}(t)\big) \tag{5.3}$$

$$x_{id}(t+1) = x_{id}(t) + v_{id}(t+1) \tag{5.4}$$

Where the acceleration coefficients and are two positive constants; is an inertia weight and is a uniformly generated random number from the range [0, 1] which is generated every time for each iteration. Proper control of global exploration and local exploitation is crucial in finding the optimum solution efficiently to PSO algorithm. Equation (5.3) shows that, when calculating the new velocity for a particle, the previous velocity of the particle (v_{id}), their own best location that the particles have discovered previously (x_{id}) and the global best location all contribute some influence on the outcome of velocity update. The global best location is identified, based on its fitness, as the best particle among the population. All particles are then accelerated towards the global best particle as well as in the directions of their own best solutions that have been visited previously. While approaching the current best particle from different directions in the search space, all particles may encounter by chance even better particles en route, and the global best solution will eventually emerge. The inertia weight is critical for the convergence behavior of PSO. A suitable value for the inertia weight usually provides balance between global and local exploration abilities and consequently results in a better optimum solution. To balance between global and local exploration abilities, inertia weight is adjusted dynamically to control the process of algorithm. Due to the lack of knowledge of the searching process, it is very difficult to design a mathematical model to adapt this parameter dynamically. Hence the fuzzy adaptive PSO is proposed to design a fuzzy system, which dynamically adapts the inertia weight for the optimal sizing method of solar-hydrogen hybrid energy system. Typical inertia weight value is $0.3<\omega<1$. Both positive and negative corrections are required for the inertia weight. Therefore, a range of -0.1 to 0.1 has been chosen for the inertia weight correction.

5.4.2 Objective Function

The aim of this chapter is to achieve a standalone power system optimization with PSO algorithm; algorithm output includes the number of required components such as the number of PV panels, fuel cells and battery capacity. The number of components should be optimized so that the system required load can be supplied with high reliability.

For sizing optimization, in addition to minimizing components generation and maintenance costs, it is so important to store enough energy in the hydrogen tank and batteries to use in critical periods .

The function that must be optimized is the system performance and system costs in 20 years which includes capital cost and also maintenance and operation costs.

This function is defined as a summation of system component cost such as PV panels cost (f_{PV}), battery cost (f_{BAT}) and FC cost (f_{FC}), we assume that the hydrogen is available and don`t calculate its cost in the system.

$$f(x) = f_{PV} + f_{BAT} + f_{FC} \begin{Bmatrix} f_i = N_i \times [C_i(Y_i + 1) + M_i(20 - Y_i + 1)] \\ i = BAT\ , PV\ , FC \end{Bmatrix} \quad (5.5)$$

Where N_i is the number/size of the system component; C_i is the capital cost, M_i is operation and maintenance cost and Y_i the number of replacement in the system life time .

The proposed system optimization parameter should be within certain range

$$X = [N_{PV} + N_{BAT} + N_{FC}] \quad (5.6)$$

$$N_{PV}, N_{BAT}, N_{FC} > 0$$

System shown in fig 5.1(b) does not use battery therefore in the objective function $f_{BAT} = 0$. To achieve the high reliability in the system it is necessary the supply load by system being greater than the load required, i.e. . In the critical period and also early morning hours, the required load is supplied by batteries and fuel cell, therefore battery energy at the end of the day (in normal condition) should be equal or greater than the battery energy at the beginning of the day.

The cost of system components can be seen in Table (5.1).

Components	Life Time	Capital Cost($)	Replacement and maintenance Cost ($/year)
PV Panel	20 years	4.84($/Wpeak)	3
Fuel Cell	5000 Hours	8($/W)	6($/W)
Battery	5 years	20($/KWh)	0

5.4.3 Results:

The optimization model is a simulation tool to obtain the optimum size or optimal configuration of a hybrid solar–hydrogen system by using a PSO algorithm. An initial swarm of 10 chromosomes, comprising the 1st generation, is generated randomly and the

constraints are evaluated for each chromosome. If any of the initial population chromosomes violates the problem constraints then it is replaced by a new chromosome, which is generated randomly and fulfills these constraints. With the optimization of configurations shown in figure 5.2(a) and 5.2(b), the cost are estimated and presented in Table (5.2). The second configuration shown in figure 5.2(b) is more costly than configuration shown in figure 5.2(a), because this configuration uses only the hydrogen storage for critical periods, because of lower efficiency of hydrogen storage compare to combination of hydrogen and batteries storage, the second configuration need more PV panels to produce more energy for maintaining high reliability. Furthermore the fuel cell is also more powerful to supply required power when there is not enough radiation and this causes decreasing the fuel cell life time, therefore the fuel cell cost also increases.

The Matlab code used for PSO submitted in Appendix A.

Table 5.2 : Details of optimization

Configuration	System 5.1(a)	System 5.2(b)
PV Panel Power	2740 W	3154 W
Fuel Cell Power	1600 W	5000 W
Fuel Cell operation hours	11.7	10.1
Battery Capacity	1027 Wh	0
Total Cost($)	**361280**	**822140**

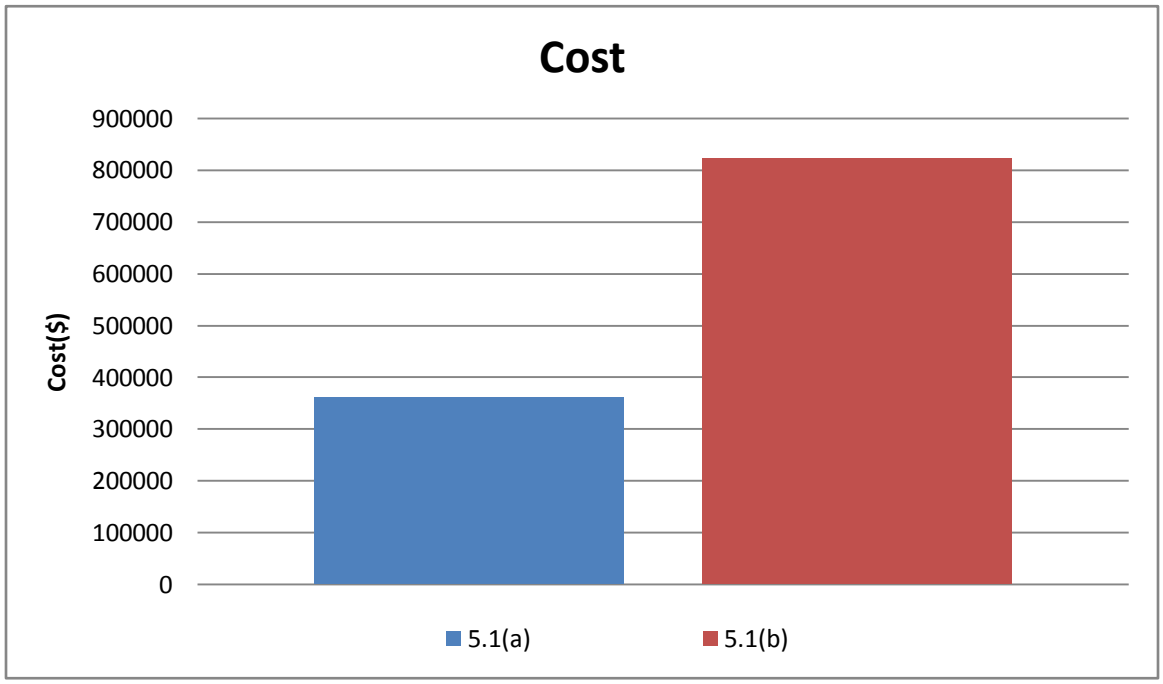

Figure 5.4: Cost comparison of two configurations

Chapter 6

Experiments and results

6.1 Introduction

In this part the project team built a hybrid system prototype using The HELEx Solar and Hydrogen Fuel Cell Trainer Add-in Module for NI ELEVIS shown in Figure 6.1 so the project team make many experiments on system components to understand the process of parts in the stand alone power systems, and to be familiar with using the solar cells, electrolyzer, fuel cells and to understand its behaviors in real systems.

Then the project team build the hybrid system and use its green energy sources to supply current to the load, by using Matlab/SIMULINK software and XPC target library to keep the voltage in the system with 1.2V to simulate the house devices voltage which is 220V.

Figure 6.1: The Emona HELEx Add-in Module along with kit components.

6.2 Emona HELEx Add-in Module

The experiments possible with the EMONA HELEx board bring together the worlds of the electromagnetic, electrical and chemical. We are able to explore, in a hands-on manner, the actions of photons, electrons and molecules upon each other. We are reminded of the interconnectedness of these complementary systems and the universal principles of

conservation of energy. Through measurements, calculations and observations we are able to consolidate our understanding of these processes.

The HELEx board customizes the instrumentation available on the NI ELVIS to create many experiment-specific instruments which can be used with the additional solar cell, electrolyzer, fuel cell equipment provided.

As well the ability to programmatically control, measure and automate our measurements using Lab VIEW brings us closer to real-world practices of system control and monitoring.

The EMONA HELEx Solar-Hydrogen Fuel Cell Experimenter (ETT-411) provides an abundance of opportunities to learn and practice experimental methodology in various fields including electrical and chemical energy.

The main EMONA HELEx equipments :

1. **The Electrolyzer** :

The HELEx Electrolyzer is used to create hydrogen and oxygen gas by decomposing water into its constituent parts, being oxygen and hydrogen. Only distilled water may be used. Only the HELEx Solar Cells or HELEx Constant current source may be used as the source of electricity to operate the Electrolyzer.

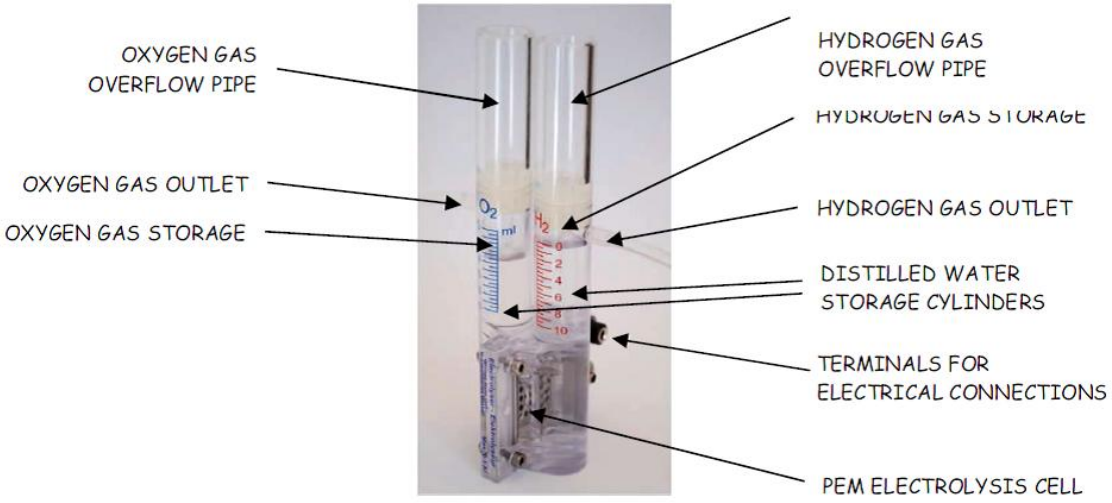

Figure 6.2: parts of the PEM electrolyzer.

The PEM electrolyzer uses a proton conducting polymer membrane coated with catalyst material on either side as the central component. PEM electrolyzer can have efficiencies of up to 85%.

Basic specifications:

Type: polymer electrolyte membrane (PEM) electrolyzer.

Filling liquid distilled water only.

Power consumption: 800 mW maximum.

Required voltage: 1.4 to 1.8 V DC.

Maximum current: 0.5A DC.

Output terminals: oxygen tube terminal and hydrogen tube terminal.

Rate of hydrogen production: 3.5ml/min (at 0.5A DC)

Consumption of distilled water: 0.1ml/h (at 0.3A)

Dimensions: 85×65×35 mm.

2. Hydrogen Fuel Cell-PEM fixed

The HELEx Hydrogen fuel cell uses an electrochemical process to directly generate electricity from hydrogen and oxygen. This fuel cell is classified as a PEM type fuel cell.

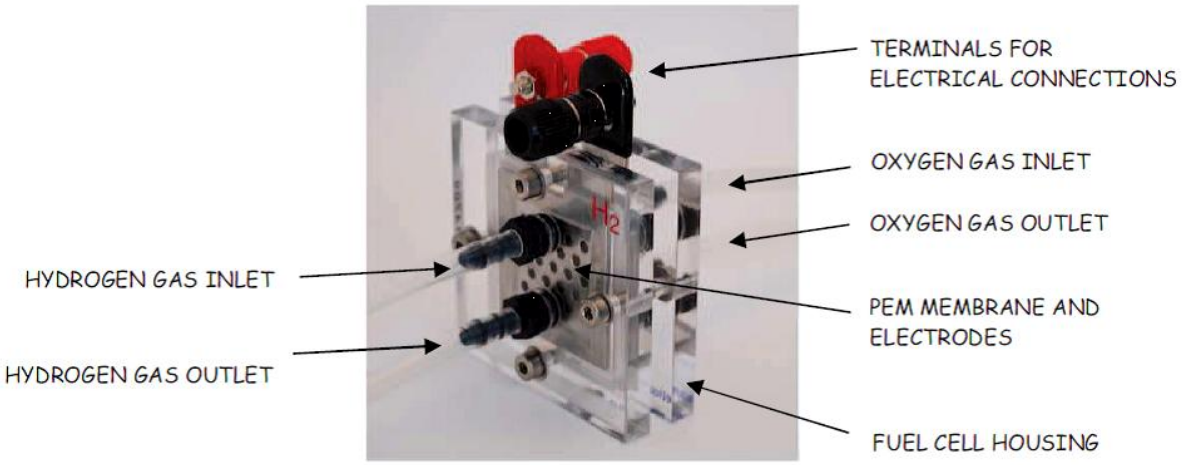

Figure 6.3: Parts of the PEM hydrogen fuel cell.

Basic specifications

Type: Polymer electrolyte membrane (PEM) hydrogen fuel cell

Membrane catalyst material: 0.4mg/cm^2 Pt

Input terminals 2× oxygen tube terminals and 2× hydrogen tube terminals.

Rate of hydrogen consumption: 7ml/min (at 1.0A DC)

Voltage output: 0.4 to 1.0V DC.

Output power: 0.5 W

Dimensions: 85×65×35mm

3. Hydrogen fuel cell-dismantlable

This fuel cell allows the user to vary particular fuel call parameters: catalyst density and oxygen concentration.

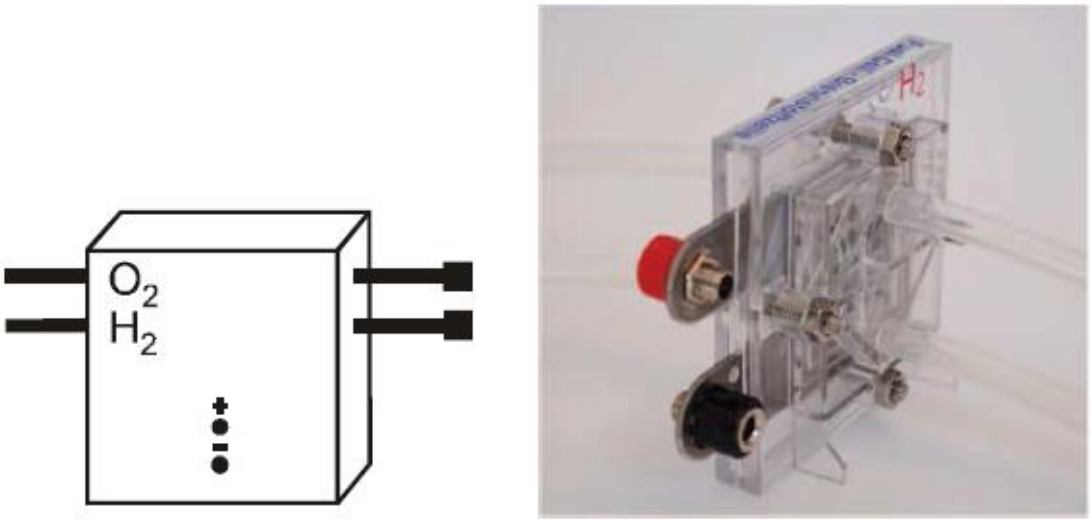

Figure 6.4: Dismantable hydrogen fuel cell.

Basic specifications:

Type: PEM hydrogen fuel cell.

Membrane catalyst material: 0.4mg/cm^2 Pt.

Input terminals: 2× oxygen tube terminals and 2× hydrogen tube terminals.

Rate of hydrogen consumption: 7ml/min (at 1.0A DC)

Voltage output: 0.4 to 1.0V DC.

Current output: 1.3A DC with air supply; 2.0A with oxygen supply.

Output power: 0.6 W

Dimensions: 85×65×65mm.

4. Resistive DC Load

The HELEx board provides a variable resistance or load, called Programmable Load, that is both manually adjustable via the board and controllable via NI Lab View from HELEx soft front panel (SFP) in a variety of ways.

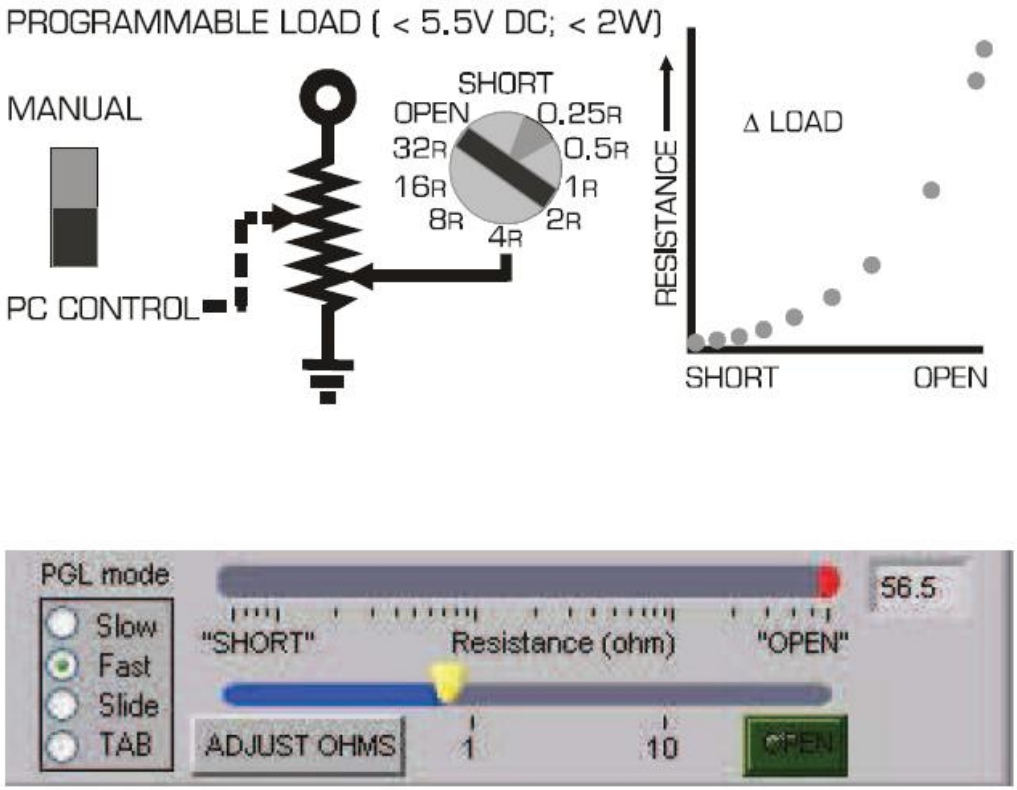

Figure 6.5: HELEx Programmable Load.

Basic specifications (HELEx board and SFP)

Operation: manual (rotary switch) and programmable under NI LabView VI control.

Load circuit one input with load resistance to Ground.

Resistance (Load) Values:

Manual control: 10 steps- 0, 0.25, 0.5, 1, 2, 4, 8, 16 and 32 ohms, open circuit.

Programmable control: 240 steps-0 to 60 ohms in 0.25 ohms step, and open.

Tolerances: 0.25±30%, other values ±10%.

Maximum allowable Input signals: <2W, <5.5V DC, DC voltage only.

Display on HELEx board: 10 LEDs.

Display on HELEx SFP: digital readout

5. Solar Photovoltaic Cells:

Two solar panels are included in the HELEx kit. Each panel will output a DC voltage when the panel is illuminated by either sun light or the Lamp. Each solar panel includes 5 silicon cells, permanently connected in series.

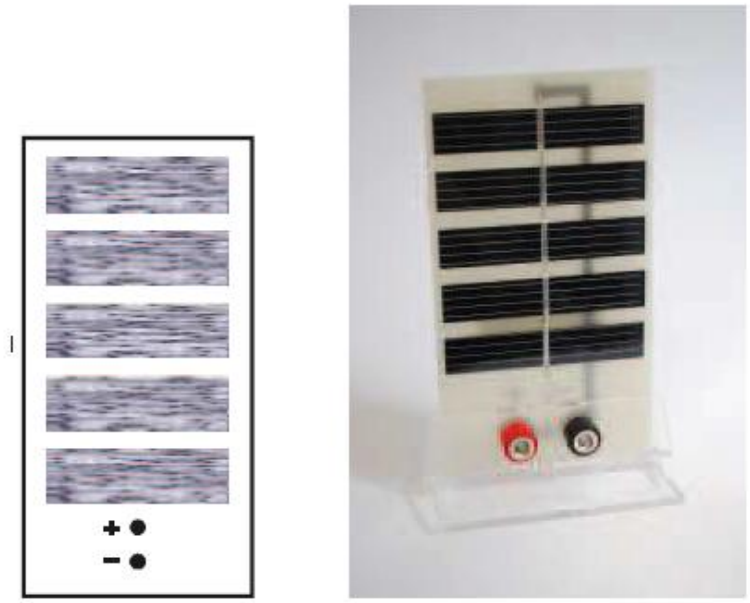

Figure 6.6: HELEx solar cell.

Basic specifications:

Number of cells per module: 5 silicon cells, series.

Voltage at Maximum power Point: 2.4V DC.

Current at maximum power point: 200mA DC.

Power output: 0.48W

OPV cell area: 37.2cm^2 (12×62mm×5)

V_{OC} = 2.8V, I_{SC} =250mA at 1000W/m^2 incident power.

Module Dimensions: 80×135×52mm.

Also the EMONA HELEx Solar-Hydrogen Fuel Cell Experimenter contains many other tools like: two current meters, two voltage meters, current source, voltage source, diodes, and timer.

6.3 Experiments and results of components

6.3.1 Solar photovoltaic cell experiments

1. Maximum power point (MPP) and fill factor (FF)

By take measurements of the solar cell's output current and voltage for various load resistance then we can determine the cell's output power (P=V×I).

Table 6.1: I-V-P data vs load for solar cell

Load (Ω)	Voltage (V)	Current (mA)	Power (mW)
Short-circuit	0	64.8	0
0.25	0.55	64	35.2
0.5	0.57	63.2	36.024
1	0.61	64.2	39.162
4	0.82	65.2	53.464
8	1.07	64.2	68.694
16	1.53	61.8	94.554
32	2.12	52.2	110.664
Open-circuit	2.67	0	0

From Table 6.1:

V_{OC} = 2.67V, I_{SC} = 64.8mA

Maximum power point (MPP) = 110.664 mW.

Current at MPP = 52.2 mA, Voltage at MPP = 2.12 V

Fill factor (FF) = MPP/ V_{OC}× I_{SC} = 0.6396

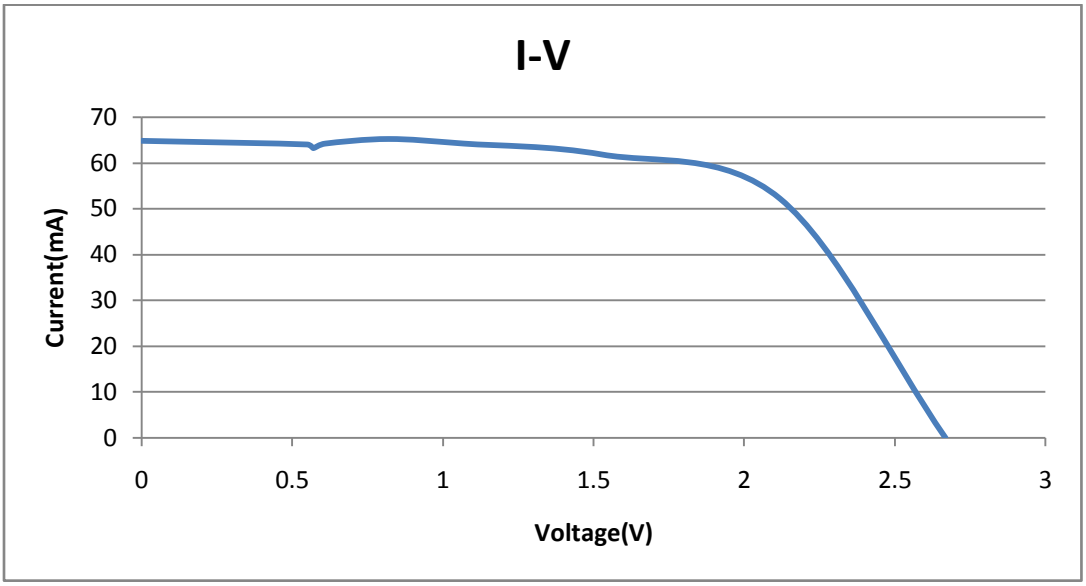

Figure 6.7: Solar cell I-V curve from Table 6.1.

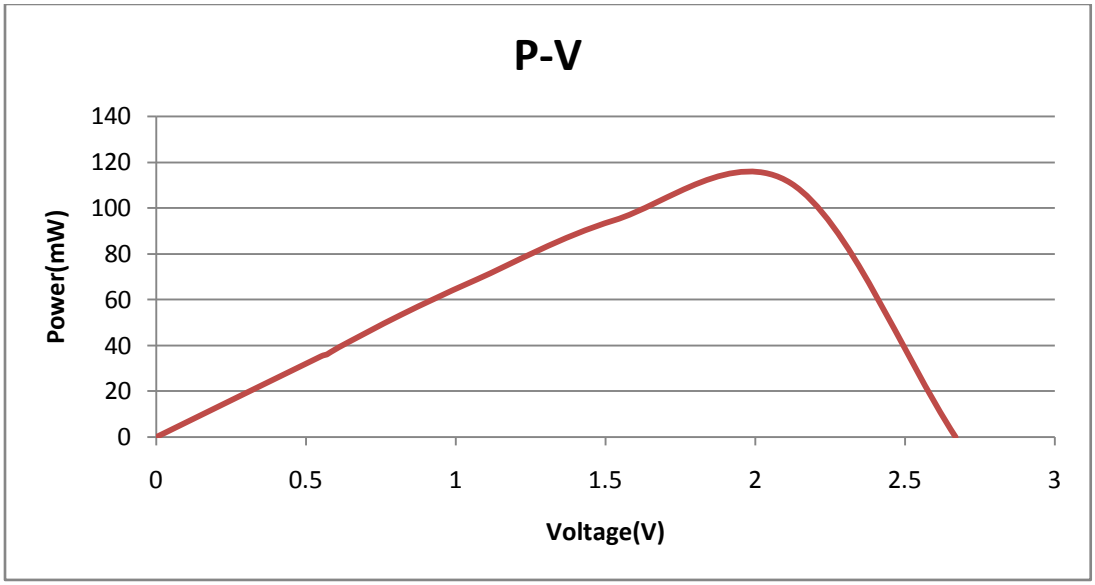

Figure 6.8: Solar cell P-V curve from Table 6.1.

2. Series and parallel connection load curves

a. Parallel connection:

Table 6.2: I-V-P reading versus load for parallel connection

Load (Ω)	Voltage (V)	Current (mA)	Power (mW)
Short-circuit	0	115	0
0.25	1	113.5	113.5
0.5	1.02	113.2	115.464
1	1.08	112.2	121.176
2	1.18	116	136.88
4	1.4	111.2	155.68
8	1.78	106.2	189.036
16	2.21	89.5	**197.795**
32	2.43	55.9	135.837
open-circuit	2.62	0	0

From Table 6.2 we can plot the I-V and P-V curves of series connection Fig. 6.9.

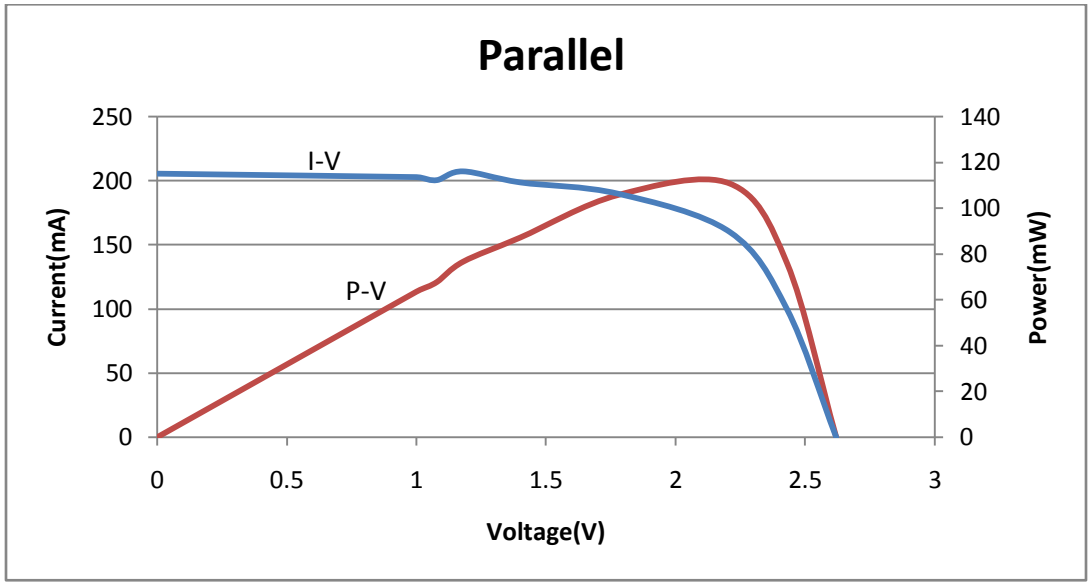

Figure 6.9: Parallel connection P-I-V curve from Table 6.2.

b. Series connection

Table 6.3: I-V-P reading versus load for series connection

Load (Ω)	Voltage (V)	Current (mA)	Power (mW)
Short-circuit	0	54	0
0.25	0.46	53.9	24.794
0.5	0.48	53.8	25.824
1	0.51	53.5	27.285
2	0.57	53.8	30.666
4	0.68	53.1	36.108
8	0.89	53.6	47.704
16	1.3	52.8	68.64
32	2.08	51	**106.08**
Open-circuit	5.26	0	0

From Table 6.3 we can plot the I-V and P-V curves of series connection Fig. 6.10.

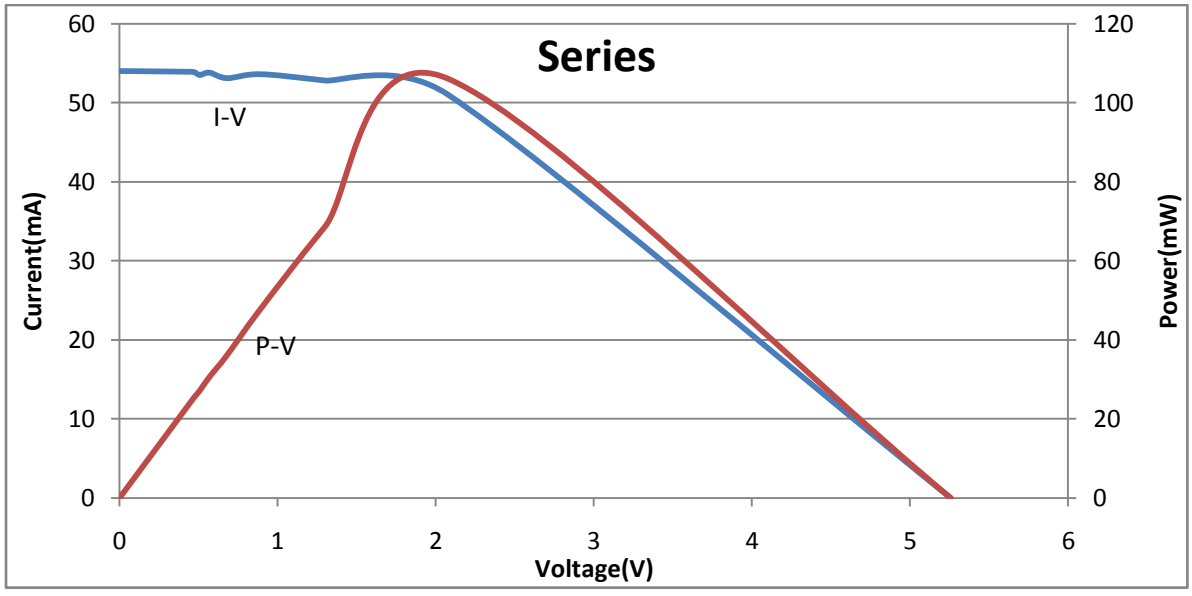

Figure 6.10: Series connection P-I-V curve from Table 6.3.

6.3.2 PEM electrolyzer

Energy efficiency of the electrolyzer:

Table 6.4: Time for 10ml H_2(s) : current(mA) :Voltage (V)

time for 10ml H_2 (s)	current (mA)	voltage (V)	
305	246	1.8	
308	246	1.78	
305	247	1.77	
306	247	1.77	
306	**246.5**	**1.78**	**Average**

The energy efficiency of the electrolyzer is the ratio between the energy constant of the hydrogen generated and the electrical energy used to create that hydrogen.

The energy relapsed when one mole of hydrogen gas is burned under the usual room conditions is 286 KJ.

1 mole of hydrogen gas has volume of 24,000 ml at normal room temperature (25^{o}C) and pressure (1atm).

Electrical energy : $E_{el} = V \times I \times t = 1.78 \times 0.2465 \times 306 = 134.264$ J

Energy relapsed by burning the 10 ml of hydrogen is :

$$E_h = 10/24000 \times 286000 = 119 \text{ J}$$

Efficiency(η) = $E_h / E_{el} \times 100\% = 119/134.264 \times 100\% =$ **88.63 %**

6.3.3 PEM Fuel cell

a. Fuel cell characteristics curve:

Table 6.5: V-I-P-t Fuel cell data vs load.

Load (Ω)	Time(sec)	Voltage(V)	Current(mA)	Power(mW)
Open circuit	20	0.861	0	0
32	40	0.786	24	18.864
16	59	0.757	46	34.822
8	79	0.717	87	62.379
4	99	0.66	156	102.96
2	119	0.578	260	150.28
1	138	0.474	387	183.438
0.5	158	0.346	543	187.878
0.25	179	0.223	695	154.985
Short-circuit	199	0.05	856	42.8

From Table 6.5 we can plot the characteristics curve of fuel cell Fig. 6.11.

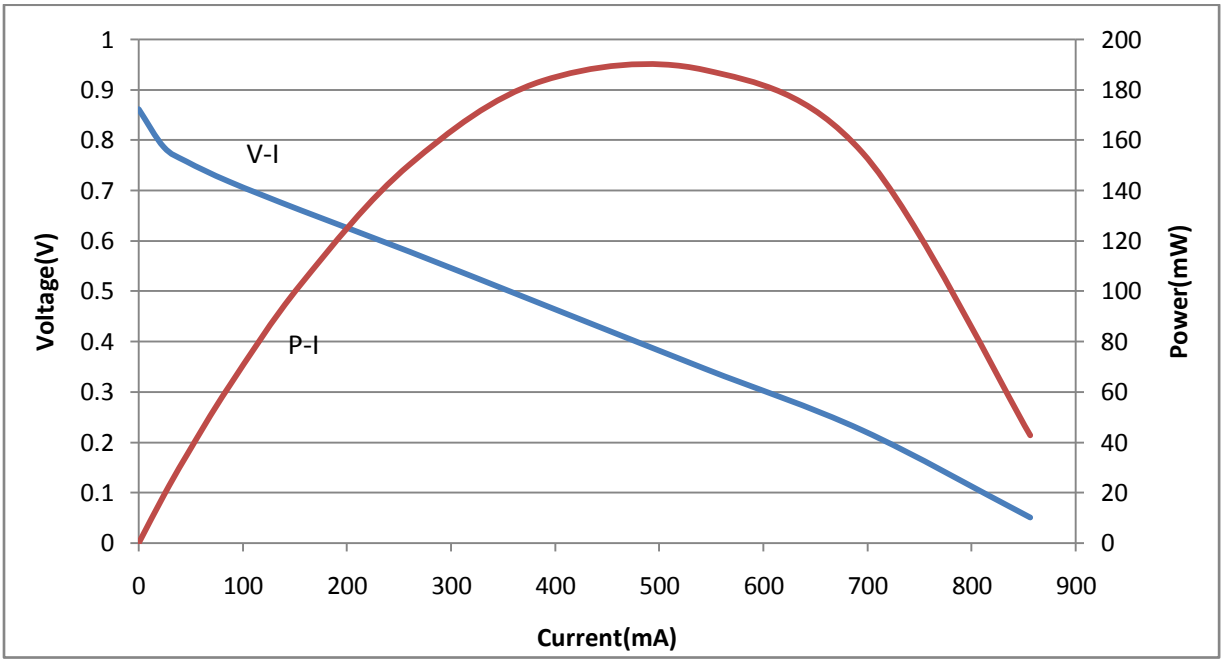

Figure 6.11: P-I and V-I fuel cell characteristics curves

b. Fuel cell energy efficiency

In this experiment we aim to calculate the maximum efficiency of the PEM fuel cell so we get the needed data to calculate the efficiency at deferent points.

$$Fuel\ cell\ energy\ efficiency\ (\eta) = \frac{Electrical\ energy\ E_{el}}{Energy\ of\ the\ hydrogen\ E_h} \times 100\%$$

The energy released when one mole of hydrogen gas is burned under the usual room conditions is 286KJ. And on mole of hydrogen has a volume of 24,000 ml at room condition, so the energy released by burning the 10ml of hydrogen is:

$$E_h = \frac{10}{24{,}000} \times 286{,}000 = 119\ J$$

Electrical energy is calculated using the following equation:

$$E_{el} = V \times I \times t$$

Where V, is the fuel cell voltage, I, the fuel cell current and t is the time needed to use the 10ml of hydrogen by the fuel cell.

Data and results:

Table 6.6: Energy efficiency of the fuel cell.

Load (Ω)	Time (sec)	Voltage (V)	Current(mA)	Volume (ml)	Efficiency(%)
30	1580	0.760	26	10	**26.24**
20	1300	0.712	35	10	**27.22**
17	1140	0.710	42	10	**28.57**
15	1050	0.760	49	10	**32.86**
12.5	880	0.713	57	10	**30.05**

As we can see in Table 6.6 the maximum efficiency of the fuel cell is **32.86%** at load of 15Ω, the efficiency is depend on the cell temperature, when the project team do this experiment the temperature was low respect to temperature of calculated values of fuel cell in the world so this value is agree with PEM fuel cell efficiencies that is in the range of 40-60% at 80^{o}c.

6.3.4 Batteries

In this experiment the charging the battery stake curve will plotted, the stack contains of two AA NI-Metal rechargeable batteries connected in parallel to increase the capacity.

Table 6.7 : Charging of battery stack data.

Time (sec)	voltage(V)	Time (sec)	voltage(V)
0	0.845	220	1.06
10	0.93	240	1.08
20	0.94	260	1.09
40	0.945	280	1.11
60	0.957	300	1.12
80	0.968	320	1.14
100	0.984	340	1.15
120	0.998	360	1.16
140	1.02	380	1.18
160	1.02	400	1.19
180	1.04	420	1.2
200	1.05	800	1.23

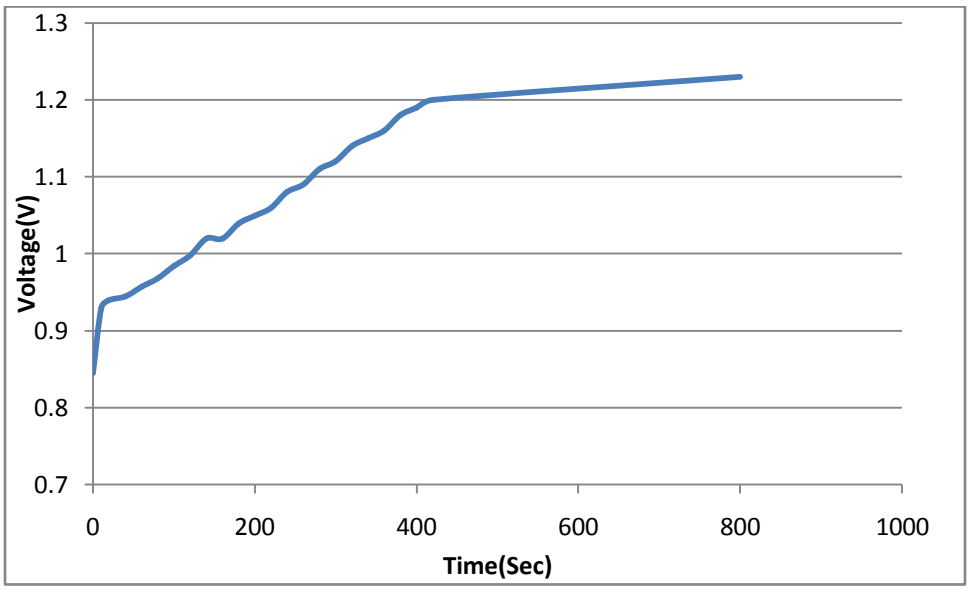

Figure 6.12: Charging curve of battery stack connected in parallel.

6.4 Prototype Building

6.4.1 SIMULINK model

For the purpose of this project, a lab built a prototype using the HELEx Solar and Hydrogen Fuel Cell Trainer Add-in Module for NI ELEVIS. SIMULINK model is developed to keep the scaled system output voltage around 1.2 Volt for variable resistance load to simulate the home electricity, which should be constant around 220 Volt and the current will change according to the load, this module shown in Figure 6.13.

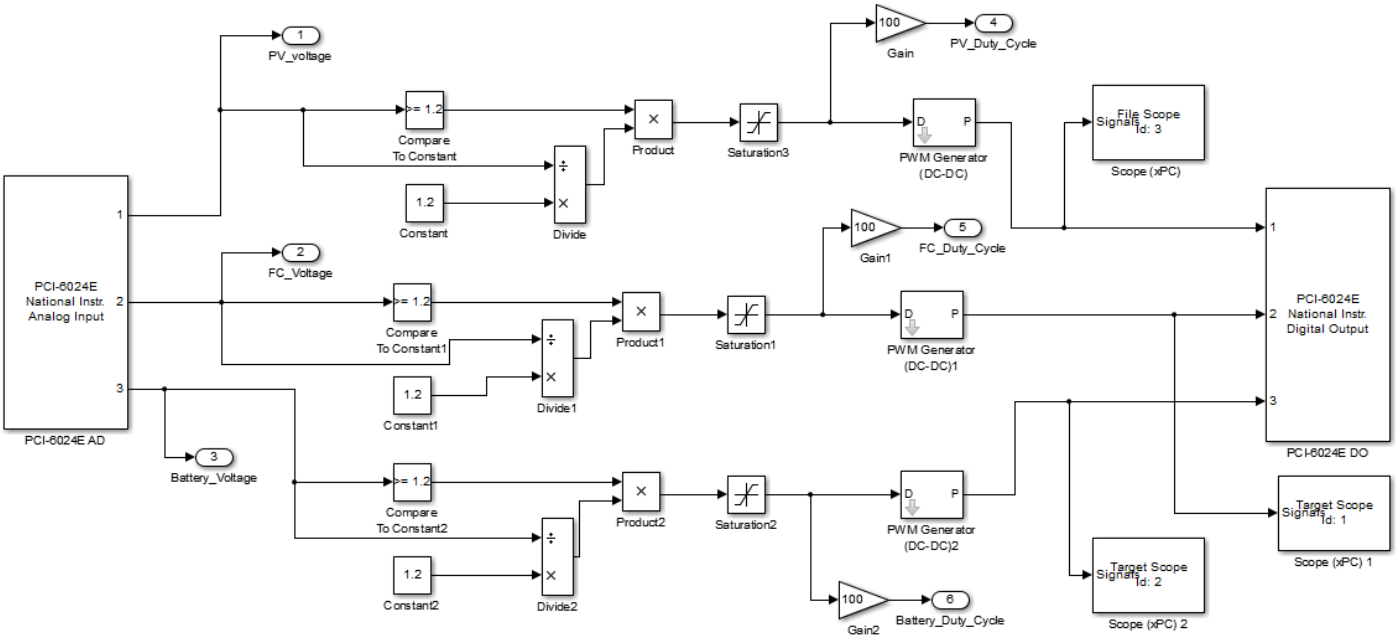

Figure 6.13: XPC Model to keep the voltage within 1.2V using PWM.

An XPC Target Library is used to build the model and to control the output voltage of PV, Fuel Cell, and battery by using PWM and DAQ (NI 6024E) is used for system control. Low pass filter is used to smooth the output signals from the power transistors which used as switches to supply the load.

The settling time chose to be 510^{-5} because it must be more than ten times from PWM block frequency to prevent loss in signal.

6.4.2 Hardware Connection

The input of the SIMULINK model is from the three sources of power (PV, FC, and Battery), the two PV module is used and connected in parallel to increase the current and the tow fuel cells connected in series to get the voltage over 1.2 V because each on has maximum voltage of 0.9V, just one battery used in this test with voltage of 1.2Vand capacity of 2700mAh.

The screw terminal is used to input the signals to the XPC Target throw the first three analog input channels of DAQ; the differential connection of signals is used to safe the DAQ from high current signals of sources. PV modules positive terminal connected to analog channel 0 (pin 68), Fuel cells positive terminal connected to analog channel 1(pin 33) and battery positive terminal connected to analog channel 2 (pin 65); also the three negative terminals of PV, FC, and battery connected together to three ground channels of analog inputs (pins 34, 66, 31).

The output of SIMULINK model is the PWM signals which connected to the first three digital output ports (pins 52, 17, and 49), three PNP transistors (2N3904) used as switches to cut the signals of the sources (PV, FC, and Battery), the transistors takes its switching signals from digital output channels then each cutting signal go to low pas filter to smooth it.

When connected the three sources the diodes are used to safe the PV modules and Fuel Cells from reverse current which may be cause damage of it.

6.4.3 Results

The project team make many test to check the system working and the system give a very good results show in the following.

In figure 6.14 the Data of PV is shown with time; the PV voltage enter the system with more than 2.4 volt , so the PWM duty cycle is approximately 50% and the output voltage is close to 1.2 V as needed with low value of error.

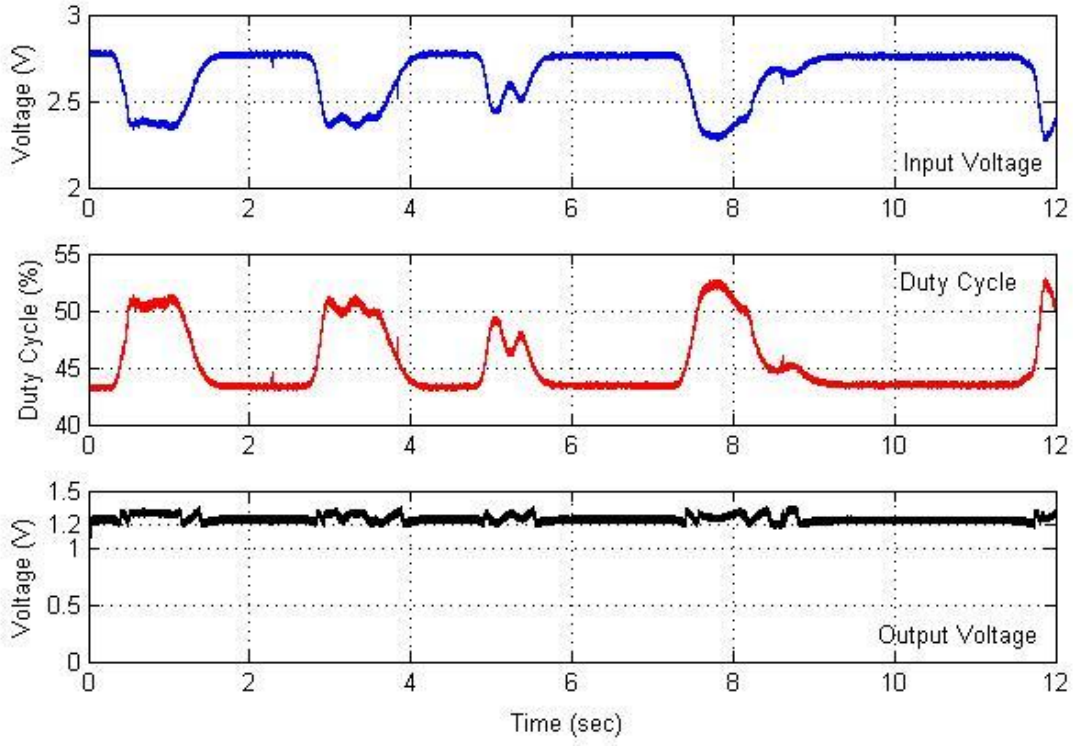

Figure 6.14 : Data of PV modules connected in parallel with Time.

The Fuel Cells Data shown in Figure 6.15 with time; as we can see in the figure the voltage enter the system from two fuel cells connected in series is approximately 1.4 volt, and so the duty cycle of PWM in range of 93% until the input voltage increase the duty cycle decrees, and the output voltage is very close to 1.2 Volt with very low error.

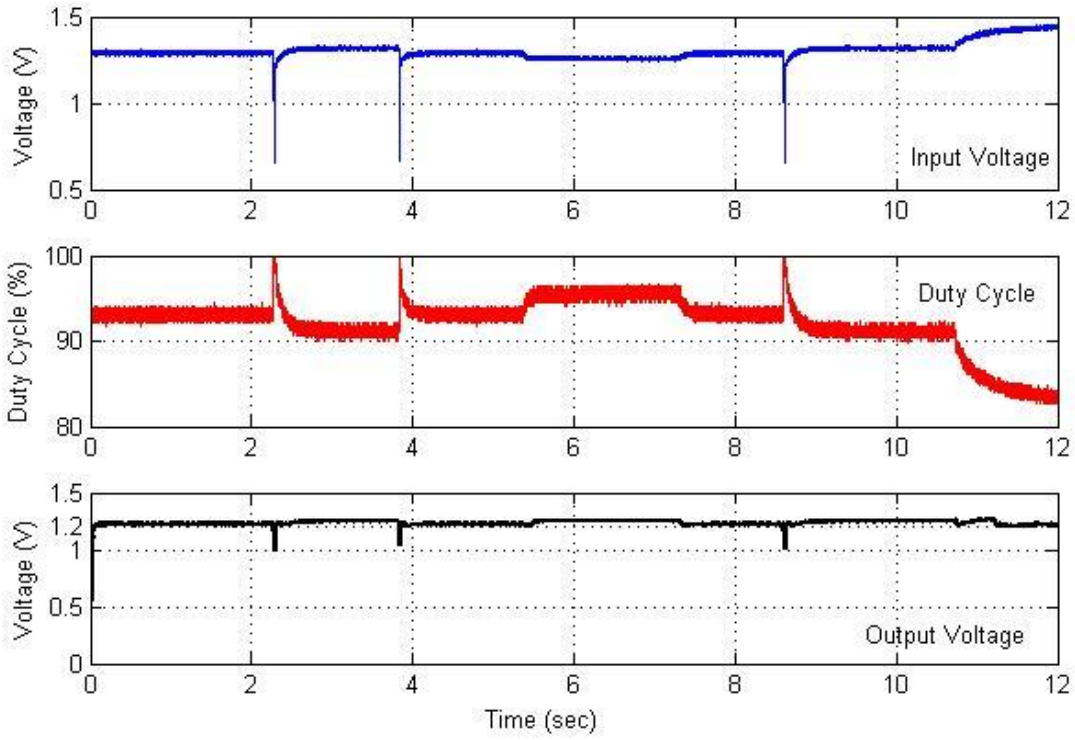

Figure 6.15 : Data of two Fuel Cells connected in series with Time.

Finally The Data of Battery with time shown in Figure 6.16; as we can see in the figure the voltage enter the system from two fuel cells connected in series is approximately 1.3 volt, and so the duty cycle of PWM in range of 98% until the input voltage increase the duty cycle decrees, and the output voltage is very close to 1.2 Volt with very low error.

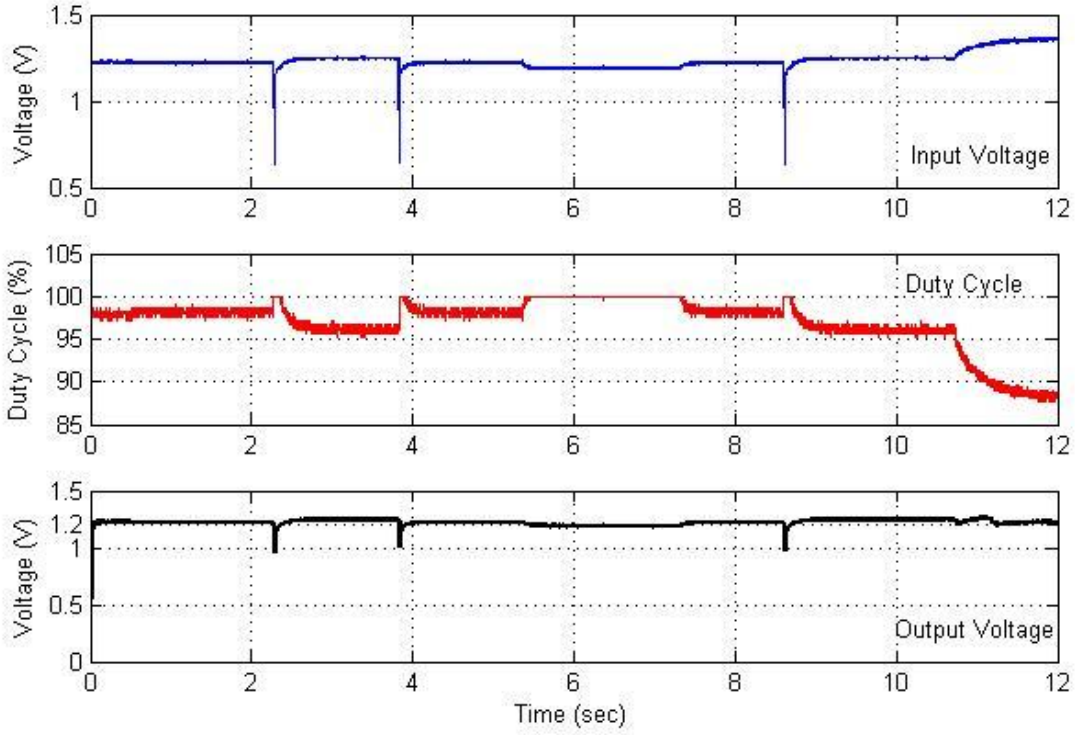

Figure 6.16 : Data of Battery with Time.

Chapter 7

Conclusion and Recommendations

7.1 Faced problems

7.2 Conclusion

7.3 Recommendations

7.1 Faced problems

In last semester the project team faced many problems, we can solved them with help and ideas from supervisor of the project and other teachers in the university, in the beginning of the experiments there is a problem in install the driver of the NI ELVES II on the computer because the CD of the unit was lost, and getting the serial number of the unit from the National Instrument company. These problems solved after we get the needed driver from the NI website and we contact the company to get the serial number.

Also a big problem we faced in the fuel cell and electrolyzer method of work, before we solve this problem the maximum short circuit current we can get from the cell not excess 100mA, this problem solved by give the fuel cell about three minutes before we close its tube to get rid out all the air in the tubes and replace it with hydrogen and oxygen by electrolyzer.

In this semester also a lot of problems faced, with god supply and hard work with our supervisor and other teachers we can solve them. For example the programming using state flow takes a lot of time and work to understand and programming it. Also The code of PSO algorithm in the first takes a lot of time from us to understand it and change the necessary things in code to satisfy our system and build our function. Another problem is to use a variable PWM duty cycle that not found in Matlab software until the new version R2013a be available on March, 2013. And so in this version a lot of problems appear like the maximum number of sample can taken from XPC target which take approximately two weeks to solve it and other problems in compiler and use XPC target.

7.2 Conclusion

The obtained results of power management strategy in chapter four showed system efficiency sensitivity to load variation, which impose limits on the switching times and fuel cell output delays. This leads to enlarge the system capacity, especially the battery bank for compensation, which leads indirectly to increase the system final cost. However, experimentation indicates some negative aspects in terms of cost, but it still have many other positive aspects in terms of renewable energy usage.

In chapter five the Practical swarm optimization (PSO) algorithm was used to optimize two different configurations of fuel cell and photovoltaic hybrid system. Two proposed configurations were optimized and the optimization results were compared; finally the best configuration of system was selected. This configuration includes PV panels, fuel cell and batteries for storage energy. Because the fuel cells are more efficient at low load profile, using the combination of battery with fuel cell as backup and storage system not only increases efficiency and life time of fuel cell, but also provides a suitable and uninterrupted power supply. Increasing battery stack size caused reduced the number of PV panels to supply required load. Therefore the best configuration of standalone power system is combination of fuel cell and battery as storage system.

The solar photovoltaic cell is dependent on the solar irradiation, so in chapter six the data in Table 6.1 is less than the nominal values because the solar irradiation is less than $100W/m^2$, also it depend on the temperature of the cells.

The electrolyzer efficiency is acceptable because the PEM electrolyzer can have efficiencies excesses 85%.

The fuel cell nominal values taken at 80^oC temperature, while when the project team takes the values of current and voltage the temperature of the lab was about 20^oC, so we can see the difference between experiment data and nominal values, for example for open circuit voltage , short circuit current and the efficiency.

7.3 Recommendations

- Make models to other system components like inverters and charge controller.
- In future include the wind turbine in the system which is an important renwable energy source.

- Build a control system for other components of fuel cell like compressor, electrolyzer and tank.

- Study the use of alkaline electrolyzer instead of PEM electrolyzer because PEM is a new technology and is twice as expensive as alkaline technology. Furthermore, alkaline technology has been used for a long time in industry and its lifetime reaches about 20 years and can use the rain water to produce hydrogen.

- Also find the method to produce hydrogen from methane gas, this method can be use in Palestine to reduce the cost of hydrogen by using waste as an organic fertilizer for crops.

- Develop the PSO algorithm to use Fuzzy logic in it.

- Use FPSO algorithm as strategy to control the power of the system.

References

[1] H. Miland, O. Ulleberg, “Testing of a small-scale stand-alone power system based on solar energy and hydrogen”, Solar Energy, In Press, Uncorrected Proof.

[2] K. Agbossou, M. Kolhe, J. Hamelin, T.K. Bose, “Performance of a stand-alone renewable energy system based on energy storage as hydrogen”, IEEE Transactions on Energy Conversion, vol. 19, pp. 633-640, 2004.

[3] A.N. Kelly, L.T. Gibson, D.B. Ouwerkerk, “A solar-powered, high-efficiency hydrogen fueling system using high pressure electrolysis of water: Design and initial results” International Journal of Hydrogen Energy, vol.33, pp.2747-2764, 2008.

[4] R. Dufo-Lopez, J.L. Bernal-Agustin, J. Contreras, “Optimization of Control Strategies for Stand-Alone Renewable Energy Systems with Hydrogen Storage”, Renewable Energy, vol. 32, pp. 1102-1126, 2007.

[5] S. Pedrazzi, G. Sini, P. Tartarini, “Complete modeling and software implementation of a virtual solar hydrogen hybrid system”, Energy Conversion and Management, vol. 51, pp.122-129, 2010.

[6] P.W. Atkins, “Physical Chemistry,” 3rd Edition, W.H. Freeman and Company, New York, NY, 1986.

[7] M.W. Chase, et al., “JANAF Thermochemical Tables,” Third Edition, American Chemical Society and the American Institute of Physics for the National Bureau of Standards (now National Institute of Standards and Technology), 1985.

[8] S.N. Simons, R.B. King and P.R. Prokopius, in Symposium Proceedings Fuel Cells Technology Status and Applications, Figure 1, p. 46, Edited by E.H. Camara, Institute of Gas Technology, Chicago, IL, 45, 1982.

[9] James Larminie, Andrew Dicks. Fuel Cell Systems Explained, Second Edition, John Wiley & Sons Ltd, 2003.

[10] EG&G Technical Services, Inc., Fuel Cell Handbook, Seventh Edition, November 2004

[11] Dursun , Acarkan , Kilic," Modeling of hydrogen production with a stand-alone renewable hybrid power system" , international journal of hydrogen energy 37(2012)309 8e3107

[12] Eroglu M, Dursun E, Sevencan S, Song J, Yazici S, Kilic O.A mobile renewable house using PV/wind/fuel cell hybrid power system. Int J Hydrogen Energy 2011;36:7985e92.

[13] Zahedi A. Maximizing solar PV energy penetration using energy storage technology. Renew Sust Energ Rev 2011; 15:866e70.

[14] Hsiao P, Chang CH, Tsai HL. Accuracy improvement of practical PV model SICE Annual Conference; 2010. 2725e30.

[15] Emin Meral M, Dinc¸er F. A review of the factors affecting operation and efficiency of photovoltaic based electricity generation systems. Renew Sust Energy Rev 2011; 15:217684.

[16] Hua CC, Shen CM. Study of maximum power tracking techniques and control of dc-dc converters for photovoltaic power system, in Proceedings of 29th annual IEEE Power Electronics Specialists Conference; 1998. 86e93.

[17] Lopes CF, Watanabe EH. Experimental and theoretical development of a PEM electrolyzer model applied to energy storage systems. Power Electronics Conference; 2009. COBEP '09. Brazilian Digital Object Identifier:10.1109/COBEP.2009.53476192009:775e82.

[18] Larminie J, Dicks A. Fuel cell systems explained. 2nd ed. Chichester, England: John Wiley & Sons; 2003.

[19] By EG&G Services Parsons, Inc. Science Applications International Corporation under contract No. DE-AM26-99FT40575. U.S. Department of Energy Office of Fossil Energy National Energy Technology Laboratory; 2007. P.O. Box 880 Morgantown, West Virginia 26507-0880, Fuel Cell Handbook.

[20] Li X. Principles of fuel cells. Taylor & Francis Group; 2006.

[21] Prentice G. Electrochemical engineering principles. Prentice-Hall International Editions; 1991.

[22] Choi P, Bessarabov DG, Datta R. Simple model for solid polymer electrolyte (SPE) water electrolysis. Solid State Ionics 2004;175:535e9.

[23] Go¨rgu¨n H. Dynamic modelling of a proton exchange membrane (PEM) electrolyzer. Int J Hydrogen Energy 2006;31:2e38.

[24] Hwang JJ, Lai LK, Wu W, Chang WR. Dynamic modeling of a photovoltaic hydrogen fuel cell hybrid system. Int J Hydrogen Energy 2009;34:9531e42.

[25] Pukrushpan JT, Stefanopoulou AG, Peng H. Control of fuel cell power systems: principles, modeling, analysis, and feedback design. Springer; 2004.

[26] Dai C, Chen W, Cheng Z, Li Q, Jiang Z, Jia J. Seeker optimization algorithm for global optimization: a case study on optimal modelling of proton exchange membrane fuel cell (PEMFC). Int J Electrical Power Energy Syst 2011;33:369e76.

[27] Ni M, Michael LKH, Dennis YC. Parametric study of solid oxide steam electrolyzer for hydrogen production. Int J Hydrogen Energy 2007;32:2305e13.

[28] Khan MJ, Iqbal MT. Dynamic modeling and simulation of a small windefuel cell hybrid energy system. Renew Energy 2005;30:421e39.

[29] Handbook of Energy Efficiency and Renewable Energy (Mechanical and Aerospace Engineering Series)

[30] A. Gilbert M. Masters, Photovoltaic Materials And electrical Characteristics, In Renewable and Efficient Electric Power System, A john Wiley &Sons, Eds.., published by john Wiley &sons, Inc , Hoboken, New Jersey,2004,pp.468-473 .

[31]A. James P .Dunlop, P.E, Batteries and Charge Controller in Stand-Alone Photovoltaic, Florida Solar Energy Center, 1997.

[32] Ismail M.S, and Mahmoud M. 2011. Simulation of a Hybrid Power System Consisting of Wind Turbine, PV, Storage Battery and diesel Generator: Design, Optimization and Economical Evaluation, pp.68-75, Fourth International Energy Conference-Palestine.

[33] Ibrik H.I. 2011. Electrification of Emnazeil Village in Palestine Multi-User Solar Hybrid Grid", pp.51-55, Fourth International Energy Conference-Palestine.

[34] Marwan M. Mahmoud , Imad Ibrik. 2003. Field experience on solar electric power systems and their potential in Palestine; Renewable and Sustainable Energy Reviews, 7:531-541.

[35] Pierre H., Jean-Marc J., Bernard L., and Klaus Y. 2000. Evaluation of a 5 kWp photovoltaic hydrogen production and storage installation for a residential home in Switzerland, International Journal of Hydrogen Energy.

APPENDIX

A

Practical Swarm Optimization (PSO) Algorithm Matlab Code

Main

```
%%
clc;
clear all;

ObjectiveFunction = @simple_fitness;
nvars = 3;    % Number of variables
LB = [3000 10 0000];   % Lower bound
UB = [8000 25 0000];  % Upper bound
Popln=100;
Genrtn=500;
WByn=1;
[x,fvalue] =
pso(ObjectiveFunction,'NumVar',nvars,'LowerBound',LB,'UpperBound',UB,
      'Population',Popln,'Genrations',Genrtn,'IncludeWB',WByn);
p=x(1)+W_FC+x(3);

disp(x);
disp(fvalue);
disp(p);
```

Objective Function

```
function y = simple_fitness(x)
clc
%PV
PV_life_time= 20; %PV life time (Year)
 x(1)=2450
C_PV = 4.84;  % PV Capital Cost ($/watt)
M_PV = 3; % PV Rep. & maintance Cost($/year)
Y_PV = (20/PV_life_time)-1; % PV Replacement Once

% Fuel Cell
FC_life_time= 5000 ;% FC life Time (Hours)
W_FC=5400;
  x(2)=24
C_FC = 8  ; % FC Capital Cost ($/W)
M_FC = 6  ; % FC Rep. & maintance Cost($/W.year)
Y_FC = (20*x(2)*365/(FC_life_time))-1; %FC Replacement Once

% Battery

Batt_Life_Time = 5; % (years)
C_Batt= 20  ;%($/Wh)
M_Batt= 0;
Y_Batt= (20/Batt_Life_Time)-1;
x(3)=0



y = (x(1) * C_PV * ( Y_PV + 1 )+ M_PV*(20 - Y_PV + 1))+((W_FC * C_FC)
      * ( Y_FC + 1 )+ (M_FC * W_FC)*(20 - Y_FC + 1))+(x(3)
      * C_Batt * ( Y_Batt + 1 ));
```

Intialise Parameters

```
%% Intialise Parameters
function init_params()
global El_lim_low El_lim_up LB UB El_range PopulationSize P Generations
iteration;
global El vel NumVer pbest_loc gbest_loc pbest_val EV gbest_val_record;
global FitVal gbest_val ev av d n p t delta_t k_pb_i k_pb_f k_gb_i k_gb_f w
El_lim_low(1,1:NumVer)=LB;
El_lim_up(1,1:NumVer)=UB;
El_range(1,1:NumVer)= El_lim_up - El_lim_low;
P=PopulationSize;% number of particles
iteration=Generations;% number of iterations
% Intialise Pbest of all agents & Gbest
El =zeros(1,NumVer,P);
vel =zeros(1,NumVer,P);
pbest_loc=zeros(1,NumVer,P);
gbest_loc=zeros(1,NumVer);
pbest_val=zeros(P);
EV=P*iteration;
gbest_val_record(1:EV) = 0;
FitVal = 1000.0;
gbest_val = 1000.0;
ev = 0;
av = 0;
d=0; n=0; p=0; t=0;
delta_t=1;
% Set parameters of the optimization problem
k_pb_i = 2.5;
k_pb_f = 0.5;
k_gb_i = 0.5;
k_gb_f = 2.5;
w = 0.9;
end
```

Intialise position & velocity of all agents

```
%% Intialise position & velocity of all agents %ini_posi_vel()
function intialise()
global El vel El_lim_low El_range P NumVer;
for p=1:P% population
        Randm=rand(1,NumVer);
        El(1,1:NumVer,p) = El_lim_low + Randm .* El_range;
        vel(1,1:NumVer,p) = El_lim_low + Randm .* El_range;
end
end
```

Update fitness for each particle and iteration

```
%% update fitness for each particle and   iteration
function update_fit()
global ell FitVal El NumVer p fhandle;
```

```
ell(1,1:NumVer)=El(1,1:NumVer,p);
FitVal = feval(fhandle,ell);
end
```

Update pbest & gbest

```
%% update pbest & gbest;
function update_pbest_gbest()
global n p ev FitVal pbest_val NumVer pbest_loc El gbest_val gbest_loc
gbest_val_record;
if (n~=1)
    if (FitVal < pbest_val(p))%% check < or >
        pbest_loc(1,1:NumVer,p)=El(1,1:NumVer,p);
        pbest_val(p)=FitVal;
    end
    if(FitVal < gbest_val)
        gbest_loc(1,1:NumVer)=El(1,1:NumVer,p);
        gbest_val = FitVal;
    end
else
    pbest_loc(1,1:NumVer,p)=El(1,1:NumVer,p);
    pbest_val(p)=FitVal;
    if(p~=1)
        if(pbest_val(p) < gbest_val)
        gbest_loc(1,1:NumVer)= El(1,1:NumVer,p);
        gbest_val = FitVal;
        end
    else
        gbest_loc(1,1:NumVer) = pbest_loc(1,1:NumVer,p);
        gbest_val = pbest_val(p);
    end
end
gbest_val_record(ev) = gbest_val;
end
```

PSO function

```
function [OptimizedElem,fval] =
pso(fhandle,~,NumVer,~,LB,~,UB,~,PopulationSize,~,Generations,~,DispWB)
warning('off');
% global pbest_loc;
% global gbest_loc;
% global pbest_val;
% global gbest_val;
% global iteration;
% global gbest_val_record;
% global El_range El_lim_low El_lim_up vel P EV p n ev DispWB
% global NumVer fhandle
% global k_pb_i  k_pb_f  k_gb_i k_gb_f w delta_t;
% global El_lim_low El_lim_up LB UB El_range PopulationSize P Generations
iteration;
```

```
% global El vel NumVer pbest_loc gbest_loc pbest_val EV gbest_val_record;
% global FitVal gbest_val ev av d n p t delta_t k_pb_i k_pb_f k_gb_i k_gb_f w


global gbest_loc;
global gbest_val;
global iteration;
global P EV p n ev DispWB
global NumVer fhandle
global LB UB  PopulationSize P Generations iteration;
global NumVer  gbest_loc  EV ;
global gbest_val ev n p

if (DispWB==1)
wb = waitbar(0,'1','Name','Shadi - Optimizer :',...
            'CreateCancelBtn',...
            'setappdata(gcbf,''canceling'',1)');
setappdata(wb,'canceling',0);
end

%% Intialise Parameters
init_params();
%%
%% Intialise position & velocity of all agents %ini_posi_vel()
intialise();
%%
for n=1:iteration
for p=1:P
ev=ev+1;
%% update fitness for each particle and iteration
update_fit();

%% update pbest & gbest;
update_pbest_gbest();
%% update_vel_pos(p,n);
update_vel_pos();
%%
if (DispWB==1)
waitbar(ev/EV,wb,sprintf('%12.9f',gbest_val));
end
end
end
OptimizedElem=gbest_loc(1,1:NumVer);
fval=gbest_val;
if(DispWB==1)
delete(wb);
end
end
```

Update velocity of PSO function

```
%% update_vel_pos(p,n);
function update_vel_pos()
global vel El El_lim_up El_lim_low
```

```
global n w k_pb_i R iteration k_pb_f  k_gb_i k_gb_f k_pb k_gb c_gb c_pb
delta_t;
global NumVer p pbest_loc gbest_loc
R = n /iteration;
k_pb = k_pb_i + R*(k_pb_f - k_pb_i);
k_gb = k_gb_i + R*(k_gb_f - k_gb_i);
c_pb = rand*k_pb;
c_gb = rand*k_gb;

      vel(1,1:NumVer,p) = w*vel(1,1:NumVer,p) + c_pb*(pbest_loc(1,1:NumVer,p)
- El(1,1:NumVer,p)) + c_gb*(gbest_loc(1,1:NumVer) - El(1,1:NumVer,p));

%Velocity Upper Bound Velocity Lower Bound
     for chgdir=1:NumVer
      if((vel(1,chgdir,p) > (El_lim_up(1,chgdir) - El(1,chgdir,p))))
          vel(1,chgdir,p) = -0.7*vel(1,chgdir,p);%(El_lim_up(1,1:NumVer) -
El(1,1:NumVer,p));%             x(i)=x(i)+2*v(i);
      end
      if((vel(1,chgdir,p) < (El_lim_low(1,chgdir) - El(1,chgdir,p))))
          vel(1,chgdir,p) = -0.7*vel(1,chgdir,p);%(El_lim_up(1,1:NumVer) -
El(1,1:NumVer,p));
      end
     end

 El(1,1:NumVer,p)= El(1,1:NumVer,p)+delta_t*vel(1,1:NumVer,p);
end
```